CODEN:LUTEDX/(TEIE-5517)/1-130/(2024)

Electrical Engineering and Automation

Industrial

# The Potential for Floating Wind Power in Power-to-X Megaprojects



**Anton Wickenberg**
**Axel Engström**

Division of Industrial Electrical Engineering and Automation
Faculty of Engineering, Lund University

EXAMENSARBETE

Ekosystemteknik

CODEN:LUTEDX/(TEIE-5517)/1-130/(2024)

# The Potential for Floating Wind Power in Power-to-X Megaprojects

**Axel Engström, Anton Wickenberg**

# The Potential for Floating Wind Power in Power-to-X Megaprojects

Axel Engström
engstroemaxel@gmail.com

Anton Wickenberg
antonwickenberg@gmail.com

June 25, 2024

Master's thesis work carried out at
Division of Industrial Electrical Engineering and Automation (IEA)
LTH, Lund University.

Supervisor: Jörgen Svensson, jorgen.svensson@iea.lth.se

Examiner: Olof Samuelsson, olof.samuelsson@iea.lth.se

## Abstract

This master's thesis explores the potential of integrating floating wind power into Power-to-X (P2X) megaprojects, with a focus on maximizing the output of chemical energy carriers through optimal energy mix strategies. The study evaluates the economic viability and technological efficiency of combining floating wind turbines with photovoltaic panels and battery energy storage systems (BESS) in off-grid settings for a P2X project. Using the Port Nolloth area in South Africa as a case study, a comprehensive simulation model was developed to assess site-specific conditions and perform techno-economic optimization. The research identifies key cost drivers and optimal component ratios, and provides a scalable tool for the analysis of the P2X system applicable to various global locations. The findings contribute to the advance of the green transition by offering a sustainable and economically feasible solution for large-scale renewable energy projects, leading to the conclusion that according to our case study, floating wind turbines play a key role in P2X applications.



**Keywords**: *Floating wind power, Power-to-X (P2X), Renewable energy, Techno-economic optimization, Photovoltaics (PV), Battery Energy Storage System (BESS), Energy storage, Off-grid energy systems, Green Hydrogen, Green Ammonia, Electrolyzer, Levelized cost of electricity (LCOE), Green transition, Simulation modelling, Renewable energy economics, Port Nolloth case study*

# Acknowledgements

We would like to express our deepest gratitude to everyone who has supported us throughout the development of this master's thesis.

Firstly, we would like to thank our supervisor at Lund University, Jörgen Svensson, for his invaluable guidance and support. His assistance in structuring the report and setting up the simulation model was crucial to the success of this project.

We also express our gratitude to Benjamin King, our supervisor at Hexicon AB, for his industry insights and practical advice. His knowledge of the floating wind power sector and the broader renewable energy industry greatly enriched our understanding and helped us align our academic research with real-world applications.

In addition, we would like to thank our classmates with whom we have exchanged ideas and support throughout this semester.

Finally, we are grateful to Lund University and Hexicon AB for providing us with the opportunity and resources to conduct this research.

Anton Wickenberg and Axel Engström

# Abbreviations

**AC** Alternating Current
**Al** Alkaline Electrolyzer
**BESS** Battery Energy Storage System
**CAPEX** Capital Expenditures
**CCS** Carbon Capture and Storage
**CF** Capacity factor
**DC** Direct Current
**DSP** Desalination plant
**ESS** Energy Storage System
**FC** Fuel Cell
**GHG** Green house gas
**HB** Haber-Bosch
**HVAC** High Voltage Alternating Current
**HVDC** High Voltage Direct Current
**LCOE** Levelized cost of electricity
**LCOH** Levelized cost of hydrogen
**LCONH3** Levelized cost of ammonia
**LIB** Lithium Ion Battery
**NCGH2** Northern Cape Green Hydrogen Project
**O& M** Operations and Maintenance
**OPEX** Operating Expenditure
**P2X** Power-to-X
**PEM** Proton Exchange Membrane Electrolyser
**PID** Proportional Integral Derivative
**PV** Photovoltaic panel
**R& D** Research and Development
**SOEC** High Temperature Solid Oxide Electrolyser
**SoC** State of charge
**SPP** Solar Power Plant
**TRL** Technology readiness level
**WPP** Wind Power Plant

# Contents

# Chapter 1

# Introduction

As a result of the climate crisis, the world is undergoing an extensive energy transition, where renewable energy is on the rise to replace existing fossil fuel-driven electricity production, enabling industries to electrify through expansion of energy production. In this transition, wind power plays an important role. Throughout the last decade, offshore wind power has been on the rise in northern Europe due to good wind conditions, water depth, and scaling possibilities. However, looking at the glosses,wind atlas, and the global sea depth map, multiple locations can be seen with great wind conditions where the coasts are too deep to use conventional fixed offshore wind turbine technology. The only possibility in multiple locations of ideal wind conditions is therefore floating wind power, with its huge potential to extend the possibilities for offshore wind power for the rest of the world. The photovoltaic industry has also seen significant development during the last decade, with increasing production, lower manufacturing costs, and technological advancements. This has been made possible due to several factors, including advancements in R& D, policies stimulating market growth, and scale economies, which have made prices significantly decline to become the cheapest electricity generation technology. [1]

As mentioned above, an effective way to decarbonize major parts of polluting sectors such as industry and transport is through electrification with electricity supplied by renewable energy. However, some sectors are hard to electrify completely, such as shipping, mining and fertilizer production, so an alternative for them to phase out their fossil fuel dependency is to transition to green hydrogen-based fuels that are produced from renewable electricity. Furthermore, regions where renewable electricity production is either too expensive or not possible due to space restrictions will depend on importing green energy, just as they are dependent on importing fossil fuels today. This green energy would then have to come from a Power-to-X (P2X) project, where sustainable energy from solar and wind production is converted to a suitable chemical energy carrier (such as Hydrogen or Ammonia) and further exported or used in local industries. These P2X projects are huge investments and have to be located in attractive locations to be competitive in the global market in the aspects of energy

yield, logistics, etc. To be more competitive, the project outline should also be carefully balanced with respect to the ratio of solar power, wind power, and battery storage technology to supply maximum production, creating the optimal composition from an economical point of view.

This Master's thesis was made in collaboration with Hexicon AB. Hexicon is a Swedish company in floating offshore wind industry. Apart from technology development, the company is also a big project developer for offshore wind in general and floating wind in particular. These are competences that give them a unique position on the market, which makes them excellent supervisors for our project.

## 1.1 Objectives

In this Masters thesis, we want to:

- Investigate the potential for floating wind in off grid P2X megaprojects aimed at maximizing chemical energy carrier output, chosen by its market viability by determining the most cost-effective mix of installed capacity for the main four system components of Electrolyzer/Haber-Bosch unit, BESS, Photovoltaics, and Wind Power at a selected case study site.
- Analyze the economical output and identifying the main cost drivers of the case study P2X project.
- Develop a general scaleable tool for P2X system analysis independent of the selected location.

## 1.2 Method Overview

To fulfill the research objectives, an overall method consisting of several steps is used. In addition, a case study of a potential location for a P2X project is presented in the background in chapter 2 to apply real-life conditions to the system. In this project, the chosen location for the case study is Port Nolloth, South Africa. This choice of location is based on local regional plans in combination with Hexicons site identification work, both presented in Section 2.7. The method starts with an extensive literature study in Chapter 3, to identify the main components of a P2X system and their functions. To then be able to dimension the system properly and validate that the system works, a power simulation model is built in the OpenModelica simulation software, where the inputs to the system come from site-specific conditions from the Port Nolloth area in South Africa which is presented in Chapter 4. Lastly, a techno-economic optimization method is used in order to ultimately give the optimal dimensioning and ratio between the components. However, the simulation model is built as general as possible, with the future goal of being applied as a tool to identify the P2X

potential for other locations. These different steps in the overall method are described in more detail in the Methodology chapter 3.

## 1.3 Delimitations

The main delimitation of this master's thesis is that the model is designed excluding grid connection, seen as an island node, which has an effect on the system where no electricity can be imported or exported.

This master's thesis is an attempt to make a very complex system of hundreds of components, more simplified to have an idea about the outcome of a P2X project for a specific location. The project is therefore restricted by the delimitations stated in the methodology, which takes into consideration both simulation and practical concerns, as well as economical optimization.

## 1.4 Disposition

As the model built in this report needs to be applicable for different cases, the background, literature study, and methodology are written independently of the case chosen. The methodology is then applied to the case study to present the results and discuss its outcome and how it can be applied for other case studies.

# Chapter 2

# Background

In this chapter, the idea is to give a background to the area of Power-to-X (P2X), including a theory of the concept, applicable usage areas for P2X products, and a brief overview of the future market potential for these products. The chapter ends with the identification of suitable locations for these types of project, including site selection work from two different sources.

## 2.1 The Concept of Power-to-X

Power-to-X (P2X) describes the idea of a renewable electricity generation system, which is transformed to other energy carriers and stored for later use in its most suitable applications. The idea behind the concept is that the "X" can be substituted to a chosen energy carrier, such as hydrogen, ammonia, methanol, or other fuels produced from renewable sources, to sustainably decarbonize today's society, where a clear majority of the energy usage originates from fossil fuels. A P2X system has the potential to produce energy derivatives to effectively phase out fossil fuels. [2]

## 2.2 Production Locations for P2X

There exist multiple interesting locations which are suitable for P2X production. For example, Africa offers multiple possibilities in desert regions. The South African and Namibian coasts have great wind and solar potential and a need for development. Morocco offers favorable pipeline possibilities, benefiting from its strategic position and strong diplomatic relations. Australia stands out with its vast land mass, renewable energy resources and stable

economy, making it an attractive destination for P2X ventures despite its remote locations. Saudi Arabia has significant space and energy potential, particularly in solar power, improving its suitability for green hydrogen production through P2X processes and facilitating exports to global markets. Meanwhile, Chile presents exclusive opportunities for wind-based P2X production, leveraging its exceptional wind resources and commitment to renewable energy. These countries collectively contribute to the global expansion of sustainable energy solutions.

## 2.3 Consumption of Hydrogen Derivative

Hydrogen derivatives are anticipated to be used over a longer time frame in nearby industries for these P2X projects, where hydrogen products have essential applications. This potential usage could draw industries to the area due to the cost-effectiveness of hydrogen products. Moreover, understanding global energy usage is crucial for comprehending its various applications and price volatility.

### Metal Production

Hydrogen can be used as an oxidizing agent, as a recycled heat supply, or converted back to electricity by using a fuel cell. Today, the metal production industry, is accountable for around 10 percent of the world carbon dioxide emissions, where steel has the main impact. At the moment, steel production relies on coke (a form of coal) as a reducing agent as well as a heat supply. Using hydrogen for these applications can effectively decarbonize the process. This process is unique in the industry and there is no other 100% decarbonized option available on the market that does not involve carbon capture and storage (CCS).[3] To implement these new processes, an increasing need for electricity in the mining and processing industry will be inevitable. As the P2X project itself also uses a lot of steel, this can be used for further green extensions.

### Agriculture

Hydrogen is widely used, as mentioned previously, in the agriculture and fertilizer industry and is therefore attractive worldwide both for domestic and export applications. The fertilizers are produced from ammonia and can therefore be produced in the importing country or industries close to the production plant to later be exported. [4]

### Transport

In the transport sector, hydrogen vehicles are an area of intense discussion and research. Fuel cell driven cars do not require customers to depend on slow charging, since they can fuel

up their cars as fast as with regular gasoline. Although the efficiency is much lower than that of the direct usage of electricity, it could be suitable for countries that depend on future energy imports, where electricity is not available. Hydrogen products such as ammonia and methanol are also believed to power the shipping and aviation industry, where batteries for these enormous vehicles would be too heavy, large and expensive.[5]

#### Emergency Electricity Generation

As a last possibility, if there is no other more efficient application of the energy carrier, both hydrogen and ammonia can be cycled back to electricity through the use of a Fuel Cell (FC). However, this should only be seen as a final possibility for emergency generation when there is a deficit in other energy storage systems (ESS), due to efficiency concerns of the conversion from hydrogen or ammonia to electricity.

### 2.3.1 P2X consumer Markets

As the ultimate goal of green energy carriers is to replace all fossil energy use, most industrialized countries have published their own target goals of domestic production and import of energy carriers.

In the following sections, to identify the consumers of a P2X project, the main three consumers are mentioned below, although hydrogen energy is a global commodity as oil is today. In these sections, hydrogen is considered for all targets , as it is one of the main focus of the world economy in terms of a long-term storage agent. However, the same reasoning is applicable to other green energy derivatives.

The European Union has huge plans for domestic production of green energy carriers, both through large-scale electricity production and hydrogen energy conversion. The European Union aims to have a continuous domestic hydrogen production of 40 GW, as well as an constant import of 40 GW of hydrogen product by the year of 2050. The import of energy from reliable sources is expected to be inevitable due to local space restrictions. EU has also launched investments of 5.6 billion dollars for research funding, as well as 3.2 billion dollars to help build the future hydrogen market. [6]The carbon taxation system for imported goods is also under active investigation in the union. This could also attract further import of sustainably produced products, fuels, and commodities, which strengthens the idea and concept of Power-to-X megaprojects.

Japan and South Korea are two countries with high population densities and ambitious climate targets. Japan is expecting to import 15-30 GW of hydrogen by 2050, and Korea is aiming to import 15 GW by 2040. [7] Because of their political relations with neighboring countries, as well as their limited potential for domestic electricity production of these magnitudes, it is likely that they will need to import green hydrogen.

The United States has better opportunities when it comes to domestic production of green

hydrogen but could still be a possible investor for projects abroad. The Biden administration recently invested 7 billion dollars in the first American hydrogen hubs.[8]

## 2.4 Economics of P2X

When designing and building large projects in general, economics plays a key role. For a P2X project the economics can be split into capital expenditure (CAPEX), and operational expenditure (OPEX). The CAPEX is the sum of all expenditures paid during project construction, while the OPEX is measured as the sum of all operational expenses during one year of operation. Further, other economical aspects such as project decommissioning also play a role in the overall economic overview.

Another economical figure is the Levelized Cost of Energy (LCOE), which quantifies all the lifetime costs associated with a certain energy production, compared to how much energy is produced during its lifetime. This gives a figure, often measured as $/kWh or $/kg of energy produced. This enables an easier comparison between different energy sources by standardizing costs to a per-unit basis considering interest rates, as well as CAPEX and OPEX. The method works for different types of energy carriers such as, for example, electricity, hydrogen, and ammonia. To calculate the cost of energy, cost and production need to be considered. These are split into the following.

**Initial investment** $I_0$: The total upfront capital cost for the project.

**Present Value of Annual Costs** $\sum_{t=1}^{n} \frac{A_t}{(1+i)^t}$: The discounted sum of all annual operation and maintenance costs over the plant's lifetime

**Present Value of Energy Produced** $\sum_{t=1}^{n} \frac{M_t}{(1+i)^t}$: The discounted sum of all annual energy produced over the plant's lifetime.

Combining these three economical terms gives the LCOE stated in the following equation.

$$LCOE = \frac{I_0 + \sum_{t=1}^{n} \frac{A_t}{(1+i)^t}}{\sum_{t=1}^{n} \frac{M_t}{(1+i)^t}} \tag{2.1}$$

Where $t$ is years, $i$ investment rate, $I_0$ is CAPEX, $A_t$ is OPEX and $M_t$ is production. [9]

For further understanding, an example assuming a wind park of 1 GW with a CF of 0.5 produces 4380 GWh. If the CAPEX is 2.2 Billion $ and OPEX is 3% of this the LCOE for the project is calculated for an interest rate of 8% and a project lifetime of 30 years.

$$LCOE = \frac{2.2 * 10^9 + \sum_{t=1}^{30} \frac{2.2*10^9*0.03}{(1+0.08)^t}}{\sum_{t=1}^{30} \frac{4380GWh}{(1+0.08)^t}} = 0.0597\$/kWh \tag{2.2}$$

## 2.5 Electricity Generation for P2X

For a P2X system to be efficient in its task of limiting carbon emissions, the electricity generated must come from renewable sources. For green power generation, today the market offers multiple alternatives, and it is important to consider that generation methods are dynamically changing. The main production of renewable electricity worldwide comes from solar, wind and hydro power. For solar and wind, this is a result of the low price of electricity generation compared to other renewable alternatives, while for hydro power it is because of storage possibilities. Other technologies such as wave/tidal power exist, but are all in their startup phase and not yet economically viable and are not expected to be competitive by 2035. Due to the scale of P2X megaprojects, the expansion possibilities of hydro power will not be enough to exclusively power it. Nuclear energy is another alternative, with the main advantage of supplying a constant load, which is preferred for hydrogen production. However, the long construction and licensing time, as well as the high LCOE, reduces its competitiveness for P2X projects where most of the consumption is elastic, and therefore the lowest LCOE value is prioritized.[10]

## 2.6 Energy Storage for P2X

Generally, for P2X projects, energy carriers are needed for both local storage and long-term storage. Renewable electricity production relies on fluctuating weather conditions, such as cloud coverage and wind availability. Therefore, short-term ESS is needed to deliver a continuous energy load to the processes that require it. As the processes are somewhat elastic, Seasonal storage is not expected to be needed, as energy carrier from the weekly storage facilities can be consumed in case it is needed.

## 2.7 Case study - South Africa

South Africa is of particular interest for the location of a Power-to-X megaproject for a variety of reasons. First, public opinion is important, as permitting in developed countries is often limited by regional and public processes. South Africa has also suffered from corruption and political instability in recent decades, leading to electricity scarcity that forced industries to shut down. Renewable power generation, especially on a scale large enough to handle severe electricity scarcity, is therefore a solution to get the entire economy back on track as the addition of new energy could re-attract green industries. The high unemployment rate is another problem that South Africa is experiencing and could be treated by implementing a P2X project that creates job opportunities. However, specific competences might be needed from an international context for some parts of a P2X megaproject. For example, competence for the deployment of floating offshore wind power currently exists mainly in Europe and the Asia-Pacific region. South Africa's relations to its neighboring countries are also generally good, making it less likely that international conflicts occur. In addition, the

country's historical relation to the major developed economies in the western world gives its investors an incentive to invest in the country.

A specific South African location of great potential is the northern cape region. The region is the least inhabited in South Africa, consisting of mainly inaccessible deserts with great solar and wind potential. The unique case of a region with desert all the way to the coast creates good conditions for a number of reasons. Placing a P2X location close to shore is good for logistics, both in the construction and operational phase. In addition, the temperature on the coast is lower, which increases the performance of the solar panels. The energy capacity of the wind is also generally better along the coast due to the lower friction coefficients. In addition, the wind conditions are even better at sea, boosted by a land breeze phenomenon causing stronger winds during the evening. [11]

In terms of space, the northern cape region also has great potential due to the absence of stakeholders in conflict, making permitting processes easier. The location is also well positioned next to large maritime trade routes, cutting costs for import/export and direct energy applications in the transport sector. For industrial applications, both in the construction phase and in the later use of energy, South Africa has a great deal of mineral processing and steel production, as well as a large chemical industry with a focus on fertilizers, which are industries suitable for application in a P2X project.[12]

### 2.7.1 Boegoebaai P2X Proposal

Currently, there are multiple proposals on how the South African economy can get back on track, including green industries and electricity production. One of them is the Northern Cape Green Hydrogen Project (NCGH2) with the initial planned investments in the Boegoebaai region on the west coast 20 km from the Namibian border. [13]

The project aims to establish a full green economy in South Africa, with an installed production capacity of more than 100 GW of green electricity from wind and solar power on land, with the main goal of producing hydrogen derivatives at an electrolysis production capacity of 40 GW continuously. The proposal comes from the region itself, which makes permitting in the area easier. The initial investor who is funding parts of this project is the largest coal company in the world, Sasol. They are planning to fund an installation of 10 GW of renewable capacity with a 4.8 GW electrolyzer. NCGH2 has presented a South African overview of the planned situation which can be seen in figure 2.1.

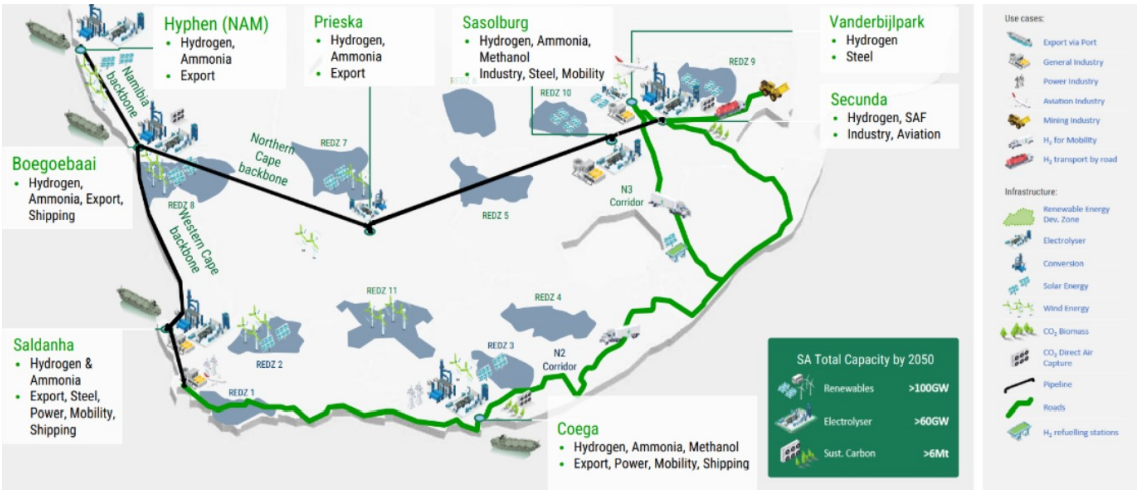


**Figure 2.1:** Map overview of the NCGH2 infrastructure plans for the whole country of South Africa.

The proposal for the final Boegoebaai production plant is illustrated by NCGH2 in figure 2.2. In this figure, one can see that the entire P2X system is illustrated, as well as other necessary parts such as residential buildings, agriculture, etc.

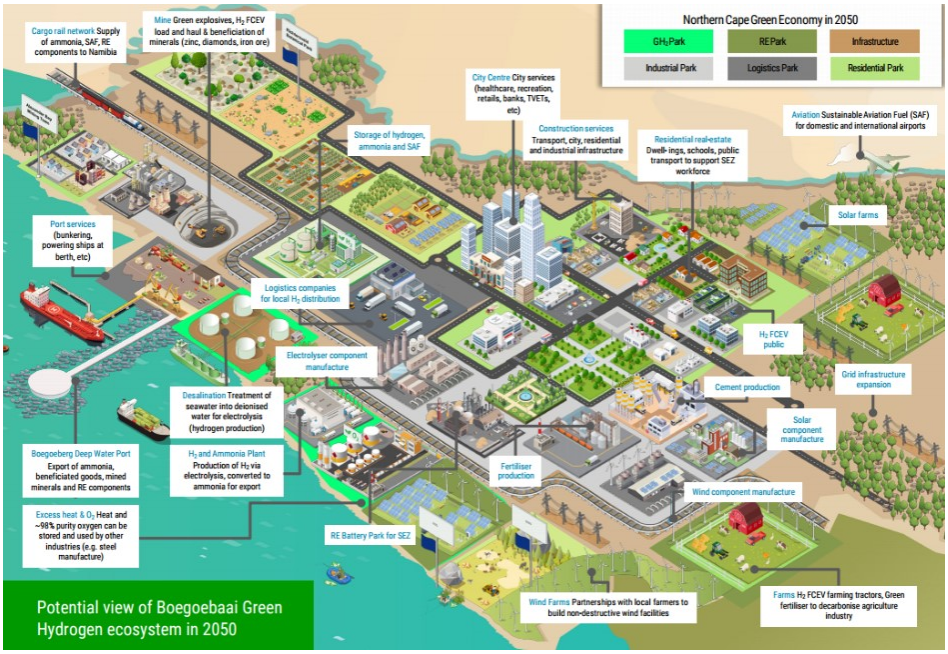


**Figure 2.2:** Map overview of the NCGH2 plans for Boegoebaii location.

### 2.7.2 Port Nolloth Generation Site Selection

Hexicon AB has made a site selection process for the deployment of a floating wind farm outside of the coast of a location called Port Nolloth, which is situated 60 km south of the Boegoebaii location in northwestern South Africa, as discussed before. The general methodology for site selection processes is described in more detail in Section 3.2.5.

Many different criteria have been taken into consideration regarding the Port Nolloth area such as, for example, coast proximity, shipping lanes, distance to grid connections, water depth, wind speed and bathymetry. In figure 2.3, some examples of different criteria and their respective grading according to certain thresholds can be seen. Some of the thresholds are fixed thresholds from rules and directives, such as shipping lanes, and some are individually set by the site developer or from frameworks made by Hexicon. However, it is worth noting that these criteria are specific for the floating WPP:s. For example, looking at column 4 in the figure, the water depths that are presented indicates that 100-350m are excellent conditions. This is because these depths of water are too deep for wind power plants with fixed foundations, meaning that floating foundations is a good alternative, which is more described in detail in Section 3.2.2.

| Score | Category | 1) Coast Proximity km | 2) Shipping lanes (density) hr/km2/month | 3) Distance to grid points Km | 4) Water depth m | 5) Wind speed m/s | 6) Slope degres |
|---|---|---|---|---|---|---|---|
| 0 | Unacceptable | 0-10 and 65-100 | > 0.1 (with a buffer of 0.5 km each side) | > 80 | 0-50 and > 1000 | 0-5 | > 20 |
| 1 | Bad | 10-15 and 50-65 | - | 70-80 | 50-60 and 800-1000 | 5-6 | 10-20 |
| 2 | Suitable | 15-20 and 45-50 | - | 60-70 | 60-80 and 500-800 | 6-7 | 7-10 |
| 3 | Good | 20-30 and 40-45 | - | 50-60 | 80-100 and 350-500 | 7-9 | 5-7 |
| 4 | Excellent | 30-40 | 0-0.1 | 0-50 | 100-350 | > 9 | < 5 |

**Figure 2.3:** Example of criterias used for WPP site selection, with corresponding thresholds for different grading.

After grading the area in colors according to certain thresholds for each specific criterion, this has resulted in the following maps seen in a-e in the figure 2.4. However, it is important to note that, in general, all the criteria might not be equally critical for the success for the project. Therefore, before assembling the final map, the criteria are weighted against each other. This weighting is often done by the site developer and is therefore based on individual or company-specific preferences or experience and learnings from earlier projects.

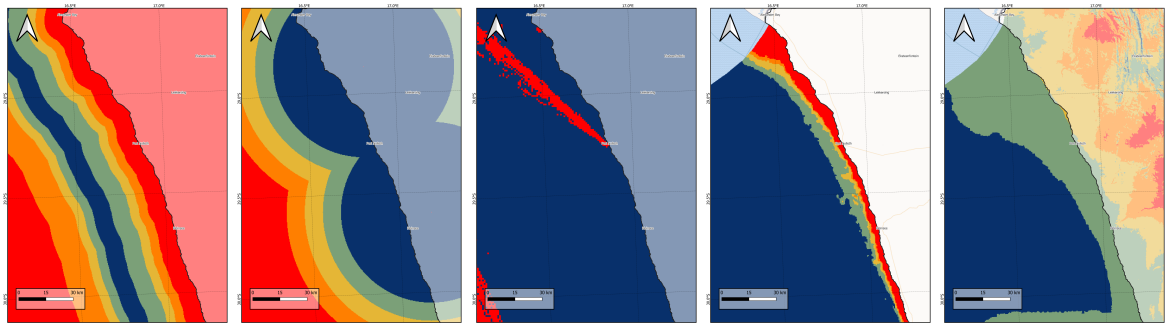

**(a)** Coast proximity. **(b)** Grid proximity. **(c)** Shipping lanes. **(d)** Bathymetry. **(e)** Wind conditions.

**Figure 2.4:** Maps including site selection criterias.

After taking all criterion's into consideration, the maps are combined into a final map of the wind power potential in the area, which can be seen in figure 2.5a, which is then converted to a more general version seen in figure 2.5b. The green area in this figure is considered a good location, while the blue area in this figure corresponds to excellent conditions. The blue area has a theoretical potential of more than 26 GW of floating wind power production. In addition, Hexicon also proposed a suitable area for a potential 900 MW wind farm, which can be seen in figure 2.5b.

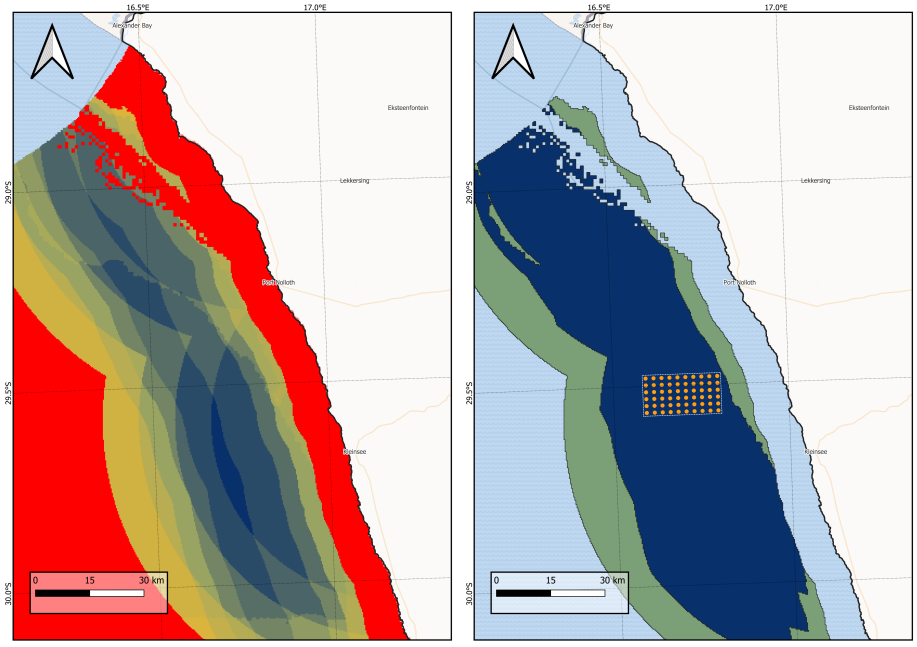


**(a)** Overlaid map. **(b)** Best zones.

**Figure 2.5:** Maps including site selection criterias and a proposed 900 MW WPP.

After choosing the area and size of the potential wind farm, Hexicon performed simulations to obtain an annual electricity yield from the WPP. The results of this simulation can be seen in figure 2.6, as well as a zoomed-in version of the proposed 900 MW WPP seen in figure 2.5 b. As can be seen in the figure, the turbine size is chosen to be 15 MW, with a column spacing of the rotor diameter multiplied by a factor of 9.15, and the row spacing with 7.95, which results in the spacing seen by the dots of the figure. These key characteristics ultimately result in a capacity factor (CF) of 55.84% for the entire WPP, with a wake loss of 5.57%. The concepts of losses and CF are explained in more detail in Sections 3.2.3 and 3.2.6.

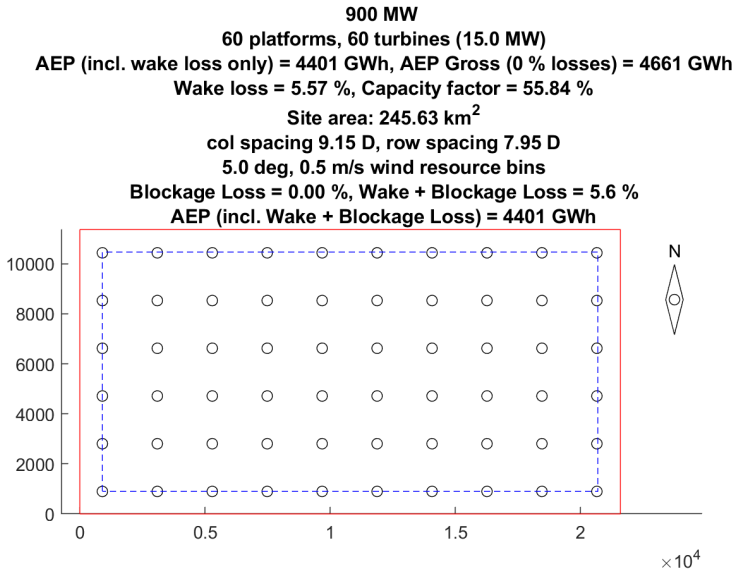


**Figure 2.6:** Results from Hexicons simulation of annual energy yield from a 900 MW WPP.

Apart from Hexicons work on the wind power potential for the area, the potential for solar power is investigated. As can be seen in Figures 2.7 a and b, the Port Nolloth area has an excellent solar power potential. The combination of excellent irradiation conditions, which can be seen in Figure 2.7 a, as well as the open landscape seen in Figure 2.7 b. makes the location close to ideal. In the figure a yearly generation of 2100 kWh/KW installed capacity is seen (with the maximum earth conditions for reference being around 2400kWh/KW at sea). Dividing this with the maximum possible power generated for the full year gives a capacity factor (CF) of 2100/8760 =0.24. However, there are more criteria that are included for the site selection work for SPP:s, which is described more in detail in Section 3.1.3.[14]

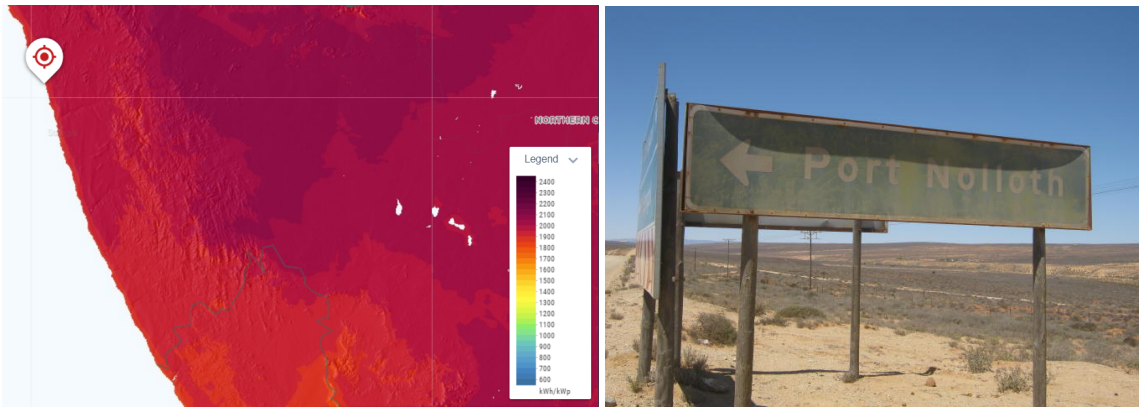


**(a)** Solar irradiance for the Northern Cape region.

**(b)** Landscape outside of Port Nolloth.

**Figure 2.7:** Solar irradiance and landscape in the Port Nolloth area.

## 2.8 Tools for P2X Simulation

When simulating a P2X system, a couple of software tools can be used. These inlude the OpenModelica software, the Renewable Ninja website, as well as Wind and Solar atlases.

OpenModelica is a free, open-source software that is great for modeling and simulating all sorts of complex system. It is built around the Modelica language, which is perfect for handling physical models. OpenModelica lets you run simulations to see how systems behave over time, making it easier to evaluate different scenarios and optimize performance. The software comes with a library of pre-made components, so you don't have to start from scratch. It is also highly customizable, making it adaptable to various research needs. OpenModelica is therefore a very useful tool for modeling and simulating the P2X system, helping to assess and fine-tune the energy mix.[15]

Renewable Ninja is an online tool that provides detailed historical and simulated data for renewable energy production. It is particularly useful for getting high-resolution data on solar and wind energy. Using weather data from NASA and ECMWF databanks, Renewable Ninja lets you input specific locations and time ranges to get data output. This hourly data are especially valuable for in-depth simulations and analyses. Renewable ninja can therefore support the OpenModellica model with the valuable simulation-based data for input of wind and solar generation.[16]

Wind and solar atlases are more about giving you a broad overview of potential energy production across different regions. The wind atlas shows details like wind speed and direction at various heights, helping to identify prime spots for wind power installations. The solar atlas provides data on solar radiation, which is key for designing and positioning solar panels. Although Renewable Ninja offers hourly data for detailed simulations, these atlases are great for getting a general sense of renewable energy potential and geographic distribution. Using this can help to simulate models accurately that reflect the real-world potential of renewable resources.[14]

In summary, using a combination of OpenModelica, Renewable Ninja, and the wind and solar atlases allows to build a solid simulation framework for evaluating the P2X system.

# Chapter 3

# Literature Study

In figure 3.1, an overview of a P2X system can be seen, with the main components included. In general, the system consists of power generation from renewable sources, as well as power consumers such as industry, city, desalination plant (DSP), and hydrogen derivate production, storage, and export. A short-term ESS is also present to provide stability to the system, as well as to maintain the voltage in the DC grid. In this chapter, the components of a P2X system are studied in more detail, in order to give a background of the technologies that can be used in the system.

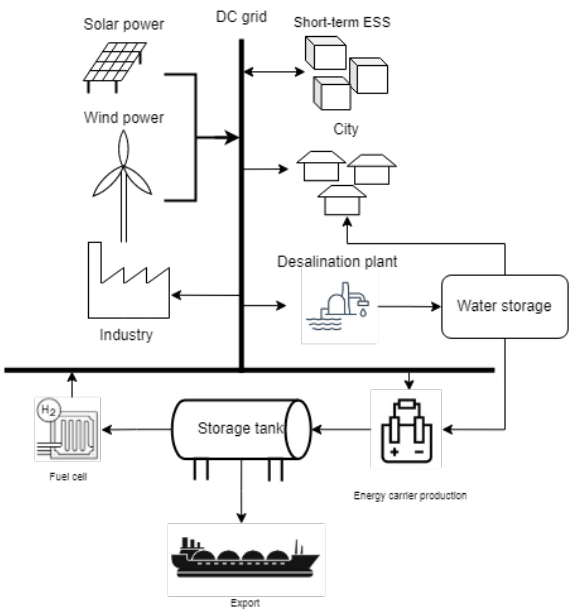


**Figure 3.1:** Overview of a P2X-system.

## 3.1 Photovoltaics

Photovoltaics play a key role in the generation for a P2X project, as seen in the P2X overview seen in figure3.1. Photovoltaic cells, or so-called solar panels, are made of semiconductor materials that convert light into electrical energy. The basic principle behind this can be seen in figure 3.2. The cell absorbs incoming photons from sunlight, and when semiconductor material has absorbed enough photons, electrons from the material's atoms are dislodged, which creates a flow of electrons, or a so-called current. Usually, panels are built out of small individual cells, each producing around 1-2 W, and are then connected in series to have a higher output voltage and power. [17]

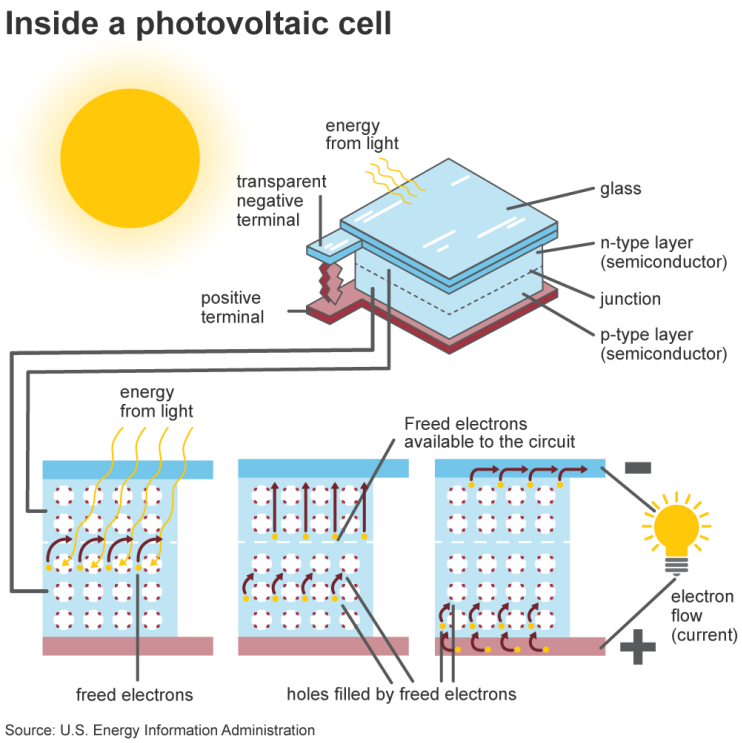


**Figure 3.2:** Structure of a photovoltaic cell.[17]

There are several factors affecting the solar panel output, and therefore its capacity factor. Firstly, the most obvious one is solar radiation. This is a measure of how many photons hit a certain surface on average, often measured in $W/m^2$. The amount of photons hitting Earth per surface area varies with latitude because the surface is hit from different angles. This makes the latitudes around the equator prone to have the highest solar radiation on Earth. In figure 3.3, a world map of a yearly average solar radiation can be seen. The figure makes it clear that the radiation is dependant on the latitude but also on area-specific weather patterns.

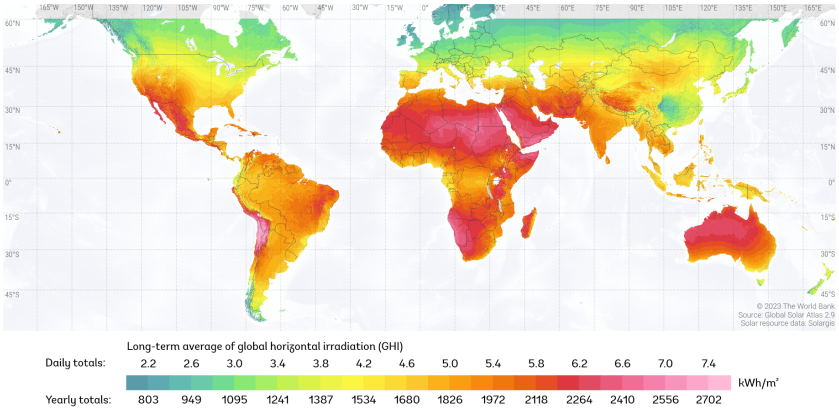


**Figure 3.3:** Caption

Temperature is another important factor affecting solar panel efficiency, as is often the case with many other semiconductor devices. If the solar panel performance is normalized around 25° C, the efficiency of the solar panel can decrease by up to 0. 5 % per degree Celsius when the temperature of the solar panel increases. The last major factor is the so-called "soiling", which includes the accumulated dirt, dust, and other contaminants on the solar panel. Depending on the type of soiling, the annual production could decrease by 5-17 %. Other factors that affect efficiency could be internal parasitic resistances, natural degradation, and the fill factor. [18]

In figure 3.4, the rapid increase in installed capacity photovoltaics can be seen. This development is clearly seen in the price drop of LCOE for photovoltaics as well. The LCOE of large-scale desert-based photovoltaic panels gives an estimate of 0.03 cent per kWh by 2030.[19] The CAPEX for a utility-scale photovoltaic system including the necessary electrical infrastructure, which is described more in detail in Section 3.1.4. The CAPEX for installed polycristalline photovoltaics are estimated to be around 500 000 $/MW for year 2035 [20], with an estimated OPEX of 13 000 $/MW/year. [21]

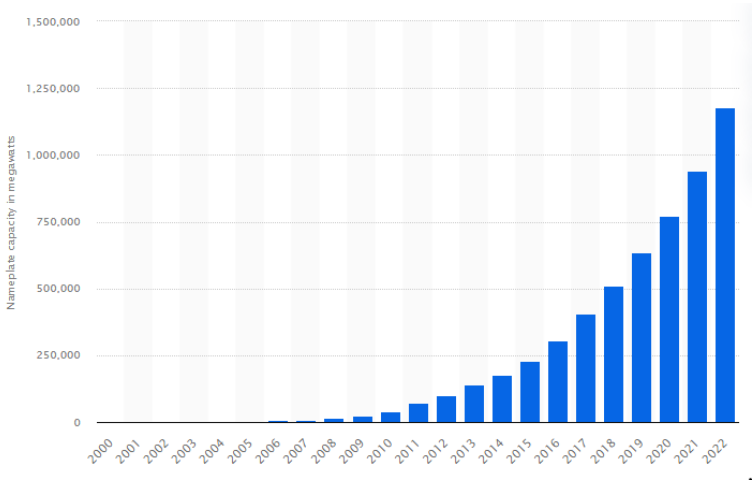


**Figure 3.4:** Development of global installed capacity of photovoltaics from year 2000-2022, measured in installed MW.

### 3.1.1 Capacity Factor

The capacity factor of a solar panel is defined as the relationship between the actual output of the SPP over a certain time period, often a year, compared to if it would have produced with its peak capacity during that time period. The equation for a yearly capacity factor can be seen in equation 3.1, where the actual yearly output of the SPP is divided by the number of hours in a year multiplied by the rated power capacity of the SPP. The capacity factor usually ranges from 10-25% [22]. The capacity factor is affected by several factors, the amount of sunlight hours, solar irradiance, as well as electrical losses, to name a few. These are described in more detail in Section 3.1.4.

$$CF = \frac{Actual\ output\ (Wh/year)}{24\ (hours/day) * 365\ (days/year) * P_{rated}\ (W)} \tag{3.1}$$

There are several different technologies that can be used for solar panels. The way most of the technology is being tested is by how much power they can generate under standard test conditions (STC). STC means that under lab conditions, an irradiance of 1000 $W/m^2$ is used, with a cell temperature of 25ºC. [23] Silicon-based solar cells currently represent 90 % of all photovoltaic modules sold on the market. These can further be divided into monocrystalline and polycrystalline with different advantages. Monocrystalline modules have higher efficiency, reaching up to 27.6%. However, they are more expensive because of the very precise manufacturing processes that are required to produce solar cells using the Czochralski process. Polycrystalline solar panels are generally slightly less efficient, with a maximum efficiency up to 23.3%. However, they are more cost-effective as manufacturing process is cheaper. There are also different alternatives to this technology that have recently made technological advancements. These are called second- and third-generation solar panels, and consist of perovskite, nanocrystal, and multijunction solar cells, to name a few examples. These new technologies have shown promising results in controlled environments, with efficiencies ranging from 18% up to 46.7%. However, more demonstrations and tests need to be performed before it can be commercialized.[24]

An effect of the efficiencies is that, logically, panels with higher efficiency utilizes less space to generate the same amount of power. For example, if the monocrystalline solar panel has an efficiency of 27.6% under STC, it would theoretically produce $1000W/m^2 * 0.276 = 276Wp/m^2$, which means that an array would need $1000/276 = 3.62m^2$ to produce 1000 W. For a polycrystalline solar panel, it would produce $1000W/m^2 * 0.233 = 233Wp/m^2$ which would give an area of $1000/233 = 4.29m^2$ instead.

Some areas are more suitable for solar panels than others due to several factors. In figure 3.5, a global map with the photovoltaic potential is shown, taking the horizontal radiation, temperature, and tilt angle of the panels. For example, looking at the marked area around Mongolia in figure 3.5, the area shows relatively good conditions. However, looking back at figure 3.3, where the global horizontal radiation (GHI) is shown, the GHI for the area is not as good as Brazil's GHI for example, but Brazil still has a lower PV potential than Mongolia when looking at figure 3.5 due to factors such as temperature.

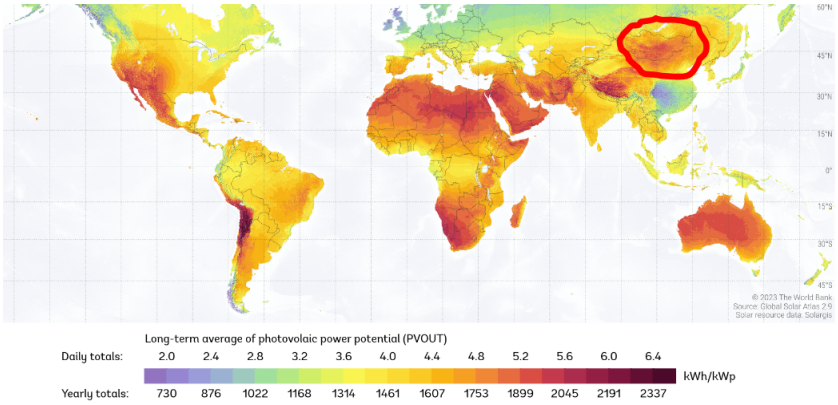


**Figure 3.5:** Global map of PV potential measured in kWh/kWp.

### 3.1.2 Ecological Impact and Area Usage

Usually, land use is considered to be one of the most significant environmental impacts of solar power plants. However, this can vary significantly because it is highly dependent on the location and placement of the solar panels. For example, solar panels can be placed on buildings and residential homes where they do not contribute to negative land use. However, if the land needs to be cleared or graded, it could have a significantly negative environmental impact on the area. There are also examples of locations where solar power plants are not considered to have a negative impact on land use. These could for example be deserts or dry scrubland, which both are excluded in the category "land competition" from a study published in Nature named "The potential land requirements and related land use change emissions of solar energy". [25]

However, photovoltaics are very efficient when it comes to production per unit of area of affected land in terms of W/m2 compared to other generation technologies. The shading and coverage of the panels can have both a positive and a negative impact on the ecosystem. An advantage could be that shading allows for possibilities for growth or animal protection, which is seen in agrovoltaic technology used in combination with agriculture.[26] Placing the panels will require foundation support, which will have a local impact on the landscape.

Another major environmental impact of solar panels comes from the mining of some of the materials that are needed in many of the photovoltaic panel technologies. For example, some photovoltaic technologies consist of toxic metals such as lead and cadmium, which can cause great harm to humans and the environment if it is leached into groundwater. The production of the PV modules themselves is also an energy intensive process that is associated with $CO_2$ emissions. [27]

### 3.1.3 Site Selection

When deciding upon a location for a large-scale SPP, it is important to consider the logistics for installation, cables, and decommissioning. The flat topography also makes the installation process easier and less visible to passing residents. Panel placement should also be done with the largest possible distance from other operating stakeholders as it facilitates the permitting procedure. The location is also favorable, with low shading and a stable underlayer to avoid erosion. The plant should also be placed as close to the consumer as possible to minimize the cost of cabling and losses.

For optimal performance, it should also be placed where the mean temperatures are within the limits discussed above. For example, along the shoreline of a desert is an optimal climate for this, as the ocean is constantly cooling/heating the nearby inland climate. This also makes the park more accessible for construction and maintenance, as most towns are along the coast. Cloud formation is more frequent along the coast, making site selection more complex. Closer to the ocean, the faster corrosion processes occur because of the ion concentration in the air. It is therefore important to save some clearing distance and at no risk to have direct contact with sea water. Furthermore, it is important to consider the landscape impact as discussed in the section above, where the panels should not be placed in protected areas, and if it affects ecology it should try to be done in a positive manner. To limit the impact of local cloud coverage, the park should be divided into multiple segments. But the more subparks, the harder permitting, installation, and maintenance will be, which often results in an optimal location. [28]

### 3.1.4 SPP Configuration

When an SPP is constructed, there is a lot of electrical infrastructure other than the photovoltaic panel itself that needs to be put in place. In figure 3.6, an example of the configuration of an SPP can be seen, which is an extension of the SPP branch in the P2X overview in figure 3.1. The figure also displays the electrical losses that are associated with every component, not including other losses mentioned previously such as degradation, soiling, temperature, etc. As the figure shows, it starts with solar irradiation reaching the SPP. The PV panels then convert solar irradiance to DC power with a technology-specific efficiency. The panels are all connected with DC cables to a DC/DC step-up converter that increases the voltage to ultimately reach a DC grid. All of these different steps are associated with losses and efficiencies, with a magnitude of around 23% for the efficiency of the PV panels depending on the technology being used as previously discussed in Section 3.1.1, 1% losses from cabling and 3% losses from the converter [29]. To give an example, if a certain SPP location had a GHI of 1000 $W/m^2$ on a sunny day, the actual electrical output would be $1000 * 0.23 * 0.99 * 0.97 = 221 W/m^2$.

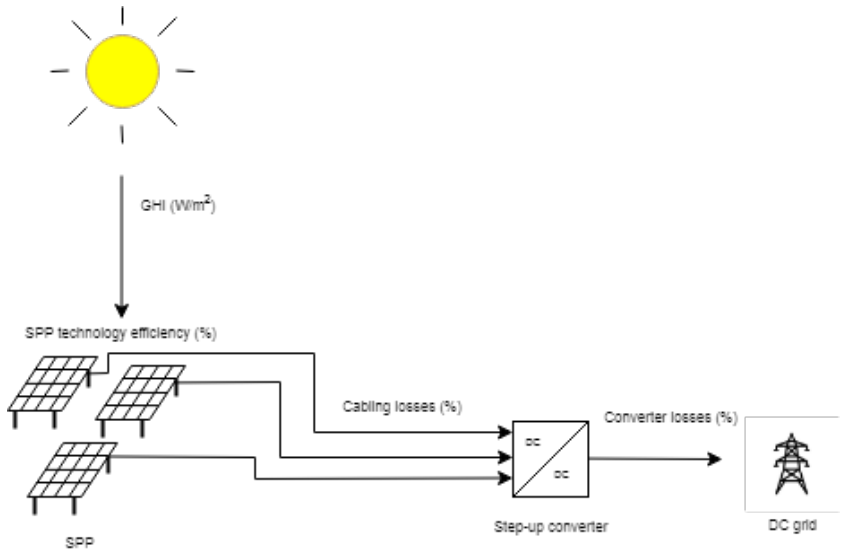


**Figure 3.6:** SPP configuration drawing.

## 3.2 Wind Power

Wind power generation play a key role for for a P2X project, as seen in the P2X overview seen in figure3.1.The principle of producing electricity from wind turbines is based on harnessing the kinetic energy from the wind, creating a lift force on the wind turbine blades, which makes them rotate because of the way they are angled. The blades are attached to a drive shaft which is connected to the rotating part of a generator that generates electricity. [30]

The wind power industry has witnessed a major expansion for the last 20 years, seeing around 17 GW installed capacity in the year 2000 turn into 899 GW in 2022. [31] This expansion has been made possible due to several factors, including technological advancements, policy making, and streamlined supply chains.

The general trend in the wind power industry has been to increase the size of wind turbines. This is due to the relationship between power production and wind characteristics. The output of the wind turbines is proportional to the swept area of the blades and the cubed wind speed. Therefore, these characteristics are pushing the industry to create larger turbines with a larger swept area and higher towers. In addition, the unit cost of the foundation and licensing processes is at the moment relatively high, which makes it unrealistic to scale linear.

### 3.2.1 Offshore Wind Power

The wind power industry is divided into two different categories, offshore and onshore, where onshore wind was dominant in the past. Looking back as far as the late 1800s, the first electricity-generating wind turbines were installed with a capacity ranging from around 5-25 kW per turbine mainly to power lamps, batteries, and electrical tools. [32] Nowadays, most onshore wind turbines are built with a capacity of a couple of megawatts. Onshore

wind power is one of the least expensive forms of renewable energy, along with solar PV, as it is installed relatively easily and quickly and is easy to perform O& M on.

Offshore wind farms, on the other hand, are a newer concept in the wind industry. The first offshore wind farm was built in Vindeby Denmark in 1991. Those days, the turbines had a capacity of 0,45 MW each, resulting in a total of 4.95 MW for the 11 turbine wind farm. [33]Since then, the turbine sizes has increased and today the largest turbines being built are up to 16 MW each. More than 3 times greater than the whole farm in Vindeby, Denmark. As mentioned above, there has been an apparent trend in the wind turbine industry to increase turbine sizes, and it is projected to increase even more in the future. [34]This trend is advantageous for offshore projects, as they can include larger components than onshore due to logistical and transportation reasons in the project installation phase.

There are several pros and cons of both onshore and offshore wind generation. Onshore generally has a lower cost and faster installation than offshore, since installation of turbines offshore requires larger components, investments, and more expensive O& M. However, there are several pros with offshore wind to compensate for this. First, the quality of the wind is better offshore, as the wind speeds are higher and less turbulent than inland, which increases the capacity factor. To harness these better winds, larger turbines can be used than onshore due to the fact that the offshore turbines are not as size limited as the ones onshore. The main cause of this is that they can be shipped and installed on site and that they do not face the difficulties of transporting the components to onshore sites. As mentioned above, the industry trend is to design larger turbines, which is beneficial for the offshore industry. Another important advantage is the fact that offshore wind farms are not as space-limited and disturbing to people as onshore wind farms, making it easier to obtain permits for the project. [35]

### 3.2.2 Floating Wind Turbines

Traditionally, the technique used for foundations in the offshore wind industry has been technologies such as monopile, jacket, and gravity foundations. These have been used because of their simplicity and cost effectiveness, and have been selected according to different depths and type of seabed. However, fixed foundations come with limitations, the two main ones being different seabed conditions and water depth. Each fixed foundation type has different geological constraints, such as for example monopile foundations not being suitable for shallow bedrock etc. [36] Regarding the depth limit, there are discrepancies in the economic viability and the technical possible water depths. Research diverges on discussions regarding the economically viable depth limits for fixed foundations. According to a report by the European Wind Energy Association, an economically viable depth limit of approximately 50 meters is suggested for fixed foundations. Beyond this threshold, floating foundations are becoming increasingly economically feasible. [37]

Like fixed structures, there are different types of foundations for floating wind. Under development, there are three main concepts ; the Spar-Buoy, Spar-Submersible as well as the Tension Leg Platform, which all can be seen in figure 3.7. Depending on the developer and

the site conditions, the most suitable option for the specific area is chosen depending on the depth, geological conditions as well as the steepness of the depth.


**Figure 3.7:** Illustration of three different floating wind power foundation concepts.

As floating fundaments are not economically feasible today on a commercial scale, it is difficult to forecast the prices. To be competitive on the market, the price cannot deviate too much from today's price for WPP:s with fixed foundations. The LCOE of a large offshore WPP electricity production gives an estimate of 0.054 $/kWh at today's prices. [38] Furthermore, the CAPEX and OPEX for a floating offshore wind park are 5.21 M$/MW installed for CAPEX, and 89 000 $/MW/year for OPEX [39] For a WPP with fixed foundations, an estimate of the CAPEX is instead 2.39 M$/MW for near-shore turbines which is the price floating wind needs to be comparable with to be profitable at large scale expansion. [40]

### 3.2.3 Capacity factor and Available Energy

As mentioned in the photovoltaic section, the capacity factor is a measure of how much power the source generates in relation to its rated output over a certain period of time, according to the formula in equation 3.1. In figure 3.8, the average capacity factor for conventional offshore wind farms worldwide can be seen. As can be seen in the figure, the capacity factor oscillates from year to year around an average of approximately 40%. However, most large-scale projects today aim to have a CF greater than 50%.

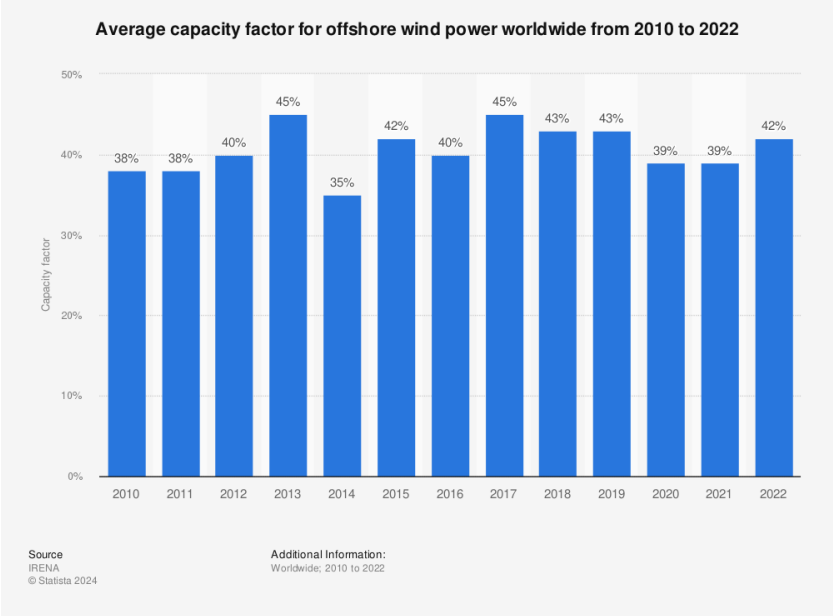


**Figure 3.8:** Average capacity factors for offshore WPP:s worldwide, constructed between 2010-2022. [41]

However, floating wind projects generally have a higher capacity factor. For example, the Hywind Scotland project, one of the first commercial floating wind power plants, has an average capacity factor of around 57.1%.[42] This particular WPP only consists of 5 turbines, meaning that the wake effects are lower than for large-scale WPP:s with, for example, up to 100 turbines, which makes the comparison a bit unfair. However, in general, the fact that they can be deployed further from shore means that the winds are generally stronger and more consistent, which contributes to a higher CF. In figure 3.9, a world map with average wind speeds can be seen. Here, the wind speeds differ depending on location due to several factors such as latitude, elevation, etc. In the case of wind power, wind speed is obviously an important factor for the capacity factor, but also the consistency of the winds.

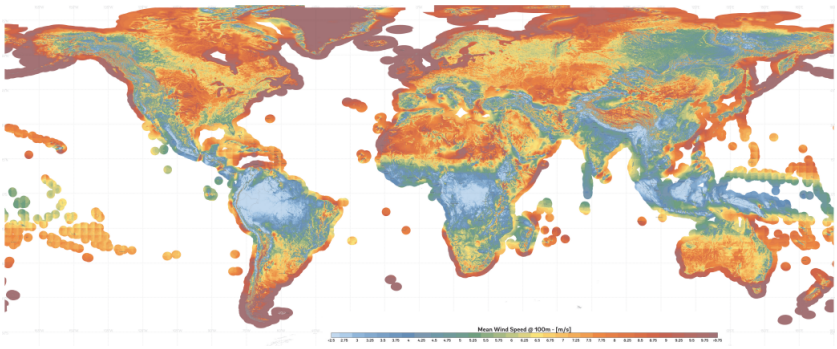

**Figure 3.9:** Global wind atlas displaying mean wind speeds (m/s) at 100m elevation.

When the wind turbine converts the wind energy into power, it follows a so-called wind power curve. The curve is technology-specific and is different for different turbines. In figure 3.10, an example of a wind power curve is shown. The figure shows the expected amount of power that the turbine should produce for a certain wind speed. The wind speeds from which the turbine starts and stops generate power are called the cut-in and cut-out wind speeds. The cut-in wind speed is logically the lowest wind speed required for the turbine to produce electricity, whereas the cut-out wind speed is the wind speed where the turbine needs to be "turned off" because of the risk of damaging the turbine.

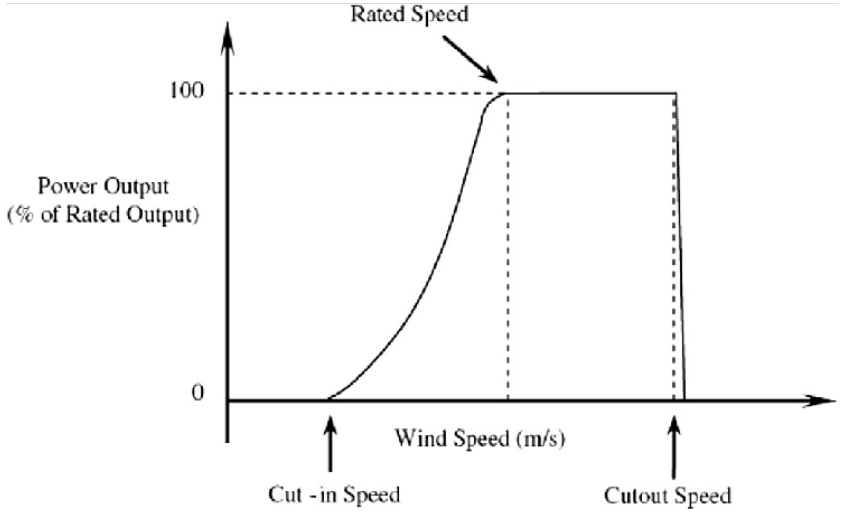


**Figure 3.10:** Power curve displaying power output as percentage of rated output, as a function of wind speed in m/s. [43]

### 3.2.4 Ecological Impact and Area Usage

The environmental impacts of floating wind power turbines are mainly associated with the carbon footprint of steel production, which in an electricity production context is relatively low. However, other environmental concerns, such as the impact on marine life, have yet to be investigated further. As floating wind turbines are a quite new concept, there have been few studies on the impact of marine life. [44]

### 3.2.5 Site Selection

The site selection process for wind turbine installation includes considerations similar to the solar power site selection process, with some major differences. In general, site selection work is done as described in Section 2.7.2, where Hexicon has worked on the site selection for a floating WPP in Port Nolloth, just outside of the coast of South Africa. Usually, the process is extensive and takes many different factors into account, such as, water depth, distance to grid connections, and wind speeds to name a few for offshore WPP:s. However, the criteria vary between the type of WPP that is going to be constructed whether it is offshore with

fixed or floating foundations, or onshore wind turbines. For example, in Hexicon's work for a floating WPP, excellent water depths were considered to be 100-350 m according to figure 2.3. However, as previously mentioned in Section 3.2.2, the economically viable depth limit for fixed foundations is at the moment 50 m, which makes the site selection different. Another considered criterion in the onshore WPP site selection is the logistics of how to transport the wind turbine parts to the site, which is not considered as much in the offshore site selection due to the fact that the turbines are transported by vessels. Another, criterion applicable for all of them is the proximity and size of the nearest port. Most wind turbine components are manufactured in different parts of the world and, therefore, it is important to have a port nearby that is large enough for the vessels that ship the components to the site. More details on the importance of ports are described in section 3.4.3

### 3.2.6 WPP Configuration

When an offshore WPP is constructed, there is a lot of electrical infrastructure that needs to be put in place. In figure 3.11, an example of the configuration of an offshore WPP can be seen, with all its main components. This figure is an extension of the WPP branch seen in the P2X overview in figure 3.1. As the figure shows, it starts with the wind reaching the turbines, which converts the wind energy into AC electrical power when rotating, with a turbine-specific efficiency depending on the wind speed. When the wind faces the blades and they start to rotate, they create turbulence behind them. This phenomenon is called the wake effect. Depending on the size of the WPP and the placement of the turbines, the wake effect decreases the power output of the turbines behind. The power then reaches a transformer that increases the voltage, to then reach a rectifier that converts it to DC, and transported to land with HVDC cables. The power is finally converted back to AC and injected to the grid, which in this case is AC. All of the steps described above are associated with losses that all affect the overall CF of the WPP.

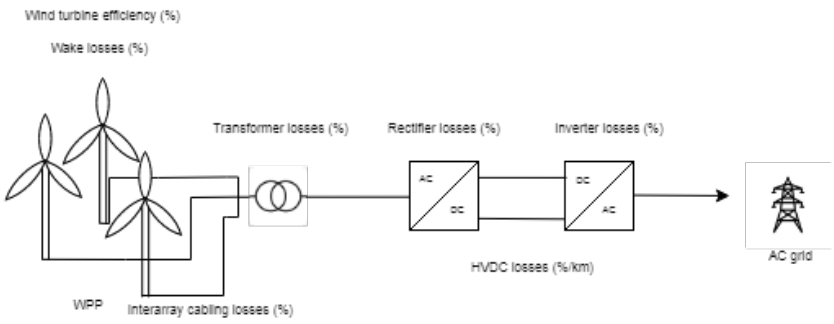


**Figure 3.11:** WPP configuration drawing.

## 3.3 Local Energy Usage

Local energy usage is a key component of a P2X setup, as seen in the P2X overview from figure3.1. Apart from the processes involved in the production of the energy carrier, people working in the industry will constitute a consumption of electricity for the society to operate. For a remote large-scale P2X project with many people involved working in the industry, a smaller village would need to be formed around the P2X industry. The society would then need power and heat for residential buildings, schools, healthcare, entertainment, waste management, and other non-elastic services. In addition, if the location is close to the coast but does not have access to freshwater for residents and agriculture, a desalination plant (DSP) would be needed. This is further presented in Section 3.7.

The energy demand from society logically varies depending on the time of day. In figure 3.12, an example of a load curve is shown where the energy demand is plotted at an interval of 15 minutes. As can be seen, the demand varies such that it is lower during the night, when most people sleep, peaks in the morning when people wake up, followed by a decrease during the day when most people are at work, to ultimately increase during the evening, when people come home again.

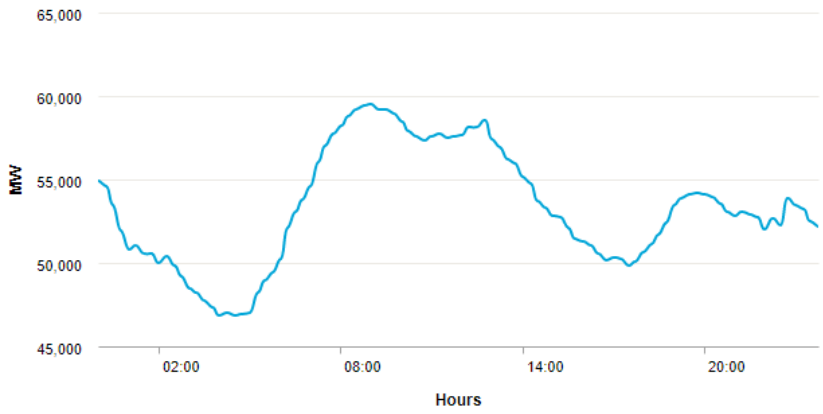


**Figure 3.12:** Example of a load curve (MW) from the energy demand in France 25/4 - 2024.

For a P2X location without a grid connection, this energy will come exclusively from electricity and possibly waste heat processes. The electricity is used directly from generation, from short-term ESS, or generated through the use of a fuel cell. As mentioned above, the energy demand is inelastic and is essential to work at all times. If the power generation source is from renewable sources, the short-term ESS is of great importance.

### 3.3.1 Energy Usage Configuration

In figure 3.13, a configuration for local energy usage around a P2X project can be seen, which is an extension of the city and industry branch in the P2X overview seen in figure 3.1. In this case, there is a DC grid that provides both residential buildings, seen in the upper right part in figure 3.13 and industries in the lower right part in the figure. A step-down DC/DC converter is needed to lower the voltage from the high voltage grid side, to a lower voltage at the consumer side. This step can be assumed to generate similar losses as for the SPP of around 3 % for the converter, followed by cabling losses between the converter to the consumer of 1%. [29].

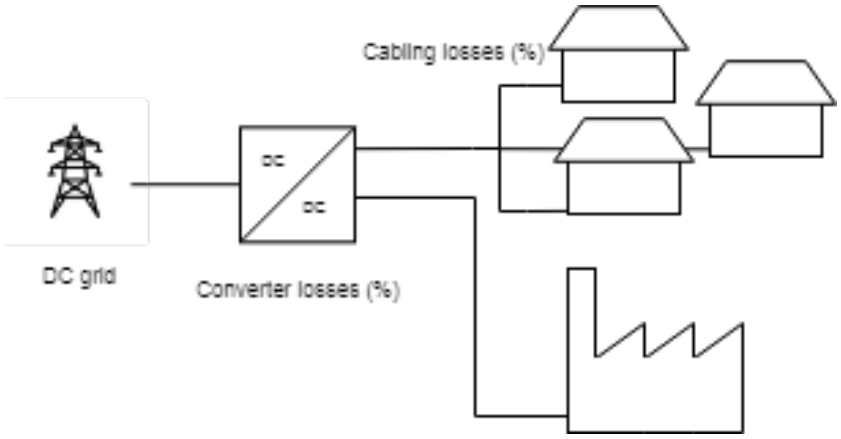


**Figure 3.13:** Local energy usage configuration drawing.

## 3.4 Energy Transport

In a P2X system, energy is transported between the main components in the form of electricity and hydrogen, which requires substantial infrastructure. Energy transport is a key component of a P2X setup, as seen in the P2X overview in figure3.1.

### 3.4.1 Electrical Infrastructure

First of, to connect all main components in the DC system, cables are needed. High-voltage direct current (HVDC) cables transmit electricity using DC over long distances. The cable consists of conductive materials enclosed in insulating layers. Today, HVDC cables are especially used for long distance subsea applications, where AC connections require power stations for voltage regulation and are less efficient exceeding distance of 25km subsea. [45]

For the cables, the CAPEX is 700 000 $/km for land-based transmission cables [46]and 3 120 000$/km submarine cable [47]. With very low OPEX values for cables , they can be assumed to be included in CAPEX costs for 30 years of operation.

In addition, different AC/DC and DC/DC converters are needed in the system, as different appliances use different voltages and technologies. An AC/DC converter transforms the alternating current (AC) from a power source to direct current (DC) for electronic devices, using rectifiers to convert the waveform. A DC/DC converter adjusts the voltage level of direct current (DC) to match the requirements of different devices, utilizing switches and inductors to regulate voltage.

The losses of transport of electrical energy are given according to equation 3.2. Here, the current (I) squared multiplied with the cable resistance (R) is equal to the losses (P) that occur when power flows through a cable.

$$P_{losses} = I^2 * R \tag{3.2}$$

### 3.4.2 Pipelines

The chemical energy carrier will be transported to consumption/offloading units as well as storage facilities through the use of pipelines. These pipelines typically consist of steel tubes, often coated internally to prevent corrosion. In addition, compression stations along the pipeline route maintain pressure, ensuring that gas flows efficiently. By maintaining the pressure of the storage unit, the pipeline itself can be seen as a part of the storage facility. Leakage prevention measures such as pipeline monitoring and maintenance are crucial because of the small molecular size of the energy carriers, such as hydrogen gas for example. [48]

### 3.4.3 Shipping Logistics

For a large-scale P2X system, shipping logistics plays a key role. Both for the cause of importing and exporting. In the installation phase of the P2X project, the ability to import components by shipping is often essential due to both the large size and the dispersed supply chains of many components for the construction and maintenance of the P2X plant. If a society formed around the P2X location, goods for residents would also need to be imported by ship.

If the main purpose of a large-scale P2X project is to produce chemical energy carriers mainly for export, shipping plays a key role here as well, due to the large volumes of chemical energy carriers being produced. To give an example of possible sizes, if the P2X project had the capacity of 1 GW constant ammonia production, its weekly production would be $1 * 24 * 7 = 168 GWh$ worth of ammonia. An example of a medium-sized ammonia carrier, which is also fueled by ammonia, is able to carry up to 40 000 $m^3$, which equals around 10 400 tonnes of ammonia. [49] To translate this weight to how much energy this holds, equation 3.3 is used, where the weight is multiplied by the amount of kWh/kg ammonia has, times an efficiency of about 70 %, which ultimately leads to the result of 37.8 GWh.

$$10400000kg * 5.2kWh/kg * 0.7 = 37.8GWh \tag{3.3}$$

This means that if ammonia were to be exported by a carrier of that size, it would need to fill up 168/37.8 = 4.4 times a week on average.

### Port

When shipping logistics plays a key role in many P2X projects, a port is needed. The port needs to have all the necessary facilities to be able to load and unload arriving ship during construction, operation, and decomissioning. The size of the port that needs to be built (if it does not already exist) obviously varies with the scale of the project. A port in a deep-water harbor with good conditions costs around 16 M$ for 300 m of berth [50], which would be large enough for the medium-sized ammonia carrier mentioned in the previous section. For the size of the port, careful calculations need to be made, taking many factors into account. For example, if the port is dimensioned for the largest planned ship in the world, carrying 93 000 $m^3$ of ammonia [51], the port needs to be larger, which is more expensive, and the P2X project also needs to have larger dimensioned ammonia storage on site, since the carriers would not come as often as for the example with the medium-sized carrier mentioned in the previous section.

## 3.5 Short-term ESS

The short-term energy storage system (ESS) plays a key role in a P2X setup, as seen in the P2X overview in Figure3.1. In a P2X project, Power stability through voltage regulation is of outmost importance, to not risk affecting production capacity by damaging power electronics and other important components, which will be met through the use of short-term storage. The storage technology will therefore account for voltage regulation, delivering a stable voltage for the high voltage DC grid. The technology is also used as peak shaving, where surplus from full production exceeding production capacity or expected average for the coming hours is stored and later used when the production is insufficient. For large-scale application voltage regulation, the most feasible options are batteries, due to their cycle of life, efficiency, and production costs. New battery technologies are also very applicable for deep discharges as well as quick responses. [52]

Battery development has up until now not been for stationary use, but has been developed for a mobile industry focusing on small devices and transportation, as well as in other space-restricted areas. But for a sustainable future, the technology is relevant in all over the world. For many P2X projects, maximum discharge possibilities and efficiency are much more important than mobility and space, whereas options not mentioned in other areas of research can be relevant.

### 3.5.1 Short-term ESS Configuration and Losses

In figure 3.14, a configuration drawing of a short-term ESS can be seen for a P2X project. This is an extension of the Short-term ESS branch in the P2X overview in figure 3.1. The power flow in this setup is bidirectional, which means that the ESS can both charge and discharge into the DC grid in this case, via a DC/DC converter that increases the voltage flowing to the grid side and decreases the voltage when flowing to the ESS side. All of these steps are associated with losses, such that charging the ESS from the DC-grid generates overall losses of 4% in one direction, including converter losses, cabling losses, and internal ESS losses. When discharged back, this means 4% losses again, which gives a round trip efficiency of $0.96 * 0.96 = 92.2\%$. However, internal losses are technology specific, and in this example taken from a BESS. [53]

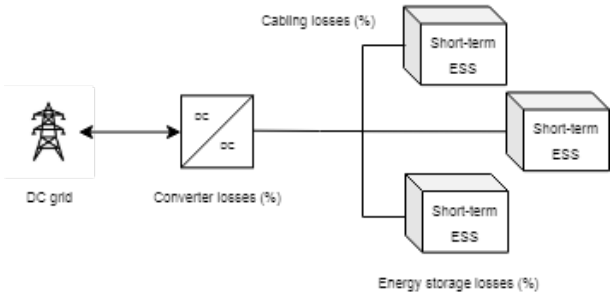


**Figure 3.14:** Short-term ESS configuration drawing.

### 3.5.2 Lithium Ion

The most developed and rapidly growing battery in the last 10 years has been lithium ion batteries (LIBs). Lithium-ion batteries operate by transferring lithium ions between the positive and negative electrodes during charge and discharge cycles. This process involves lithium ions moving from the positive electrode (cathode) to the negative electrode (anode) during charging and then back again during discharging, generating an electrical current through chemical reactions on the respective electrodes. Lithium-ion batteries are a great choice for storing energy on a large scale because they are much more efficient at charging and discharging, last a long time before needing to be replaced, and are economically viable. Therefore, most similar project requiring frequency regulation and peak shaving for rapid changes in production from wind and solar is currently using lithium batteries. [52]

The fact that the sector has been embracing this technology and made quick technological advancement has made lithium batteries a good all-around reserve for multiple industries. Lithium batteries have fallen 90% in price during the last decade, and the cheapest technology is expected to be reduced from 2023's 139 to 80 $/kWh by 2030. However, in this stage of development, it is not a matter of pervasive technological advances but rather a matter of the mineral prices used in the processes. [54][55]

The following problem of the high demand for lithium batteries is the possibility of lithium

scarcity. A green future requires large volumes, which could make a less energy dense metal reaction more applicable, such as sodium batteries, using the same technology but with much lower energy and power density. Although whether lithium scarcity is a future problem or not is heavily debated as new reservoirs are explored continuously, mentioning the option where there is no space restriction is relevant. [56]

For the application of the lithium ion battery in a P2X project, the forecasted CAPEX can be seen in figure 3.15. This figure shows the forecasted CAPEX for three different examples of lithium ion batteries that have a discharge time of 2, 4 and 6 hours, respectively. The CAPEX differs between the three due to that the faster the batteries is able to discharge, the higher rated power output it needs to have, which makes it more expensive. The figure also shows a steady decline in CAPEX until 2050 for all battery alternatives presented.

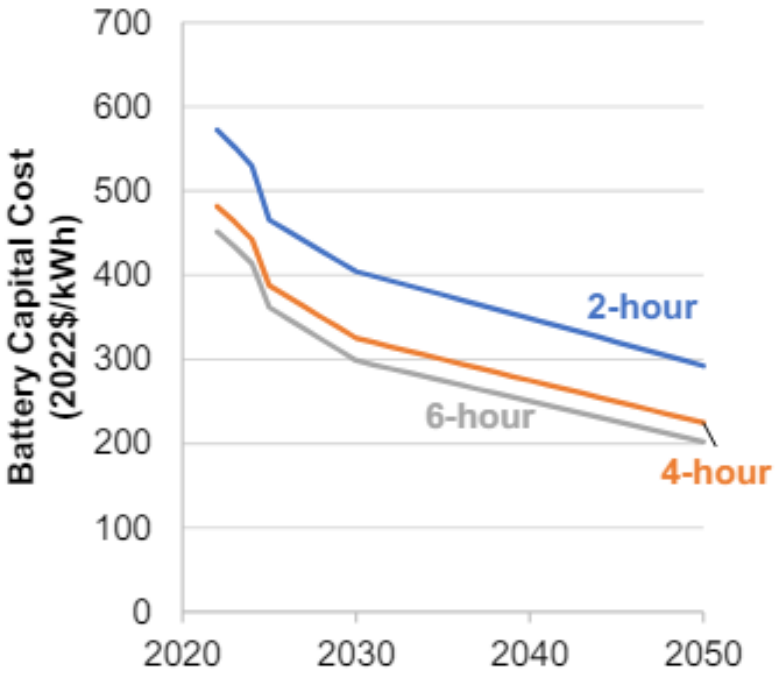


**Figure 3.15:** CAPEX BESS. [57]

As lithium batteries are limited by their cycle life, it is important to consider this in the calculations. The CAPEX mentioned above are therefore valid for 5000 cycles of 75-25 discharge. [58] The OPEX for a BESS system is forecasted to be 2500$/MWh/year. [59]

### 3.5.3 Supercapacitors

When an application requires high power outputs, especially for stationary uses, an alternative is to use supercapacitors. Supercapacitors use a technology that is based on an electrostatic process. In this process, the energy is stored in a double layer procedure in contrast to lithium-ion batteries where chemical reactions occur which slowly degrade the capacity of the cell. Supercapacitors therefore have a much longer cycle life and tolerated a higher Depth of Discharge, as well as efficiency where near-no heat is generated because of low internal resistance from movement of ions. The fact that electricity is stored electrostatically further leads to a higher self-discharge rate of around 30% per month compared to 10 % for lithium-ion. Another advantage is that the supercapacitors have a lifetime of many more cycles with an expectancy of 500 000, meaning full charge and discharge 45 times a day for 30 years and a high energy efficiency of 99%.[60]

The main advantage of the supercapacitors for a P2X setup is that they allow for a much higher power density compared to lithium-ion, meaning that the storage unit can be charged and discharged much faster. This makes them very interesting for applications where extreme loads of energy are expected, which can happen when solar farms are suddenly cloud-covered. Meanwhile, the forecasted energy density for 2030 is only 100-200Wh/kg, which can be compared to lithium potential of 650 for 2030 Wh/kg. [61]The low energy density means that the ESS requires much more space, which for the applications of a P2X system rarely is a problem. This, in combination with the more diverse application of lithium-ion technology, makes investments in supercapacitors less attractive, which makes the LCOE much higher than for lithium-ion. With future increase of applications, it is although expected to decrease to 1500-3000 $/kWh for 2030. [61]

Studies have although shown that for similar application with expected short-term shortage, using capacitors is more viable per kWh installed as less energy needs to be stored to deliver the energy for the need, which means that a combination of the two technologies might be an option, where both very variable and static load occurs. [60]

## 3.6 Energy Carrier Production

Energy Carrier production is a key component of a P2X setup, as seen in the P2X overview in figure 3.1. For this masters thesis, hydrogen derivatives were investigated. Hydrogen is the simplest and most abundant element in the universe, composed of a single proton and electron. Hydrogen has a high energy potential, which makes it suitable as an efficient energy carrier in for example transportation and renewable energy sectors. The energy carrier can be used directly after production or processed further to be used as energy in a later stage. [62]

### 3.6.1 Energy Carrier Production Configuration

In figure 3.16, a more detailed configuration drawing can be seen of the energy carrier production branch in the system overview in figure 3.1. The energy production facility draws power from the DC grid, through a DC/DC converter, to produce the energy carrier with a certain efficiency. The product is then stored in a storage tank, which is nearly emptied when a ship arrives to export the product. The system also has a fuel cell installed, which produces electricity for emergency cases when the short-term ESS in the overall system is empty. The fuel cell then empties the storage tank to convert the energy carrier to electricity with some efficiency.

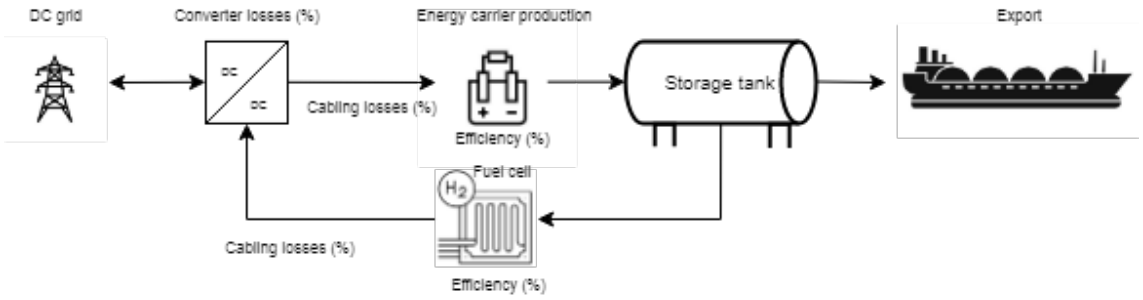


**Figure 3.16:** Energy carrier production configuration drawing.

### 3.6.2 Electrolysis

Today, hydrogen is conventionally produced through a steam reforming process, where natural gas is combusted in the presence of water and hydrogen. This process generates the so-called grey hydrogen, with the main disadvantage that the process emits carbon monoxide and is not considered sustainable. If the same process is used but the carbon emissions are stored underground, the product is called blue hydrogen. It is sustainable as long as the carbon is kept in the underground reservoirs. Therefore, limited research and pilot plants limit the possibilities. The third option is to create green hydrogen through the use of electrolysis. In electrolysis, desalinated water is decomposed into oxygen and hydrogen by passing electricity through the otherwise non spontaneous reaction.

There are three main electrolyzer technologies on the market, all of which have different properties and targeted applications.[63][64] In addition to these three electrolyzer technologies investigated in this report, there are other alternatives to these as well. For example, in China, an electrolyzer that can generate hydrogen from salt water is being tested. However, immature technology makes it impossible to use for P2X projects on a megascale, and therefore the electrolyzer needs freshwater input, either from a nearby reservoir or a desalination plant. [65]

### Alkaline

The alkaline electrolyzer is the conventional electrolyzer, as it has been used in the chlorine industry for several decades, although hydrogen-specific electrolyzers have been in construction for the last decade. The Alkaline electrolysis operates through the use of two platinum electrodes separated by a diaphragm, dividing the cell, where the water is reduced on one side and transporting one electron to the other side, where the hydrogen is produced. The technology is currently the cheapest on the market, although the need for a constant electricity supply makes it dependent on a large short-term storage system if it is integrated with solar and wind generation. [64]

Today, the Alkaline electrolyzer reaches an efficiency of 61 % with an ultimate target of 70%. The aim is to reach a production cost of around 2 $, with the aim of being competitive to gray and blue technologies in an unregulated market. Today, technology is ready to be used with a technology readiness Level classification of technology readiness level (TRL) 9 out of 10.[63]

### PEM

The Proton Exchange Membrane electrolysis (PEM) utilizes a solid proton exchange membrane to split water into hydrogen and oxygen using electricity. One advantage of the PEM electrolyser is that it is much more tolerant to variable energy input, which is preferable for renewable energy production from wind and solar energy, as it limits the need for short-term ESS capacity. Meanwhile, the technology is more complex and relies on more rare components than the Alkaline. [64]

The PEM electrolyzer today reaches an efficiency of 61 % with an ultimate target of 72%. The PEM electrolyzer is targeting a price of 1 $. Today, the technology is ready to be used with a technology readiness Level classification of TRL 9.[63]. Other literature although states that higher targets are possible with efficiencies expected to exceed 80% by 2035 [66].

### SOEC

The high temperature solid oxide electrolyzer (SOEC) operates above 600 ° C, using solid oxide electrolytes for efficient hydrogen production from high temperature sources. This makes it possible to reach higher efficiencies using thermal energy that otherwise would be wasted. The SOEC electrolyser can tolerate smaller variations in electrical load and heat supply. However, if the reactor differs too much from the optimum, studies have shown that crack formation occurs, which greatly decreases the lifetime. [67] Because of the higher temperature, and because steam is separated to a greater extent from pollutants, the inflow does not have to be as clean as for the competitors. Saving other water filtration expenses.

The SOEC electrolyzer today reaches an efficiency of 71 % efficiency (88% with thermal input) with an ultimate target of 79% (95 with thermal input) and is therefore much more efficient

than its competitors. Recent small-scale studies have even shown a thermal input efficiency of 98%.[68] The electrolyzer currently targets prices of around 4 dollars, with the further goal of decreasing it to 1 dollar. Today, the technology is in the demonstration phase with a TRL 7/8 classification.[63]

### 3.6.3 Fuel Cells

To use the energy of the hydrogen molecules, the gas can be burned if the energy is needed as a heat source, used as an oxidation agent if applicable, or put in a fuel cell to generate electricity.

A fuel cell works in the same way as an electrolyser, while the reaction is opposite, generating an electric current from the spontaneous process. The fuel cell technology is therefore the same as the three technologies of the electrolyzer previously mentioned. For a P2X project, the development of the fuel cell is interesting for two reasons, first as its a main component of long term storage in the system itself , but also because the development of the technology also impacts whether the worldwide hydrogen economy will break through (and the project becomes successful where the energy can be sold), as this depends on the viability and efficiency of the technology.

The efficiencies of the fuel cell for the respective technology are for the conversion back to electrcity significantly lower than for PEM, Alkaline and SOEC electrolyzers, with 60% efficiency for all three technologies. Although the advancement in one technology will directly link to the other. [69] Some fuel cells on the market are also possible to be run bidirectionally, which means that in case local consumption of long-term storage components (produced hydrogen) would be needed, although the technology is more expensive, a second unit does not have to be bought, cutting investment expenditure for this component [70].

### 3.6.4 Hydrogen

Using hydrogen directly as an energy source can be integrated in a range of sectors and industries. It can be applied both as a heat source and converted back to electricity through the use of a fuel cell. Hydrogen is a very light component while being extremely energy dense by weight. This means that its weight energy density is very high, as it stores a large amount of energy per unit of weight. However, in its gaseous form, its volumetric energy density is low because hydrogen gas occupies a large volume. The gas also has a very low melting point, making storage even more complex. The heat value of hydrogen is 39.39 kWh/kg, underscoring its high energy density by weight. When compressed or liquefied, hydrogen's volumetric energy density increases, making storage more efficient considering weight, but not volume.

Transporting hydrogen is very difficult due to its properties, as it requires a very high pressure of up to 800 bar or liquefaction at a temperature of 259,2 ° C to be viable. The additional properties of the gas, such as its explosive nature, invisible flame, and undetectable smell, further complicate storage. Although not poisonous to humans, these characteristics pose

significant challenges. A combination of these properties sets high requirements for the safety concerns of technology where complicated and expensive infrastructure is necessary.

The forecast LCOH2 for producing green hydrogen varies a lot, because of volatility prices for the technology used, most government targets 1-3 $/kg, which is far from reality of actual projects. An estimate is that it instead ranges in between 5 and 8 $/kg. All depending on the forecasted technological development and material availability. [71] The estimated CAPEX prices for 3035 are 650 000 $/MW installed capacity, [72] and 40 000 $/MW/year for the OPEX.[73]

### 3.6.5 Ammonia

With the disadvantages in the process of storing and transporting hydrogen, an alternative is to further process it into ammonia. Ammonia does not require the liquefaction of a temperature as low as that of hydrogen gas, as it has a boiling point of -33.34 º C. It also has a much higher volumetric energy density, making it easier to transport both as a liquid and as a gas. The chemical is, although toxic for humans and flammable, but with a flash point lower than hydrogen. This still makes it important to treat the chemical with care, especially when transporting, as emissions can have a tremendous environmental impact. The heating value of ammonia is 5.2 kWh/kg making it less energy dense considering weight, although the density makes the chemical interesting. [74] [75]

Today, ammonia is used in industries all over the world, being the second most produced chemical. Mainly used in the fertilizer industry, where conventional ammonia is produced through the use of gray hydrogen (from steam reforming of natural gas) to later be used in the Haber-Bosch process (HB). The Haber-Bosch process combines nitrogen (which is the most abundant component in the air) with hydrogen. The air is processed in an air-separation mechanism, where the concentrated nitrogen can be used in the Haber-Bosch process. [76]

As energy storage in ammonia (if not further processed to fertilizers or other chemicals) requires the steps of both transforming to ammonia and cracking back to hydrogen, the process is not only more expensive but also results in a lower efficiency through production and decomposition if not storage is considered. However, when the round-trip efficiencies of suitable liquefied storage methods for transportation are compared, it becomes evident that the additional energy required for compression, storage, and controlled vaporization is significantly higher for pure hydrogen than for ammonia, including the extra energy used for producing and cracking ammonia. The results show a round-trip efficiency that breaks even in 30 days, with favorable conditions for ammonia for storage longer than this and favorable conditions for hydrogen for shorter time periods. This makes the use of ammonia as export energy carrier favorable.[77] Ammonia also has comparable efficiencies in terms of production. [78] This reference also states that in combination with electrolysis, the process only requires and extra 10 percent input of energy. With the targeted 72% PEM electrolyzer, the combined will be 65%.

Research is also investigating possibilities to directly convert ammonia in a fuel cell. This

direct reaction may be much more efficient and cheaper than it is today, which may lead to further advantages in the logistical chain and development of the energy use. [79]

The main disadvantage of ammonia cracking and combustion is the emissions of NOX particles and nitrous oxide (laughing gas). In perfect combustion and application in fuel cells, they are not formed, but the high temperature and presence of oxygen make side reactions inevitable. Studies show that fuel cells are much more efficient and some studies say that no side reactions are formed.[80] To address the problem, catalysts need to be used, which is expensive technology but necessary to mitigate the poisonous and GHG emissions. [81]

In the same way as for hydrogen, the forecasted price for LCONH3 varies a lot due to the volatility prices for the used technology. However, an estimate is that it will range between 0.475 and 0.950 $/kg by 2030. [82]

The cost of a Haber Bosch plant varies greatly, but in combination with an electrolyzer, some management and treatment costs can be avoided. An estimate is that 9.35 % of the power supplied to the electrolyzer is needed for the Haber-Bosch plant. In these conditions, the CAPEX for the Haber-Bosch plant stands for 37.65% of the electrolyzer cost. Although the estimated Opex is 1.5 percent of the Capex per year. [83] [84]

### 3.6.6 Methanol

Another hydrogen derivatives chemical energy carrier is methanol, which has very interesting properties when it comes to carbon limiting actions. The chemical has a high energy density and is much safer to handle than hydrogen and ammonia, as it is liquid under atmospheric pressure.

In the production process, carbon dioxide is combined with hydrogen to form methanol. In an initial phase, carbon dioxide could be captured from industries. The chemical can later be burned to power steam generators, with the only reactants being water and carbon dioxide. Through this process, the carbon atoms are cycled again, and huge carbon emissions can be mitigated. As carbon dioxide still is let into the atmosphere, this is not considered a final solution but a solution for the transitional phase, toward a full ammonia/hydrogen infrastructure and is therefore not considered as an exclusive candidate for production in this report.

## 3.7 Desalination Plant

The desalination plant (DSP) plays a key role in a P2X setup, as seen in the P2X overview in Figure3.1. As the main electrolyser technologies mentioned above need an input of desalinated water, a freshwater reserve or a desalination plant is needed in a P2X project. In addition, desalinated water is also needed for residential use, to serve exporting ships as well as agriculture. In a DSP, seawater is pumped into the desalination plant. Then, it goes

through a series of filtration stages to remove larger particles and debris. Later, the water is pressurized and forced through the reverse osmosis membranes, separating freshwater from salt and minerals. Freshwater is collected and treated further to meet quality standards, while concentrated brine containing the removed salts is disposed. A desalination plant typically consumes 3-4 kWh of energy for every cubic meter of water, making it a very efficient process. On average, a resident (and deckhand on an exporting ship) consumes about 200 liters of water a day, and the electrolysis process requires 9 liters per kg of hydrogen produced. Also important to consider for a P2X project is agricultural use, which on average accounts for around 70% of the world's freshwater consumption. [85] The CAPEX for a desalination plant is estimated to be 3 968 254 $ per MW, and for OPEX as low as $0.5\$/m3 * 0.59 = 0.295\$/MW$, as 41% of the original OPEX consists of the energy price.[85].[86]

### 3.7.1 Desalination Plant Configuration

In figure 3.17, a configuration for a DSP with water storage included used in a P2X project can be seen. This figure is an extension of the DSP part of the system overview described in figure 3.1. The DSP draws power from the DC grid, which is passed through a DC/DC converter to lower the voltage from the grid side. As the DSP draws power from the grid, it produces desalinated water that is ultimately used to provide the city, agriculture, and the energy carrier production facility with enough desalinated water.

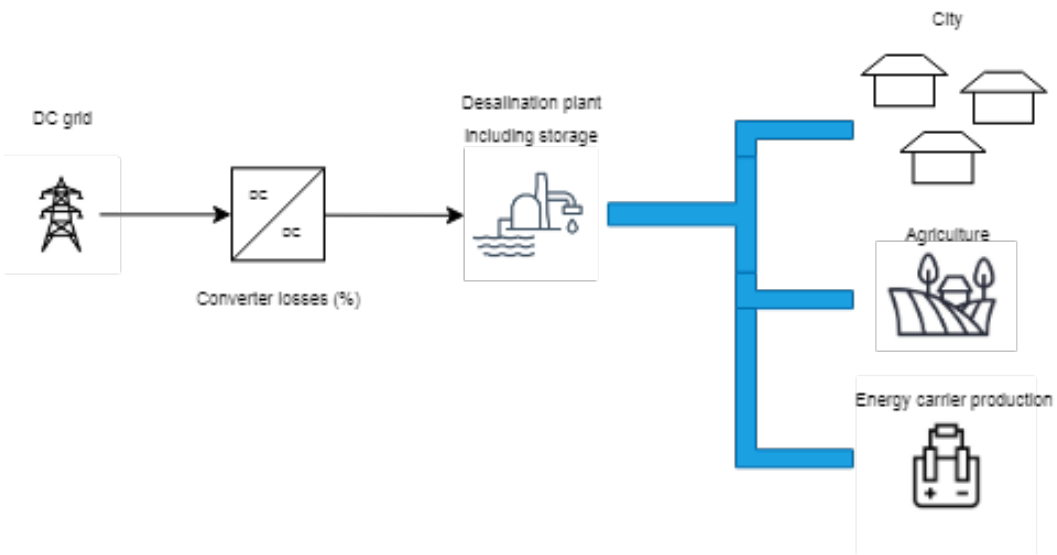


**Figure 3.17:** Desalination plant configuration drawing.

## 3.8 Tank Storage

Tank storage for DSP and chemical energy carrier play a key role in a P2X setup, as seen in the P2X overview in figure3.1. When different chemical components are stored, a wide range of technologies can be used, depending on the planned application and available technology. As for many P2X projects, the need for long-term storage on site is limited, and the product is expected to be exported/consumed in a short time from production. However, in the short term it is needed in case of logistical failure or a temporary imbalance in supply and demand.

The standard storage method for such an application is the use of tanks. In the tank, the stored agent can either be compressed to a pressure of 300-800 bar or be liquefied and kept chilled until further application. What technology is used depends on further application, for example, whether it is used on site use or exported, as well as what space limitations the site has. [87]

An alternative to storing hydrogen is to convert it to ammonia, as it is much easier to store with its higher boiling point. This simplifies not only the storage procedure, but also the export. The Capex and OPEX for the storage of refrigerated ammonia is 1.04 $/kg for CAPEX and 3% of this for OPEX. [88]

The water that is desalinated for use in the electrolyzer, residential and agricultural uses also needs to be stored temporarily. This is a much simpler process because water is in liquid form at room temperature and it is non-toxic. The CAPEX of this is assumed to be 100 $/m3. [89]

### 3.8.1 Others Storage Alternatives

In addition to conventional storage in gas/liquid tanks, there are multiple other storage methods, using different types of natural geological formation, such as empty gas fields, salt caverns, or old mine shafts. First, these technologies require that local conditions have the possibilities for such a storage system. Because these types of technology are mainly applicable for long-term large-scale storage, they are not further investigated.

Hydrogen gas can also be stored in metal hydrates, where the gas is subjected to a sponge structure, undergoing a non-spontaneous reaction, allowing metal-hydrogen bonds. In a later stage, the bond breaks when exposed to a lower pressure or temperature. This technology is especially suitable for transportation because hydrogen can be transported with a volumetric energy density of 4.3 kWh/dm3 compared to 1.3 kWh/dm3 at 700 bar for hydrogen.[90] This allows more energy per carrier, as the transport is most often space-limited and not weight-limited, where the alternative is much heavier than other technologies. Another advantage is that the storage technology is considered much safer, as the metal is neither flammable nor poisonous. The main disadvantages are the increased cost of application and the losses in the conversion in both binding to the metal and decomposition. Studies have shown that the technology is applicable to hydrogen storage with a dimension of up to 100 MWh. [91]

## 3.9 Specification Summary

For the technologies mentioned in this literature study, the main efficiencies and CAPEX / OPEX prices are stated in table 3.1, to be used later in the construction of the P2X set-up.

**Table 3.1:** Summary for Specifications of stated technologies.

| Component | Efficiency | CAPEX | OPEX | Unit |
|---|---|---|---|---|
| **Solar - Mono** | 27.60% | Not Stated - more expensive | | |
| **Solar - Poly** | 23.30% | 500000 | 13000 | $/MW |
| **Wind farm** | Not stated | 2100000 | 89000 | $/MW |
| **BESS** | 95% (for Max Power) | 270000 | 2500 | $/MWh |
| **Cables Transmission** | LOSSES 2GW: 1.44%/1000km (R=0.0072 ohm/km) | 700000 | 0 | $/Km |
| **Cable Submarine** | | 3120000 | 0 | $/Km |
| **DSP** | Combined: 3-4 $MWh/m^3$ | 3968254 | 1095000 | $/MW |
| **Desalinated water storage** | | 100 | 0 | $/$m^3$ |
| **Electrolyzer - PEM** | 72% | 650000 | 40000 | $/MW |
| **Electrolyzer - AL** | 72% | Not stated | | |
| **Electrolyzer - SOEC** | 95% (with thermal input) | | | |
| **PEM + HB process** | Combined: 65% | 241475 | 3622.125 | $/MW |
| **Ammonia storage** | | 1.04 | 0.0312 | $/kg |
| **Offloading port and equipment** | | 16000000 | 160000 | $/300m berth |
| **Hydrogen Fuel Cell** | 60% | Integrated in PEM | | |

The levelized costs of energy stated in the literature study for hydrogen, ammonia and electricity are stated in table 3.2 and are to be compared with the result of the P2X project.

**Table 3.2:** Forecasted LCOE Prices for Hydrogen, Ammonia, Wind and Solar Power

| Type | Range |
|---|---|
| Levelized Cost of Hydrogen ($/kg) | 5.00 - 8.00 (1.00 - 3.00 target) |
| Levelized Cost of Ammonia ($/kg) | 0.475 - 0.95 |
| Levelized Cost of Wind Power ($/kWh) | 0.054 |
| Levelized Cost of Solar Power ($/kWh) | 0.03 |

# Chapter 4

# Method

The general methodology photovoltaic, described in Section 1.2, as a part of the literature study. In the following part of the report, an overview flow chart of how the objectives are met is illustrated in Figure 4.1,

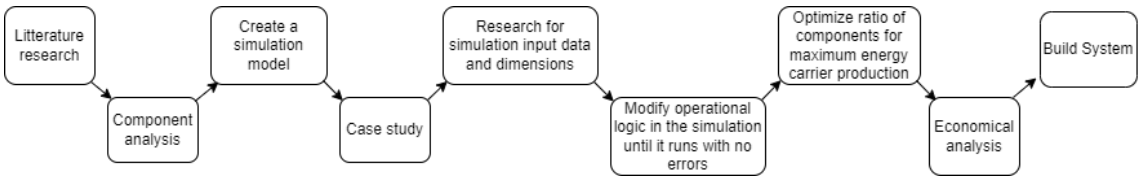


**Figure 4.1:** Method overview flow chart.

In the figure, it can be seen how the methodology starts with the literature research to identify the main components of a P2X system made in the literature study. In addition, a component analysis is performed to identify and compare the technologies investigated in the literature study, which is presented in the result. In addition, a simulation model is built to be applied for a case study for which the components are chosen and the inputs determined. The built model is also adjusted on the basis of these inputs to be further optimized for maximum energy carrier output. Lastly, the economic analysis is carried out, where the final results are analyzed.

The structure of the method is chosen to be in the presented way to make it easy to scale or apply the tool to other situations relating to the objectives. In this way, for a new set-up, the methodology can start from the fourth step in the figure above.

## 4.1 System Component Analysis

Before being able to simulate the key component of the P2X system, different technological alternatives and its specifications are being investigated. This is made to know how to build the simulation in an efficient way to reach the main goal of maximizing production. To do this, the main components within the generation, storage, consumption, production, and logistics of a P2X system are presented in the literature study chapter 3. The analysis is made to get an understanding for how the system needs to be built and does not to a final setup result before the simulation is done, where the technology is determined based on the required specification in the system.

## 4.2 Simulation Method

The simulation of the P2X system in figure 3.1 in the beginning of the literature study is carried out using the OpenModelica simulation tool. The simulation software, which was described in more detail in Section 2.8, is chosen because of its great properties when simulating the performance of energy systems. When designing the system, the main objective is to maximize the energy carrier production while still maintaining the necessary functions by providing residents and industries with a sufficient amount of power every hour of the year. The simulation model has been made to replicate the conditions and components of a P2X system including component configurations described for all the components in the literature study. In figure 4.2, an overview of the simulation model can be seen, with all its components. The green headings represent the potential input of the power injection into the grid, while the red ones represent the power consumption. The black heading of the battery means that it is bidirectional and both injects and draws power from the grid.

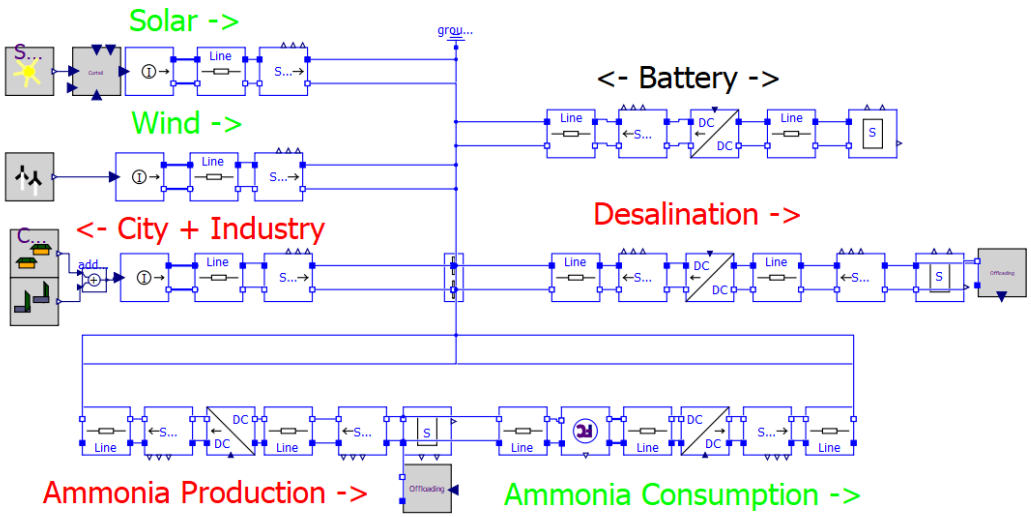


**Figure 4.2:** System overview with the main components without controllers.

For the system to function properly according to the specified requirements, some of the components need controllers in order for the system to work. The complete simulation model including the controllers and logic's can be seen in Figure 4.3. The system has 7 components with 5 controllers and 2 offloading units. The gray blocks connected to DC/DC converters represent controllers, while the gray blocks connected to storage units are offloading units. The general logics behind these controllers and offloading units are described briefly for the respective component in this section.

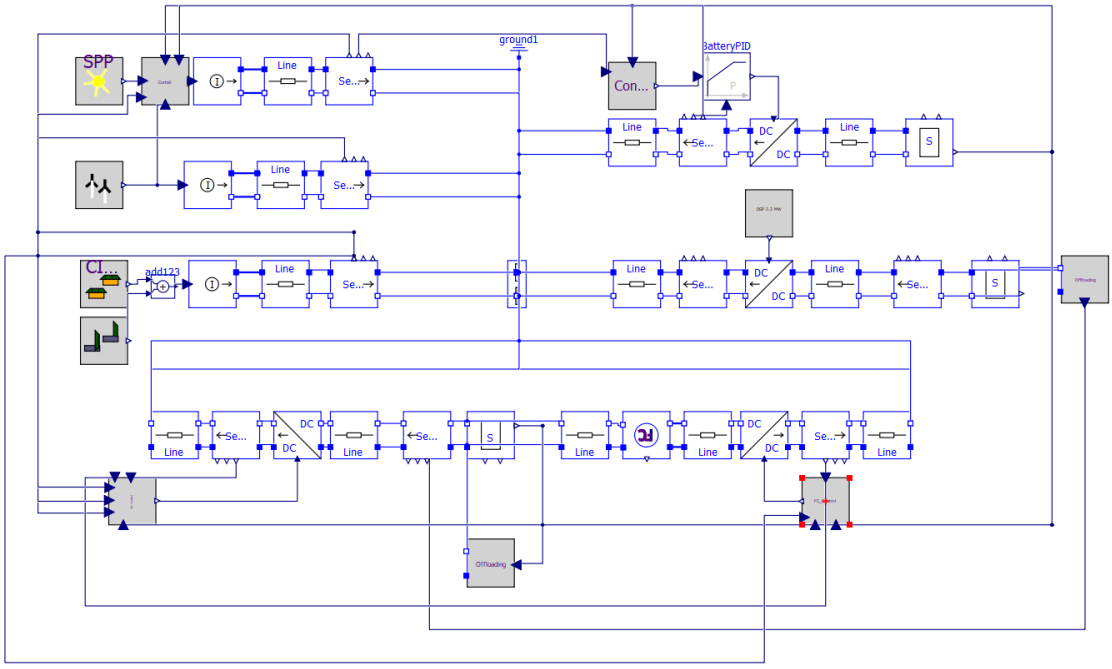


**Figure 4.3:** Full system overview including controllers and logics.

When the gray blocks are opened, the controllers can be seen in more detail. To give an example of how a controller can look, Figure 4.4 shows the complete electrolyzer controller. The controller functions such that the excessive power in the grid is calculated by taking the power generation subtracted by the consumption. This excess power then becomes the set-point value for the power the electrolyzer should draw from the grid to produce hydrogen. In addition to this, the SoC of the BESS is taken as input in the controller in order to allow the electrolyzer to produce more hydrogen when the SoC of the BESS is high and make the electrolyzer produce less when the SoC is low.

To implement these functions in the controller, mathematical operation blocks are used for the calculations, while switches and hysteresis blocks are used for the logical operations. When the calculations and logical operations have been made, a PID controller takes the power as a setpoint value, to ultimately convert it to an electrical current signal that makes the electrolyzer draw power from the grid.

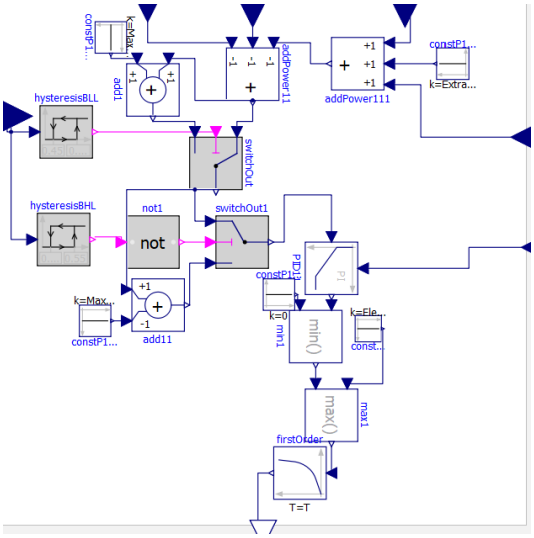


**Figure 4.4:** Electrolyzer controller logic.

In figure 4.5, an example of an offloading controller can be seen. Here, the controller measures the storage level in the tank, and if the tank is 90 % full, it offloads the tank to the storage level 50 %, mimicking the situation where a medium-sized carrier comes to export ammonia.

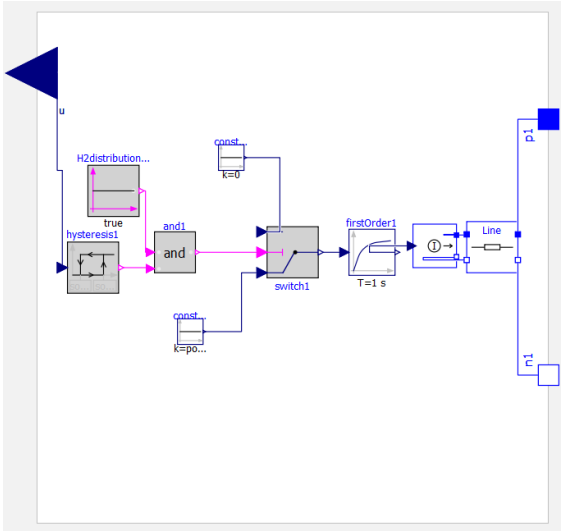


**Figure 4.5:** Offloading controller of energy carrier storage.

### 4.2.1 Timeseries Data

In a P2X system with no grid connections, all components which are generating or consuming power needs to be simulated based on accurate time-series data for a full year of operation. Due to the fact that all power in the system is generated from fluctuating renewable energy sources, overlaps and counter-overlap in generation therefore lead to a big variation of power present in the system.

To achieve realistic simulations, power generation and consumption should be updated as frequently as possible. However, for remote locations, accurate hourly data from measurements for the specific location is not within the budget of this master thesis.

For power generation, solar and wind power generation have a strong dependency on each other. Therefore, simulation-based data for a specific year must be prioritized. The simulated dataset is obtained from the renewable Ninja website presented in section 2.8. This data is based on satellite measurements and site recordings to generate estimated hourly weather data for any location for the year 2019. Using this database, an output file is supplied with a resolution of 1 hour for the full year which is suitable for the project.

In reality, for especially solar but also wind, the output can vary from 0 to 100 capacity in a matter of seconds due to cloud coverage or winds. However, since the scale of the WPP and SPP can be large, these changes in capacity do not often occur at the same time for the whole plant, since it takes some time for a cloud, for example, to cover the whole SPP. One way this is combated in the modeling is through the use of four delays, with the purpose of smoothening out the variations in a realistic manner although its still based on the same dataset. The dataset can also be interpolated in different ways in between the datapoints to give realistic outputs.

For the energy consumption of the industrial town, actual data for this do not exist as the town is not built yet. There is also no nearby town that would be comparable to the scale and energy usage of the town described in the P2X system. Therefore, data from another location with a similar energy usage pattern is used and scaled to match realistic values based on the size of the P2X project.

### 4.2.2 Microgrid

To transport the generated electricity from producers to consumers, all different components are connected through the use of HVDC transmission lines and cables, creating a DC microgrid. Using DC/DC converters between components and the grid, the voltage of the grid can be kept at a desired unified voltage level while the different components can use the voltage they are designed for.

### 4.2.3 Wind Power

When implementing the WPP in the simulation model in Figure 4.2, the WPP configuration seen in figure 3.11 from section 3.2.6 is used as a template. In the simulation model this is implemented by inserting a table with hourly power output from one turbine. This table is then amplified with the number of turbines that is chosen for the project, and then divided into 4 different input tables, each with a time delay of 10 minutes. This is done to imitate a realistic scenario in which the wind turbines have spacing between each other and do not produce the exact same power output every second. With a time delay of 10 minutes, a 10 m/s wind will travel a distance of 6 km, which was considered a reasonable distance. Finally, the four power output tables are fed into a current source, which injects power into the system, resulting in the top left branch in figure 4.2.

The time series data for the turbine are gathered for a chosen location as described in Section 4.2.1. In order for the data to be translated from a wind speed to an actual power output from a wind turbine, the formula seen in equation 4.1 is used. Here, 0.5 is multiplied by the power coefficient $C_p$, air density, $\rho$, the swept rotor area, A, and cubed wind speed U to ultimately obtain the power output for the given wind speed. The air density used is 1.225 $kg/m^3$, and the $C_p$ value is calculated by inserting a turbine-specific rated output at rated wind speed in equation 4.1 and solving for $C_p$.

$$P = 0.5 * C_p * A * \rho * U^3 \tag{4.1}$$

For example, for a Vestas 15 MW turbine, $C_p$ at rated power becomes 0.41 at rated wind speed, as can be seen in equation 4.2.[92]

$$\frac{15000000}{0.5 * 43742 * 1.225 * 11.1^3} = 0.41 \tag{4.2}$$

This $C_p$ value is then held constant when calculating the power output for all wind speeds. For wind speeds higher than the turbines rated wind speed, the power output is capped at rated power. Finally, the cut-in and cut-out wind speeds are applied, such that power outputs for wind speeds less than cut-in and greater than cut-out are set to 0.

### 4.2.4 Solar Power

When implementing the SPP in the simulation model in figure 4.2, the SPP configuration seen in figure 3.6 from section 3.1.4 is used as a template. In the simulation model, this is implemented in the same way as for the WPP, by inserting a table with hourly power output from one square meter of solar panel. This table is then amplified with the capacity that is chosen for the project and then divided into 4 different input tables, each with a time delay of 5 minutes. This is done to imitate a realistic scenario in which the wind turbines have spacing between each other and do not produce the exact same power output every second.

Finally, the four power output tables are fed into a current source, which injects power into the system, resulting in the left-hand middle branch in figure 4.2.

In the SPP case, the site-specific data is collected in the format of percentage of actual output compared to the installed capacity. When implemented in the simulation model, a similar methodology is used as for the wind power. The table of hourly percentage of installed capacity is amplified by the desired installed capacity. This table is then divided into 4 different input tables, all with a time delay of 5 minutes each. These four input signals are then fed into a current source, which injects power in to the system, resulting in the top left solar branch seen in figure 4.2.

In addition to the SPP, there is also an associated controller that is regulating the power output from the SPP in the simulation model. The controller is needed because during some periods of the year, the system is producing more power than it is consuming while the battery is full, and therefore there is a need to curtail the surplus energy in order for the system components not to be damaged. To implement this logic in the controller, it takes both production and consumption units as input, as well as the SoC of the battery, and calculates the instantaneous power balance of the system. If the system has a surplus of power when the BESS is fully charged, logics in the controller make the SPP curtail the excessive power that cannot be consumed in the system. The controller also makes the SPP curtail if the power exceeds the rated limit of the battery, in order for the battery to not draw a larger power than its rated capacity.

### 4.2.5 Local Energy Usage

When implementing the local energy usage in the simulation model in figure 4.2, the configuration seen in figure 3.6 from section 3.1.4 is used as a template. In the simulation model, this is implemented by inserting hourly electricity consumption data for the desired area, which is gathered according to the methodology described in Section 4.2.1. This is then used as input to a current source, which draws power from the system according to the data, resulting in the left-hand middle branch in figure 4.2.

### 4.2.6 Battery Energy Storage System

When implementing the BESS in the simulation model in figure 4.2, the short-term ESS configuration seen in Figure 3.14 of Section 3.5.1 is used as a template. In the system, the BESS plays an important role in voltage regulation, peak shaving, and to deliver power to processes requiring a constant power input, as the local energy usage for example. Due to the versatile applications of BESS, there has to be a controller connected to it. For example, the controller makes the BESS to regulate the voltage by measuring the current grid voltage and comparing it with a reference voltage of 1 MV DC. If the voltage is higher, the battery draws power from the grid until the measured voltage is equal to the reference voltage, and vice versa, if the voltage is lower than the reference, the battery discharges power into the grid. Another function of the controller is to measure the SoC of the BESS to keep it within

the desired range of 10-90% using a so-called hysteresis logic. An example of this can be seen in figure 4.2.6. When the battery reaches 90% SoC, the hysteresis logic prevents the battery from charging again until it reaches 85%. However, due to other operational logic, such as the curtailment of solar power that starts when the SoC of the BESS is 85%, the battery will rarely reach over 85%, so hysteresis should be seen as an emergency logic. An example of how this should work can be seen in figure 4.2.6, by looking at the first SoC increase. When the battery reaches 85%, the SoC does not increase further, and is then discharged to around 50%. Vice versa, if the battery discharges to 10%, hysteresis prevents the battery from discharge further, until the SoC is 15%. When the SoC reaches 15%, the fuel cell starts to supply the system with power instead, which can be seen as an example at the end of figure 4.6. The BESS can be seen in the upper right part in figure 4.2.

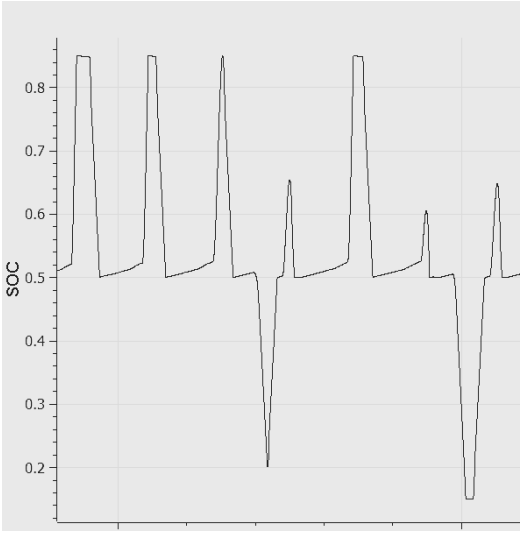


**Figure 4.6:** SoC of the BESS as a function of time.

### 4.2.7 Fuel Cell

When implementing the fuel cell in the simulation model in figure 4.2, the energy carrier production configuration seen in figure 3.16 from section 3.6.1 is used as a template. A fuel cell is used when the battery is running low and processes in the system require energy. The way that the fuel cell is implemented in the simulation model is by inserting a storage unit that is connected to a DC/DC converter that is further connected to the grid. In this DC/DC converter, the losses and efficiencies are stated such that if energy flows through the converter, it is multiplied with the losses and efficiencies. The fuel cell can be seen in the bottom right branch in figure 4.2.

As mentioned above in section 4.2.6, if the battery reaches 15%, the fuel cell is activated to help provide the system with power. Similarly to BESS, the fuel cell has a controller that includes hysteresis logic based on the SoC of the BESS such that if it reaches 15%, the fuel cell starts producing power equal to the power demand at that time, until the SoC of the battery is back at 20%. An example of this situation can be seen in the end of figure 4.2.6, where the SoC of the BESS reaches 15%, and the fuel cell starts to produce. Further, the fuel cell is also

logically connected to the hydrogen storage, such that if the hydrogen storage SoC is too low, the logic prohibits the fuel cell from producing power by using hydrogen from the tank until it has enough hydrogen again.

### 4.2.8 Desalination Plant

When implementing the DSP in the simulation model in figure 4.2, the DSP configuration seen in figure 3.17 from section 3.7.1 is used as a template. As mentioned above, desalinated water is needed for various purposes and processes in the simulation model. Since many suitable P2X locations do not have a stable freshwater supply, a desalination plant (DSP) is needed to convert seawater to desalinated water, which in the model can be seen in the middle right branch in the figure 4.2. In the simulation model, the DSP is based on the operational logic which draws constant power from the system based on the rated power for the DSP. This electrical power is then converted to desalinated water using the equation 4.3, where the constant power consumption P of the DSP is multiplied by the efficiency with which it can convert seawater to desalinated water, measured in kg/kW.

$$m_{H_2O} = P\,(W) * Efficiency\,(kg/kW) \tag{4.3}$$

This results in an output of desalinated water that fills up the water tank that is controlled by an offloading unit controller. The offloading unit then emptys the tank according to the instantaneous water needs of the system. The water needs from the city and agriculture are modeled as constant, while the water consumption from the electrolyzer varies depending on the production rate of hydrogen, by using 9 liters of water for every kg of hydrogen.

### 4.2.9 Electrolyzer/Haber-Bosch

When implementing the electrolyzer in the simulation model in Figure 4.2, the energy carrier production configuration seen in Figure 3.16 of Section 3.6.1 is used as a template. The electrolyzer is where all hydrogen is produced from electricity and desalinated water, which can be further processed in the haber-Bosch unit (HB), which is modeled in the same step. In this section, for simplicity, this process will only be stated as an electrolyzer.

The electrolyzer is controlled by several mechanisms, which is described in more detail in the example in Figure 4.4, as well as an offloading unit, which is also described in more detail in Figure 4.5. The electrolyzer is implemented in the simulation model is by inserting a storage unit that is connected to a DC/DC converter that is further connected to the grid. In this DC/DC converter, the losses and efficiencies are stated such that if energy flows through the converter, it is multiplied with the losses and efficiencies.

In order to translate the electricity consumption of the electrolyzer, the signal is converted to ammonia using the formula seen in equation 4.4. Here, the mass of ammonia that is produced, $m_{NH_3}$, is calculated by taking the power consumption P of the electrolyzer, multiplied by the

efficiency of the electrolyzer, $\eta$, and the heating value, HV, for ammonia. The heating value is the theoretical amount of energy that is needed to convert electricity to ammonia.

$$m_{NH_3} = P\,(W) * \eta * HV_{NH_3} \tag{4.4}$$

### 4.2.10 Data Collection

To manage the measured signals in the system for further techno-economical optimization and system validation, many data measurements are needed. In addition to using measurement unit blocks for instantaneous signals such as SoC, voltage, current, and power, other time-based readings are needed. For instance, this measure unit block converts all powers to energy by taking the integral of the power curve. This way one can see the accumulated energy for a specific measure unit and how it varies throughout the year. This is for example used to see the kWh of curtailed energy, generated energy, weight of produced ammonia and water, for instance. This logic is also used to have an estimate of how many cycles the battery undergoes by using a counter mechanism. This is done by dividing the BESS capacity by the absolute value of the total energy used. All the measured data in the block are presented in table 4.1

**Table 4.1:** Yearly Production Data - Parameters and Units from data collection block

| **Parameter** | **Unit** |
|---|---|
| Total electricity production (incl Curtailed) | kWh |
| Wind electricity production | kWh |
| Solar electricity production | kWh |
| Curtailed electricity | kWh |
| Wasted electricity | kWh |
| Ammonia Production Electricity Consumption | kWh |
| City electricity Usage | kWh |
| BESS Bidirectional electricity usage | kWh |
| Fuel Cell electricity Production | kWh |
| Ammonia Production | kg |
| Ammonia Consumption | kg |
| Exported Ammonia | kg |

## 4.3 Model Input Method

At this stage, when the model is built and the components are identified, one has to choose an estimated location to implement the model at. The first analysis is made by scouting using global solar and wind atlas and other site-specific information gathering from case-studies conditions, presented in the background. In addition, the inputs are set by plugging in the site-specific characteristics for this location. Through this, the model input can be specified, which is described below along with how they are decided for the location.

- Wind Power generation - Timeseries data from suitable location according to section 3.2.5, where renewable ninja data is used to extract hourly data.
- Solar Power generation - Timeseries data from suitable location according to 3.1.3, where renewable ninja data is used to extract hourly data.
- Water demand - based on local characteristics
- City and Industry energy demand - based on local expectancy
- Export possibilities - based on local geography

To chose between the use of inland or offshore wind the power generation, trends have to be analyzed. By plotting the data set sorted by the time of day for the difference seasons, the hourly variation in power output can be seen. Further, shifting the dataset forward and backwards by around 6 hours, to reach maximum and minimum overlap, and then re-running the simulation is done to see what influence the power curve overlap has on ammonia production and fuel cell operation.

Further, based on the location, model requirement and research method, the technologies and specifications of the chosen technology can be stated, where the model has all required inputs.

## 4.4 Technical Assumptions

The main technological assumptions for the built system are stated below.

One key assumption is that none of the components capacity is degrading with time. In reality, degredation occurs for both BESS, photovoltaic, and electrolyzer. In reality, a larger capacity would, therefore, be needed to compensate for this to maintain production.

The Fuel cell is also assumed to be integrated in the electrolyzer, which for the project means that it has a higher efficiency than in reality, as well as that the reversible technology in reality should be more expensive than the CAPEX and OPEX of the stated technology.

The OPEX of HVDC cables as well as water storage are assumed to be included in the CAPEX price for the respective component, as low costs are expected. In addition, the cost of pipes within the production plant is excluded, as well as the efficiency losses associated with this.

Another assumption in how the system is built is that no water is reused in the system. In reality, the current overproduction is even higher in reality when including a water treatment plant and cycling back the water. For the used setup, all used water is instead desalinated sea water.

## 4.5 Techno-Economic System Optimizing Method

When the system in the simulation model system can be run without simulation errors, the next methodology is to further optimize it. This is done through the use of a feedback-oriented trial-and-error methodology, which is described in the flow chart in figure 4.7.

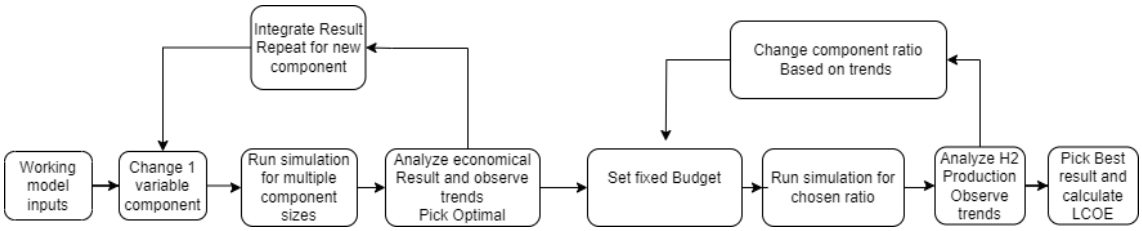


**Figure 4.7:** Flow chart of techno-economical Method overview

The methodology consists of two loops, which are described in the two following sections of "Initial component size optimization" and "Budget based component ratio optimization".

### 4.5.1 Initial Component Size Optimization

When the simulation method is performed, the system is efficiently constructed based on dimensions, making it possible to run for the full time period. By avoiding bugs and crashes as well as unrealistic appearances of the plots, reasonable orders of magnitude of the different components are identified during model exploration.

Using this, to further optimize the system, the capacity of all components but one is fixed to find the optimum of production depending on the price of the component. Here, the price of a range of component sizes is simulated around the initial component size of the model construction seen in the third step from figure 4.7. This methodology is made for all different components, with some small differences, as derived in the following sections.

To do this optimization for batteries, linear prices cannot be assumed as it depends on both the power output and cycles. The following equation therefore gives the actual price on the battery, which has to be modelled for different scenarios.

$$Price_{battery/year} = BESS_{price/kWh} * BESS_{lifetime} \tag{4.5}$$

Here, $BESS_{price}$ varies depending on the size of the battery, as smaller batteries require a higher rated power output and are therefore more expensive per kWh installed. Furthermore, a smaller battery undergoes more heavy deep-charge cycles and is therefore faster worn down, leading to a shorter lifetime and therefore to a higher battery price. Therefore, for battery calculations, it cannot be scaled linearly, as the price per kWh of the battery depends on the installed capacity itself. For the battery, the counter mechanism described in section 4.2.10 is used to identify the useful lifetime. In contrast, for the electrolyzer, which is assumed to scale linearly with respect to properties and lifetime, the equation is seen in figure 4.6.

$$Price_{component} = capacity_{component} * price/kW_{component} \tag{4.6}$$

When the system instead is optimized based on the optimal wind and solar ratio, instead of one variable, it is optimized for two variables of different prices. To do this, the total price of the generation technology is fixed, while the economical ratio between the installed capacity of wind and solar is varied. Therefore, the sum of the cost for the installed wind and solar is constant and calculated using 4.6 above. The simulation is then run, fixing the total cost for generation and applying different ratios of installed capacity to maximize the production.

To find the most beneficial size of the installed component as illustrated in the fourth step in figure 4.7, the revenue for the different sizes of the component can thereafter be calculated as seen in equation 4.7.

$$Revenue_{hydrogen/year} = ExportedH2_{year} * Targetprice \tag{4.7}$$

The difference between $Price_{component/year}$ and the revenue from exported hydrogen is then calculated for the different sizes of the components, and the highest production is therefore the most economically viable according to the equation,

$$Optimum = max(Revenue_{Soldhydrogen} - Price_{component/year}) \tag{4.8}$$

The result of this can be further plotted for the different scenarios of component sizes, to find the size which brings the maximum value for the analyzed project setup. The same analysis is carried out for different installed capacities, to have an estimate of sizes.

### Checking Independence

To further check for the independence of the previous input, the method is carried out over and over again seen in the first loop in method 4.7, varying the installed capacity of a new component and using the optimum of another setup. Based on this, the ratios are tested

for other dimensions of the components. The more independent situations tested, the better outcome. This is because situations far from the economical optimum above need to be tested to make sure that there are not only detected local extreme points but also the optimum of the total system.

### 4.5.2 Budget Based Component Ratio Optimizing

When the best option of reasonable dimensional ratios from the methodology above is found, the total cost of the main components is fixed, consisting of the electrolyzer, BESS, SPP, and WPP. The costs of the other components of the system are not considered at this stage of the analysis, as they are assumed to be the same for all ratios of the four components above.

From this stage, a trial-and-error method is further carried out to test different ratios in which the total budget of the project is fixed starting in the fifth step in figure4.7. Instead of maximizing the revenue, at this stage simply production can, therefore, be maximized. To do this, the economics of the main components is plotted in pie charts to get a visual presentation of the economics when analyzing the result in step seven in figure 4.7. The result is then analyzed for every tested ratio to test new ratios in the second loop of figure 4.7. If a positive correlation of a certain mix is discovered, similar mixes are tested to look for combinations of even higher production. During this process of trial and error method, it is also explored if some ratios between certain components can be identified to have a stronger correlation and impact on the system than others. For example, the overlap in generation and cost between WPP and SPP in theory has a great impact on when the power generation occurs, which can affect the system a lot.

To do this efficiently for initial investigations, the main components are identified only considering the CAPEX costs. Based on these costs, the optimal ratio of the components can be found for a fixed budget. Later, the same methodology can be made including CAPEX and OPEX, both considering an interest rate of 8% and 0% for 30 years of simulation. Here, the different economic analyses are always based on the previous results of establishing a fixed budget and maximizing production.

When as many tests as possible are performed, and all the results are collected for the different scenarios, the best ratio found is presented in the final step of figure 4.7, which is heavily dependent on the assumed prices for the different components. Further, the total economics of the system can be presented in a table of CAPEX and OPEX, including the other components of transmission, storage, DSP and port.

### 4.5.3 Site Dimensioning

The methodology used to select a location for the SPP and the WPP was to first look at the global wind and solar atlas maps in figures 3.5 and 3.9 to identify potential areas with good wind and solar conditions. When an overall area has been identified, a more detailed area is selected by taking many criteria into account according to the site selection processes

described in Sections 3.1.3 and 3.2.5. The method of selecting a suitable area for the rest of the components in the system is to place them as logistically favorable for the project as possible, without interfering with the local residents. Later through "on field" studies through Google Street View is brought out to identify SPP locations which together with site selection work of offshore wind to be placed on a map using Google Earth.

## 4.6 Final Economical Analysis Method

When the system is designed and the simulation results for one year are extracted from the model, the expected economic outcome can be listed for the project after its full lifetime to analyze the advantages and disadvantages of investments for different scenarios. Initially, the full economics of the CAPEX and OPEX of all components are shown as pie charts to see the ratio of economics.

In addition, the LCOE-method stated in Section2.4 is used to calculate the levelized cost of energy for the result of different energy carriers. It is important to note that all prices should be considered when calculating the LCOE for the chemical energy carrier, whereas the prices for the energy carrier production and storage are excluded when calculating the LCOE for electricity.

### 4.6.1 Economic Assumptions

This masters thesis includes a range of economical assumptions as follows.

The price for the floating wind turbines is assumed to reach today's cost for fixed foundations by 2035; this assumption is made because the technology otherwise is not expected to be competitive for a P2X megaproject application.

All the CAPEX and OPEX prices are scaled linearly and are therefore assumed to be independent of the size of the technology for all technologies apart from BESS. This is done because of scaling simplicity, where the economical methodology would be much more complex otherwise, redoing the economical calculation for every tested setup.

All economical prices are forecasted, although there is a slight variation depending on which year is taken, the prices are assumed to be valid for year 2035 as well.

OPEX and CAPEX of power electronics except for cables, such as DC/DC converters, are also assumed to be included in the respective main components of the system.

For all components apart from the BESS, which is cycle-dependent, a lifetime of 30 years is assumed for simplicity reasons.

The price of decomissioning the project is not accounted for in the project, as it is hard to forecast the value the components have on the market after 30 years. Furthermore, since many

of the technologies are newly developed, there is very little information on decomissioning costs after the project life.

The ratio optimization is only considering the 4 main components. For most components, this does not have an influence on the optimum as a fixed cost is added to every model. However, the price of an electrolyzer is directly related to the HB size, which means that the expenditure of the electrolyzer component in the optimization should be greater, assuming ammonia production is selected.

In addition, expenses are not included for the city itself. Residents are assumed to pay for their own needs as in a normal city. However, extra expenses for DSP and electricity in the area are covered, as the circumstances are special with the location of the city in the desert without a water reservoir or electrical grid.

## 4.7 Input Correction Method

At this point, the methodology built to meet the objectives of the master thesis is executed. However, to work through the entire methodology takes a lot of time, and to redo all steps in case of found errors is very time-consuming, as validation of the final results only can be done when the entire methodology is brought out, where steps are direct dependent on the previous method step.

Inputs can therefore, when analyzing the final results, be changed to redo specific steps of the methodology, which generate interesting findings although the accuracy of the results can be criticized. For the first experimented method in this master's thesis, the analyzed results presented in Chapter 5 showed some unrealistic values for capacity factors, and certain efficiencies could be criticized after comparing LCOE values and production with theory.

For the setup, the capacity factor of the initial dataset used had to be increased to match the values of the case study of Port Nolloth in South Africa in Section 2.7. To scale up the input values for Wind and solar Power generation presented in 4.2, the wind speeds are scaled linearly until the total yearly generation matches the value given from the theory in Section 2.7. In the same way, the solar power generation also given from the simulation method is further linearly scaled to match the total yearly power generation also stated in 2.7. However, for both generation technologies, the electricity production should not exceed the rated power. In addition, the efficiencies stated in the literature study are also changed to match other sources for the efficiency of the fuel cell and electrolyzer, which can be directly integrated in the model.

# Chapter 5

# Results

In this chapter, the results are presented. The structure mirrors that of the methodology section, initially introducing the identified components and then selecting and sizing these components for the chosen case study. Secondly, we discuss the system's performance over a full year and the results for the full project lifetime.

## 5.1 Research Results

In the literature study, all key components and their technological alternatives are identified for the system. The main technologies identified together with the main arguments are listed in table 5.1. In the table, the components of the literature study are summarized, with their main advantages and disadvantages for a P2X project application. In addition to the information stated in the table, the fuel cell uses reversible electrolyzer technology as presented in 3.6.3.

**Table 5.1:** Overview of the researched technology with pros and cons, and identified components of interest in the simulation.

| Solar | | Wind | | | BESS | |
|---|---|---|---|---|---|---|
| Mono | Poly | Inland | Fixed | Floating | Lithium | Supercapacitor |
| High efficiency, More expensive | Low efficiency, Cheaper | Cheapest, Size limited, worse wind conditions | Cheaper, restricted by depth, less good wind conditions | Most expensive, suitible deep water,good wind conditions | Cheaper, less cycles, less power density, low discharge rate | Expensive, more cycles, high power density,high discharge rate |

| Energy Carrier | | Electrolyzer | | |
|---|---|---|---|---|
| Ammonia | Hydrogen | PEM | SOEC | Alkine |
| Suitable for storage and transport, active market,less efficient, more expensive, pollutants | More efficient, Cheaper, high market possibility, clean | Variable input, low efficiency,expensive | Const input, high efficiency (if thermal input), expensive | Constant input,Cheapest, low efficiency |

| Cables | DSP | Storage Bank |
|---|---|---|
| Low losses, subsea suitable, DC components | Main technology available | Depend on Carrier, most availible chosen |

| Port |
|---|
| Pier only alternative |

## 5.2 Case Study Model Inputs

In table 5.2 the main characteristics of the South African Case Study Section 2.7 are listed that are relevant for the construction of the P2X model. Apart from all these specific characteristics, the case study is identified as attractive for a range of other national reasons such as industrial expansion and similar that is also stated in the South African Case Study section.

**Table 5.2:** Site specific input for Port Nolloth

| Port Nolloth | | | | |
|---|---|---|---|---|
| Wind | Solar | Water demand/supply | City and Industry | Export |
| Average wind speeds in the region is high, offshore power curve is shifted to the night | Desert climate makes location very suitable for solar, temperature along coast are good because of atlantic climate | There is no nearby water reservoir but great asset of salt water, DSP production is needed. Neither there is any agriculture possible with local climate, so agriculture needs excessive production. | City and Industry for the site are expected to be normal | Export possibilities by ship are good |
| Model Input | | | | |
| 20 km offshore Renewable ninja data | 10 km inland renewable ninja data | 200 l/day x 10 000 expected inhabitants + 9l per produced kg $H_2$ + 100 l/s to agriculture | Romanian data scaled by industrialized city energy use,scaled to 10 000 people consumption. 50MW baseload from industry and port operation | Constructing own port, average ship of 100 m possible any time |

In figure 5.1, the power variability of solar and wind trends during an average day is shown. The figure is based on the dataset used in the simulations. In the figure, the trend of solar and wind power output is seen for every hour of the day. From this, its clear that the solar energy is matching the irradiance curve while the wind is more stable throughout the day, with a dip countering the solar peak, and a peak in evening when solar power is lower.

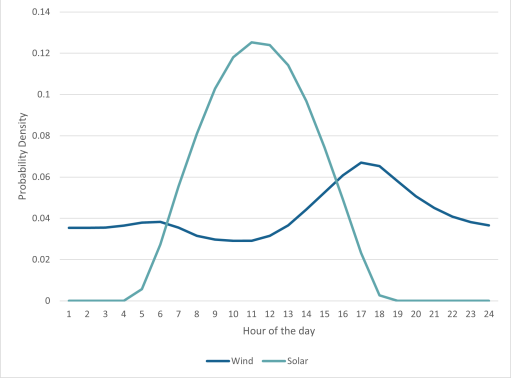


**Figure 5.1:** Comparison between the average wind and solar output during for every hour of the day.

In addition, seasonal variations for the location of Port Nolloth for inland and offshore wind conditions as well as solar conditions can be seen in the figure 5.2. Here, one can see that for solar power, the irradiance trend of longer days in summer (November-February) flattens out the curve, as the days are getting longer, with the opposite trend during winter (May-August). For the offshore wind power trend, the energy distribution is very similar for seasons, which ends up in the same trend as for figure 5.1, throughout the year. For the inland wind site, the power availability is very different between summer and winter, with opposing trends. Building a resistant system for such high seasonal variability makes dimension problematic, as it leads to that ideal ratios of components being very different from summer to winter.

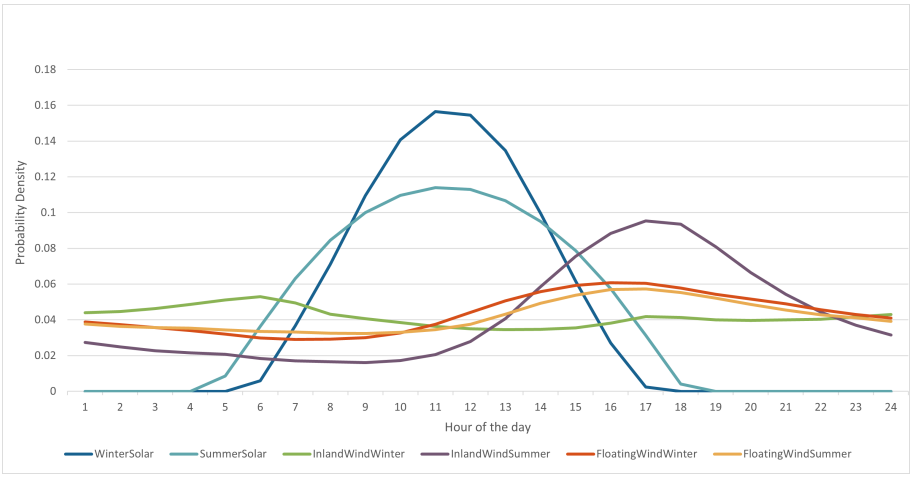


**Figure 5.2:** Seasonal average power potential for every hour of the day for both 20 km offshore and 20 km inland for Summer (Nov-Feb) and Winter (May-Aug)

By shifting the wind peak dataset by 6 hours forward to perfectly match the peak of solar, or backwards, simulating maximum opposition one gets the result seen in table 5.3. In the figure, electricity production and fuel cell usage where the simulation is performed using the final set-up from properties stated in the later investigated table 5.6. In table 5.3, one can see that the operation of the fuel cell varies greatly with the overlap of the power generation trend, which also results in a difference in total ammonia production explained by the fact that less power needs to be converted. More overlap results in less production and more consumption, while the other way around has the opposite effect.

**Table 5.3:** The Fuel cell consumption and Ammonia production change by 6 h wind data shift

| | NH3 Consumption | NH3 Production |
|---|---|---|
| Minus 6 h | 51% | -2% |
| Plus 6 h | -57% | 2% |

Based on the performance of the system and the research results, the technology that is decided to use for Port Nolloth is presented in figure 5.4, where orange colour represents the chosen technology. With local characteristics in combination with the technologies available from the research result in section 5.1, there is enough information to select the alternatives that are most suitable for the site-specific characteristics of the P2X project.

For solar panels, polycrystalline solar cells are selected due to lack of space constraints, and lower costs per MW installed for economic viability are prioritized. In wind generation, floating offshore turbines are the only feasible option, as fixed structures are not viable given the depth of the water. Onshore turbines are excluded based on logistical considerations and the power shift stated in the previous figure. The electrolyzer uses PEM technology, chosen for its ability to withstand variable loads, which is critical to the success of the project. Although SOEC technology in combination with increased BESS capacity could offer higher efficiency, it is excluded because of the availability and cost concerns of BESS. In the choice between ammonia and hydrogen, ammonia is preferred due to logistical advantages, being easier to store and more suitable for export by ships. In addition, the initial market demand for green ammonia is expected to be higher than that for hydrogen, which requires the development of infrastructure for production and utilization.

**Table 5.4:** Selected technologies based on site specific constraints, model method and research method.

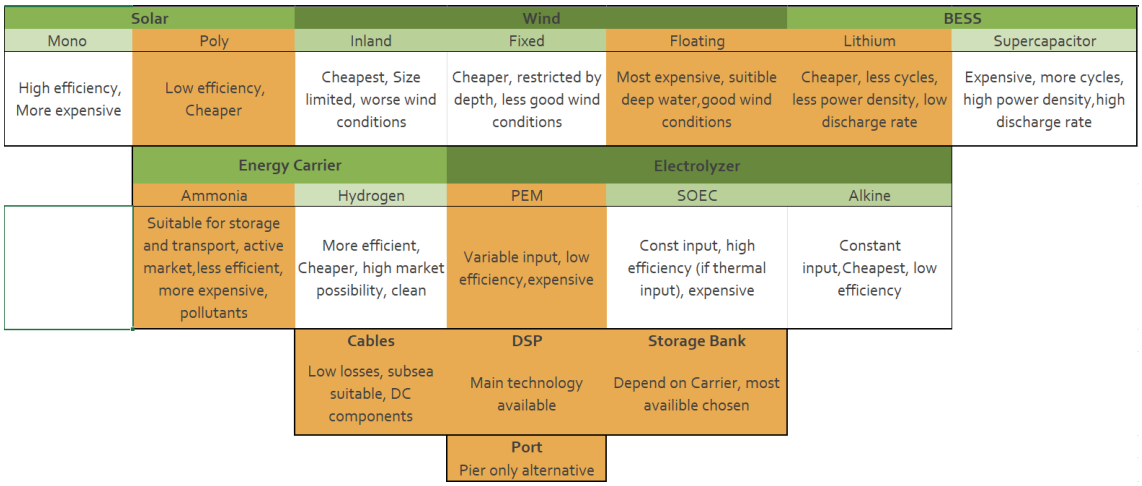


The specifications of the technologies decided are presented in Table 5.5. In this table, the assumed efficiencies for power conversion, sizes, as well as other necessary properties are stated according to the information given in table 3.1 in the literature study. For BESS and HVDC, the efficiency is stated for the maximum power, as the losses increase with the current according to the loss equation 3.2 mentioned in the electrical infrastructure section. The properties of the offloading are dimensioned on the basis of a medium-sized ammonia carrier ship and storage facility based on yearly maximum production, to generate viable offloading intervals, with a margin for logistical errors. The combined efficiency of Ammonia production, storage, and offloading is taken from the combination of Haber-Bosch and electrolysis, as stated in the literature study. The area of space-wise minor components is stated in the report as standard factory slots. With the assumption that each such slot requires a space of 1 ha which is reserved as a minimal size for the components. In the figure, the chosen technology and its competitive alternatives for the Port Nolloth case are illustrated as follows.

**Table 5.5:** Technological Details

| Technology | Efficiencies | Size | Properties |
|---|---|---|---|
| Photovoltaics | 23.3% | 4.3m$^2$/kW | Polycrystalline |
| Floating Turbines | Not applicable for model | 10 D spacing | 15 MW Turbine |
| Li ion BESS | 95% (Max Power) | Std. factory (1 ha) | Max Power: 250 MW |
| NH3 Production (PEM+HB) | 65% | Std. factory (1 ha) | Direct Conversion |
| NH3 Storage | Integrated above | 25,000 ton | Refrigerated |
| Offloading | Integrated above | 300 m pier | 10,000 ton |
| HVDC | **LOSSES 2GW:** 1.44 %/1000km (R=0.0072 ohm/km) | Length of cable | 1 MV DC ($\pm 500 kV DC$) |
| DSP | 70% | Std. factory (1 ha) | Constant Prod. |

## 5.3 Techno-Economical Model Optimization

In this section, the ratio of the four main components of the system (WPP, SPP, BESS, and Electrolyzer) is optimized for hydrogen production although, according to Table 5.4 ammonia production is stated. However, this is not a problem, as all hydrogen derivatives are directly dependent on hydrogen production, the findings regarding the ratio of the components can be applied to other hydrogen-based energy carriers such as ammonia. The optimization is therefore not made considering the added cost of HB, which in reality is increasing expenditure for the electrolyzer process.

The plots in Figure 5.3 illustrate the results of the initial optimization of the system, focusing on the variation in revenue and cost when altering one parameter at a time. The plot on the left shows how revenue changes with different installed capacities of the electrolyzer (in GW). As installed capacity increases, revenue initially increases, reaching a peak before declining. This shows that there is an optimal electrolyzer capacity, which maximizes revenue considering both production and installation costs. The right plot depicts the effect of varying the installed MW ratio of solar to wind energy on the revenue. For this specific example presented to have an understanding of the method, revenue increases with the solar-to-wind ratio, peaks at 0.6, and then decreases, and the best possible ratio is identified. Observe that the two examples cannot be compared to each other, especially regarding project profit, as the different setups have different total economical setup.

In both plots, only one parameter is varied while all other variables are kept constant. This approach helps identify the optimal points for each parameter in terms of revenue generation. By isolating the effect of each variable, the analysis provides a clear understanding of how different configurations impact the economic performance of the system. This is the first step in finding the optimal optimized system.

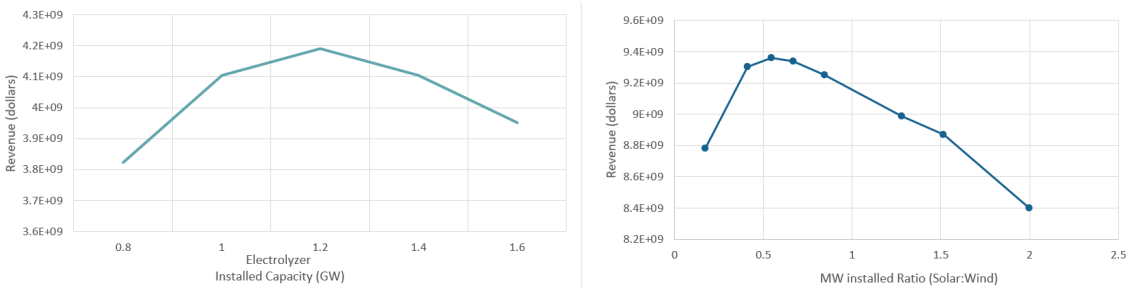


**Figure 5.3:** Initial optimizing for specific situation gives perception of sizes.

When an initial ratio investigation is done by varying different components for a variable budget, the step forward is to fix the budget while varying multiple components. The figure 5.4 displays the results of 16 different simulation setups, showing the accumulated hydrogen production over a year. Each line represents a different setup where multiple parameters have been adjusted while keeping the budget constant. The x-axis represents the time in megaseconds (Ms) over a full year, and the y-axis represents the accumulated hydrogen production in Kg. Variations in the slopes of the lines indicate seasonal changes in power production. A

flatter middle section of a line displays lower hydrogen production during the winter, while steeper slopes at the beginning and end of the year indicate higher production rates during the summer. This pattern highlights the seasonal dependency of hydrogen production in these setups.

It is crucial to distinguish this plot from similar ones for ammonia production. Although optimizing hydrogen production also affects ammonia production, ammonia has different efficiency and heating values, resulting in significantly lower production rates. This figure specifically focuses on hydrogen production and should not be confused with ammonia production plots, but the same argument of appearance of the curves applies. The primary purpose of this figure is not to find and compare individual outputs but rather to measure the variability of hydrogen production across a large variation in the ratios of the installed system components. By comparing the different setups, one can assess how changes in system parameters affect the consistency and reliability of hydrogen production throughout the year.

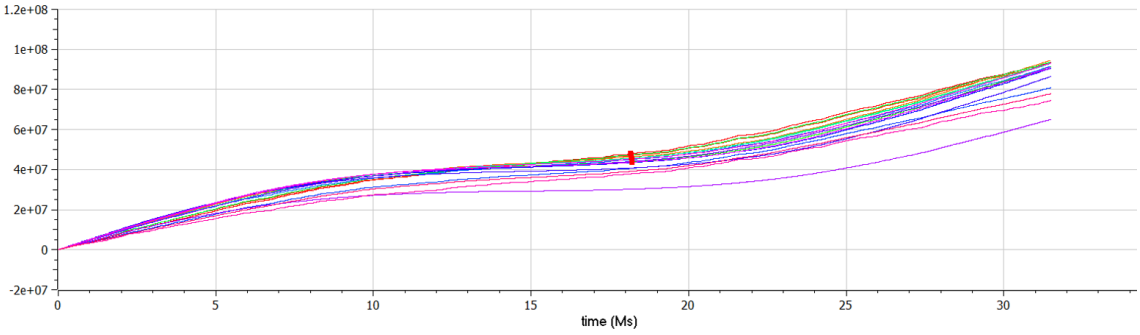


**Figure 5.4:** Exported Hydrogen for all ratios tested in Capex method

To further illustrate the complex methodology, the results of 17 selected simulations of different ratios from the previous figure are presented in Figure 5.5 showing the economic ratio of the 4 main components of the system and its connection to production. This result for this stage only considers CAPEX costs for overall understanding of the relations. The results are sorted after production, where the x-axis represents the chronological test number, corresponding to different simulation setups. The left y-axis shows the share of each component considering total CAPEX economics for Electrolyzer, BESS, Solar, Wind, assuming the main 4 components account for the total economy, which is fixed for all simulation setups. The right y-axis displays the hydrogen production. Each colored line indicates the share of a specific component, and the orange line represents hydrogen production. Observe that only the actual data points should be interpreted as the results in the figure, as the plot is not of a continuous time scale. Where connective lines are only present to identify trends.

From this figure, it is evident that there is significant variability in the share of each component across different tests, with wind and solar power showing the most fluctuation. As stated in the initial phase of the techno-economic optimization method in section 4.5.2, correlations between different components were explored. One example of such discovered correlation was the ratio of solar power and electrolyzer, which can be seen following approximately a 1:1 ratio in figure 5.5. This is also logical, since a higher ratio of solar power means a higher peak power output, which favors an electrolyzer with higher rated power. In contrast to this, the WPP does not follow the same correlation with the electrolyzer, as can be seen in

figure 5.5, since its output power during the year and during the hours of the day does not have as high peak power output, and therefore it is not necessary to have an electrolyzer with higher rated power.

The Electrolyzer and Battery shares remain relatively stable. Hydrogen production increases with certain configurations, but does not show a straightforward correlation with any single component's share. This lack of a clear pattern is one reason why a trial-and-error method was employed, as finding the optimal ratio for each component does not directly translate to increased hydrogen production. The main result of this method is therefore that very different ratios of components ended up in very similar hydrogen production. The large variation in the result for similar compositions also illustrates the difficulty of finding an optimum in a system with many variables.

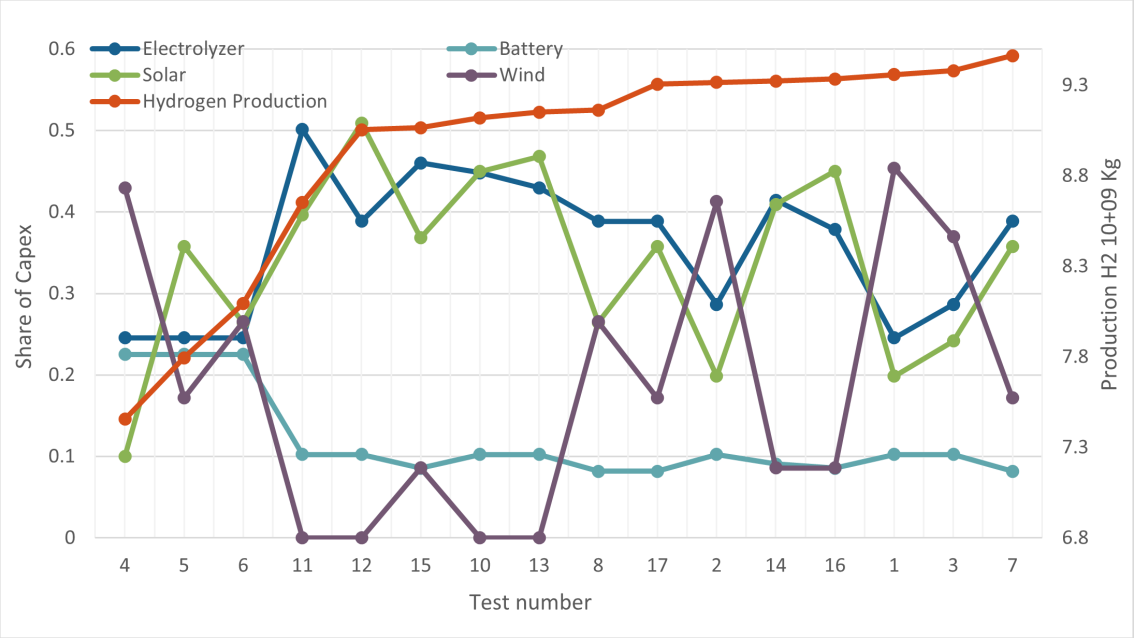


**Figure 5.5:** Ratios for 16 test setups with fixed CAPEX budget for the main 4 components.

For the best alternatives with the highest production, further analysis was performed to test the impact of OPEX by running 6 simulations presented in 5.6. These results resemble those with the highest production when considering an interest rate of 0 % where the total costs are still fixed as in the previous method. However, a new higher budget was set when including OPEX, which explains the higher produced hydrogen numbers seen in figure 5.6, meaning that it is the ratios of the components that is important in this figure.

The plot has the same appearance as figure 5.5. This analysis reveals that OPEX was significantly higher for certain components, with electrolyzers and wind turbines being particularly costly. As a result, the focus shifted to solar power as a result of its lower OPEX. According to this method, when considering an interest rate 0%, wind energy showed a slightly higher economic share than solar.

The outcome of these economic analyses, as depicted in the figure, indicates that all optimal

configurations incorporate both solar and wind power. This suggests a balanced approach to harnessing the strengths of both renewable sources to achieve the most cost-effective and efficient production setup.

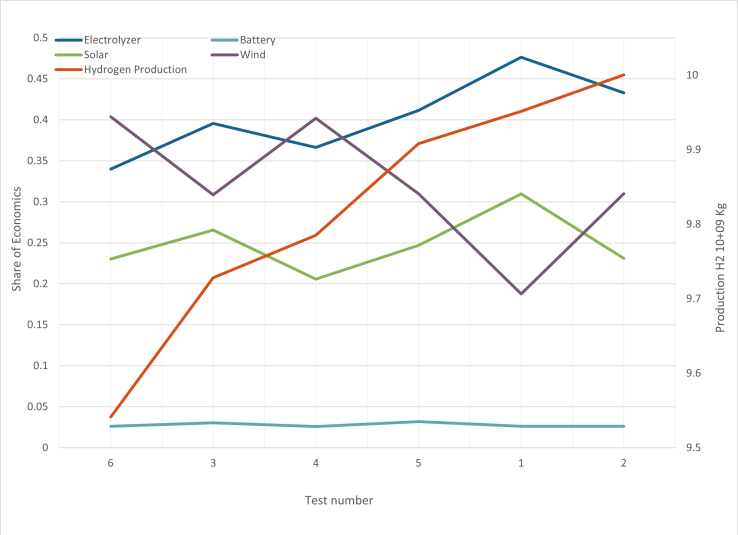


**Figure 5.6:** Ratios for 6 test setups with fixed budget of CAPEX and OPEX 0% interest rate for the main 4 components.

Finally, an interest rate of 8% was included in the analysis and several simulations and optimizations were carried out to optimize the previous result but calculating for a new fixed budget to meet the same installed ratios. None of the new installed capacity ratios exceeded those from the previous analysis, the best ratio found is for the new analysis the same as before as seen in figure 5.7, and in this stage the ratio of the best optimized alternative is decided.

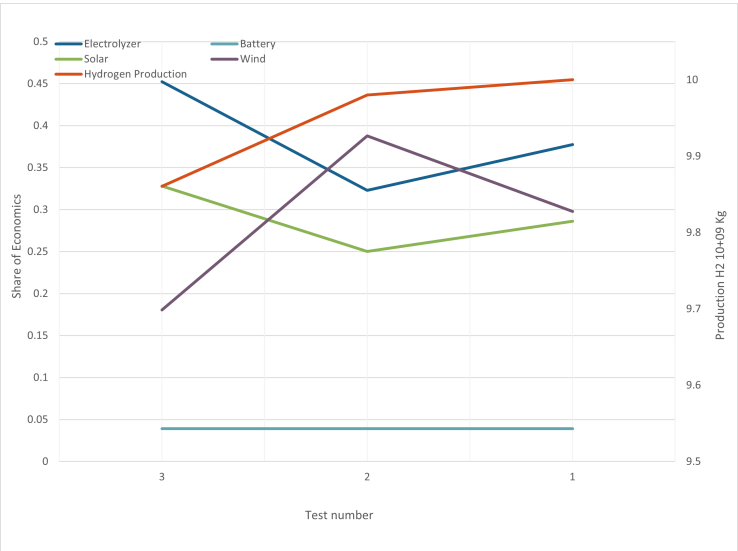


**Figure 5.7:** Ratios for 3 test setups with fixed budget of CAPEX and OPEX with 8% interest rate for the main 4 components.

### 5.3.1 Dimensioning Overview

Based on the above techno-economic optimizing method, the optimal ratios of the main four components have been determined and are presented in the fifth column of the table 5.6. In addition to the forecasted CAPEX and OPEX derived from the previous dimensioning, these are supplemented with economic values according to table 3.1 in the literature study to further calculate the final CAPEX and OPEX for the installed components. Unlike the previous analysis, which considered only four components, this comprehensive table includes all components of the system. The sizes for components are stated according to the information provided in the case study model input and techno-economic dimensioning, which are listed in column 5. The cost of OPEX for 30 years at an interest rate of 8% is also calculated according to the present value of the annual cost theory explained in Section 2.4.

**Table 5.6:** Final economics and sizes of system components.

| Component | CAPEX | OPEX | Unit | Our size | CapexCost ($) | OpexCost ($) | OpexCost ($) (30 y 8% interest) |
|---|---|---|---|---|---|---|---|
| DSP | 3968254 | 1095000 | $/MW | 2.2 | 8.73E+06 | 1.42E+06 | 1.60E+07 |
| Solar farm | 500000 | 13000 | $/MW | 3044 | 1.52E+09 | 3.96E+07 | 4.45E+08 |
| Wind farm | 2100000 | 89000 | $/MW | 660 | 1.39E+09 | 5.87E+07 | 6.61E+08 |
| Electrolyzer | 650000 | 40000 | $/MW | 1835 | 1.19E+09 | 7.34E+07 | 8.26E+08 |
| HB converter | 241475 | 3622.125 | $/MW | 1840 | 4.44E+08 | 6.66E+06 | 7.50E+07 |
| BESS | 270000 | 2500 | $/MWh | 900 | 2.43E+08 | 2.25E+06 | 2.53E+07 |
| Cables Transmission | 700000 | 0 | $/Km | 80 | 5.60E+07 | 0 | 0 |
| Cable Submarine | 3120000 | 0 | $/Km | 20 | 6.24E+07 | 0 | 0 |
| Desalinated water storage | 100 | 0 | $/m$^3$ | 25000 | 2.50E+06 | 0 | 0 |
| Ammonia storage | 1.04 | 0.0312 | $/kg | 25000000 | 2.60E+07 | 7.80E+05 | 8.78E+06 |
| Offloading port and equipment | 1.6E+07 | 160000 | $/300m berth | 1 | 1.60E+07 | 1.60E+05 | 1.80E+06 |

In table 5.7, the total costs after the project lifetime of 30 years for the present value are presented. In the first row, the total CAPEX and OPEX as well as the total cost are stated for all system components with an interest rate of 8%. Secondly, the same information is calculated excluding the costs of HB, electrolysis, and ammonia storage, to present the cost of an alternative project setup solely producing electricity. The added cost for the conversion of power to ammonia therefore account for 37% of the total costs in addition to the costs of energy losses. This makes it clear that to have efficient energy usage for nearby industries, the most viable option is to directly use electricity as a power source if the demand is flexible and there are no other restrictions.

**Table 5.7:** Final economics for CAPEX and OPEX at the project lifetime of 30 years for a interest rate of 8%.

| | CapexCost ($) | OpexCost ($) (30 y 8% interest) | Total Cost ($) |
|---|---|---|---|
| All components | 4.960E+09 | 2.060E+09 | 7.020E+09 |
| Excl $NH_3$ Tech | 3.297E+09 | 1.150E+09 | 4.447E+09 |

The CAPEX and first year OPEX columns from the table 5.7 are presented in pie charts in figure 5.8. Each segment of the pie charts represents the proportion of the total cost attributed to each component, providing a visual representation of the cost structure. These costs include all components, although the labels are only stated for the main 5 as the shares of the rest are too small to identify in the chart, with a combined cost of less than 5%. This provides a breakdown of the economic distribution for all main components, which clearly states that the main 5 components holds the main cost considering both CAPEX and OPEX.


**Figure 5.8:** Capex and 1 year Opex of the final optimized setup for all system components.

In addition, the total economics of the project, including 30 years of operation, are presented in the pie charts in figure 5.9. This considers the present value for 30 years with an interest rate of 8 % taken from Table 5.6. This figure shows very similar results to the CAPEX pie chart presented above.

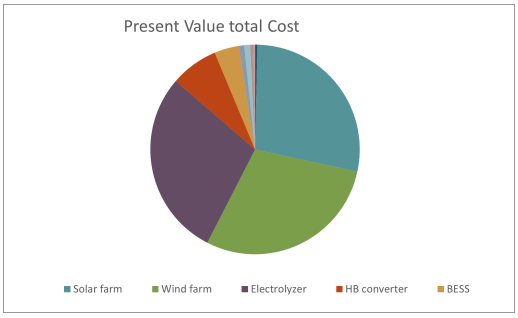


**Figure 5.9:** Total economics considering 30 years of operational costs at an interest rate of 8% and initial CAPEX costs.

The result of the total cost and CAPEX plot looking very similar, are investigated through looking at the relation between CAPEX and OPEX for a lifetime of 30 years for the different components. In the CAPEX:(CAPEX + OPEX) ratio of the main 5 components, shown in table 5.8, the CAPEX represents a similar share of the total economics for the five main components. If these ratios were identical, the total cost and CAPEX plot would be identical.

**Table 5.8:** Economical Ratio for the main 5 components

| | Solar farm | Wind farm | Electrolyzer | HB converter | BESS |
|---|---|---|---|---|---|
| CAPEX:(CAPEX+OPEX) | 77% | 68% | 59% | 86% | 91% |

### 5.3.2 Power-to-X Setup

At this stage, the dimension of the components in Table 5.6, is combined with the technological area coverage of 5.5 to obtain the area coverage of the specific components of the site stated in 5.9,

**Table 5.9:** Site Specific component area coverage

| Technology | Dimension | Size | Area coverage |
|---|---|---|---|
| Photovoltaics | 3044 MW | 4.3$m^2$/kW | 13.1$km^2$ =4x(3.28$km^2$) |
| Floating Turbines | 660 MW | 44 turbines with 10 D spacing | 180.1 $km^2$ |
| Offloading | 1 pier | 300 m/pier | 300 m |
| HVDC | 80+20 km | Length of cable | 80+20 km |
| Pipelines | 600m | Length of pipe | 600m |
| Li-ion BESS | 900 MW | Std. factory | 1 ha |
| NH3 Production (PEM+HB) | (1840+1835) MW | Std. factory | 1 ha |
| NH3 Storage | 25000 ton | 34246 $m^3$ | 33*33*33 $m^3$ = Std. factory (1 ha) |
| DSP | 2.2 MW | Std. factory | 1 ha |
| DSP tank | 25000 ton | 25000$m^3$ | Std. factory (1 ha) |

Figure 5.10 shows a screenshot from the "on-site" investigation made in Google Earth to identify suitable areas. From the Port Nolloth, South Africa case study in section2.7, one can see that there are major expansion possibilities. Both for generation, where Hexicon states that there is water suitable for wind power generation of up to 26 GW presented in section 2.7.2, as well as P2X production and other industries interested, as seen in Figure 5.10.


**Figure 5.10:** Picture of the landscape from a location outside of Port Nolloth.

Following all the constraints discussed in the selection of the wind and solar generation site from the literature study in Chapter 3 and combining this with the site-specific characteristics of the South African case study section 2.7, the proposed site of the project is made in the Port Nolloth area. By further combining the "on-site" observations through street view such as the observations seen in Figure 5.10, suitable sites for respective components are identified. Based on the coverage of the component area seen in Table 5.9, the locations of the different components are identified, where a detailed view of the Port Nolloth area is shown in Figure 5.11,

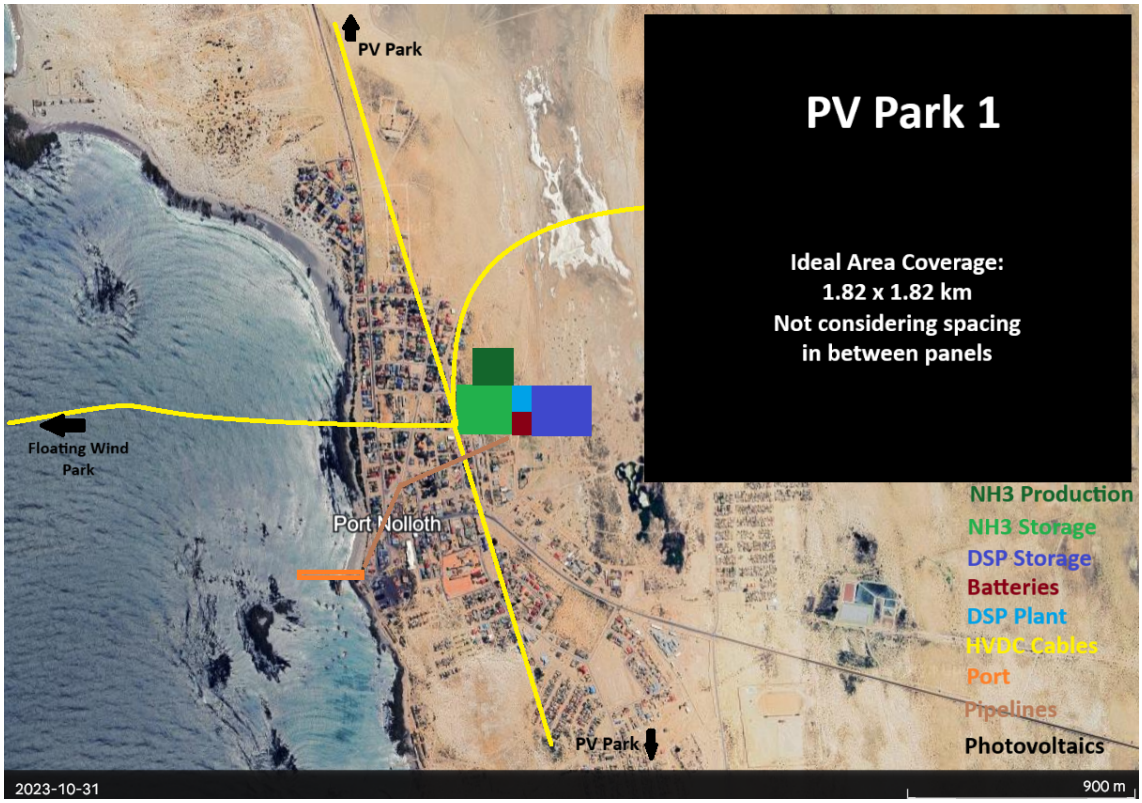


**Figure 5.11:** Port Nolloth overview of production plant

In addition, a zoomed-out map of the region with generation sites is seen in Figure 5.12, where the solar and wind generation area coverage is presented in 5.9. Further, one can see that the solar area coverage is divided into four parks marked as black and the Hexicon site selection work is linearly scaled down from 60 to 44 turbines marked as yellow.

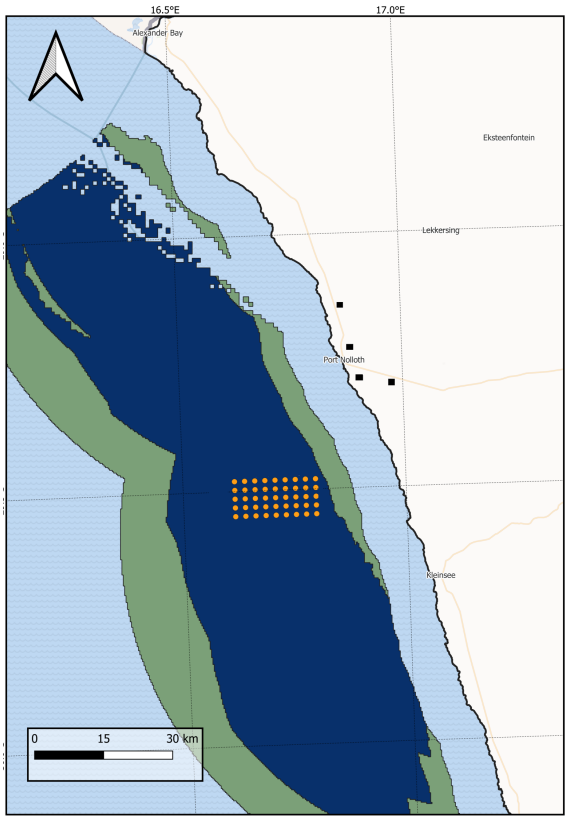


**Figure 5.12:** Region overview of generation sites

## 5.4 Simulation Results

In this section, the simulation results for the location of the Port Nolloth case study are presented. The simulation is run with a time step of 10 seconds for the renewable ninja dataset from 2019 with the key dimensioning inputs from the tables 5.6 and 5.2.

The sum of the wind production for the 44 turbines varies from zero to the rated power as seen in the figure 5.13. Looking at the graph a profile of the production matching theory can be seen. At first glance, it can be interpreted as that generation is fluctuating drastically during the 20 day timeline, but looking at individual days, the trends smooth. The cut in and rated power are clearly seen, where the production suddenly is capped at 640 MW and started at 0 MW. Observe that the trend is somewhat smoothed by the delay of the wind integrated in the model, whereas this graph should not be compared with wind profile of a single turbine at the site.

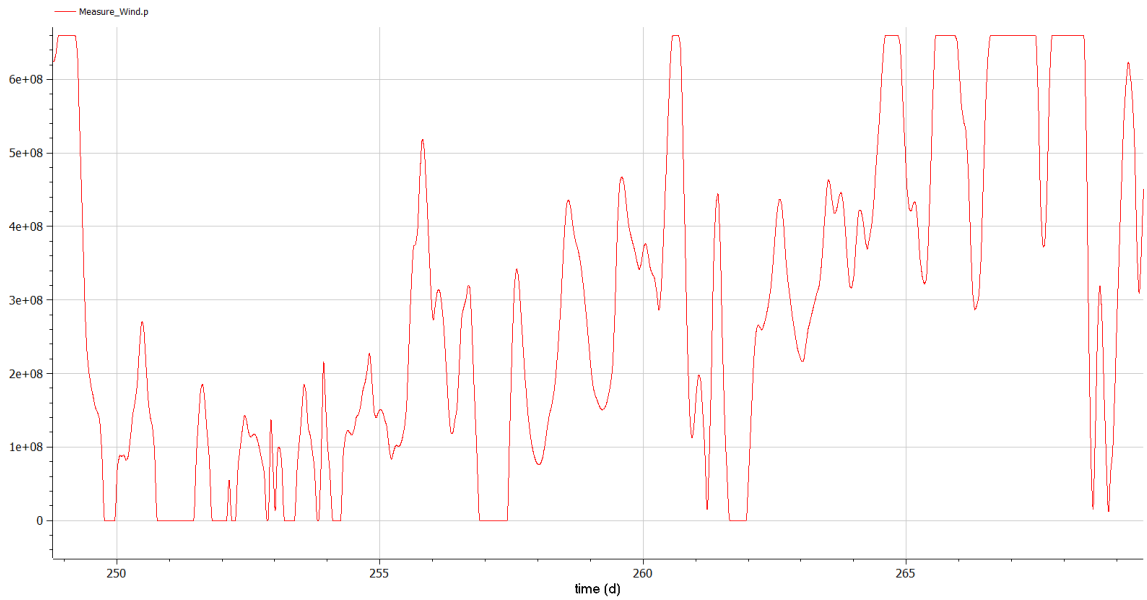


**Figure 5.13:** Wind production for 20 days

In figure 5.14, the power generation for the 3044 MW of photovoltaic can be seen. The peak for these specific days in mid February is just above 2000 MW, and during night there is no generation. For the plotted 5 days the data illustrates perfect irradiation curves as seen in the blue curve. One can see that the temperature affects the power output of the solar as the height of the curves otherwise should slope downward and that cloud interference is low for these specific days. To not overpower the system during peak hours where combined with wind, a fraction of the energy is curtailed, as seen in the red curve. The red curve is therefore the actual power output for these days. One can clearly see that the curtailment works as it should. First, a limited curtail occurs, where the battery power is capped to 200 MW; further, when the battery reaches 85 percent, the full curtailment is activated, not letting any more power into the battery.

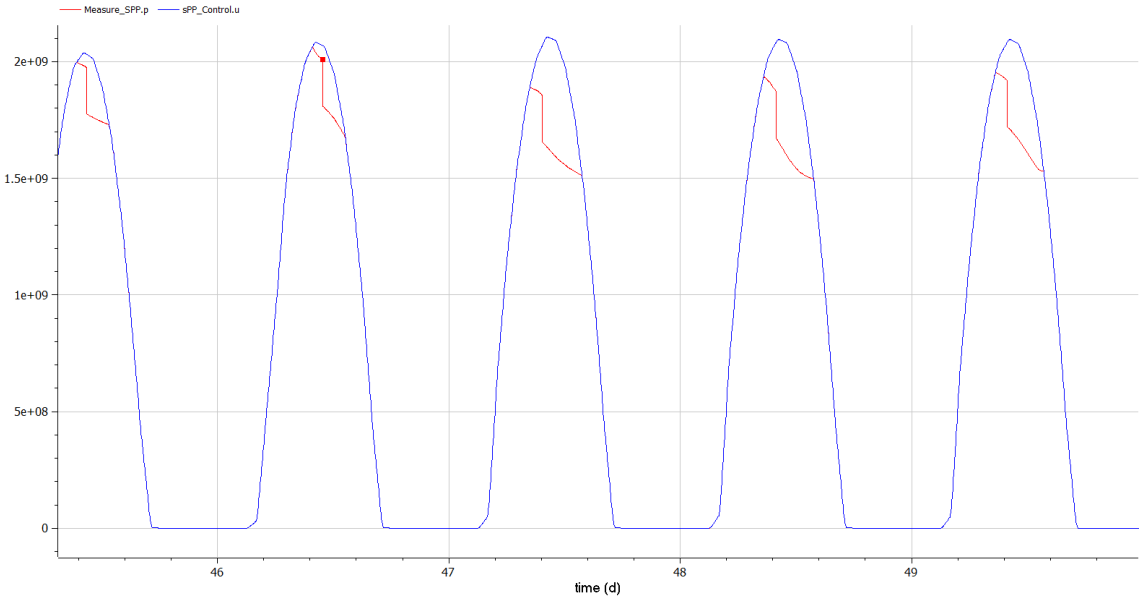


**Figure 5.14:** Solar Production for 5 days with curtail

For the whole year, the output of wind and solar production is illustrated in the figure 5.15 below. Wind production for the full year fluctuates between the rated power and zero, with no clear difference in the seasonal trend. For solar production, a seasonal trend is clearly visible, where it perfectly matches the yearly irradiation curve. Observe that solar production is curtailed as explained in the graph above, whereas the power for the peak irradiation has the potential of being even higher. In this ratio, in general, solar energy represents bulk production, whereas wind energy is used mainly to support the electrolyzer during nights and winters.

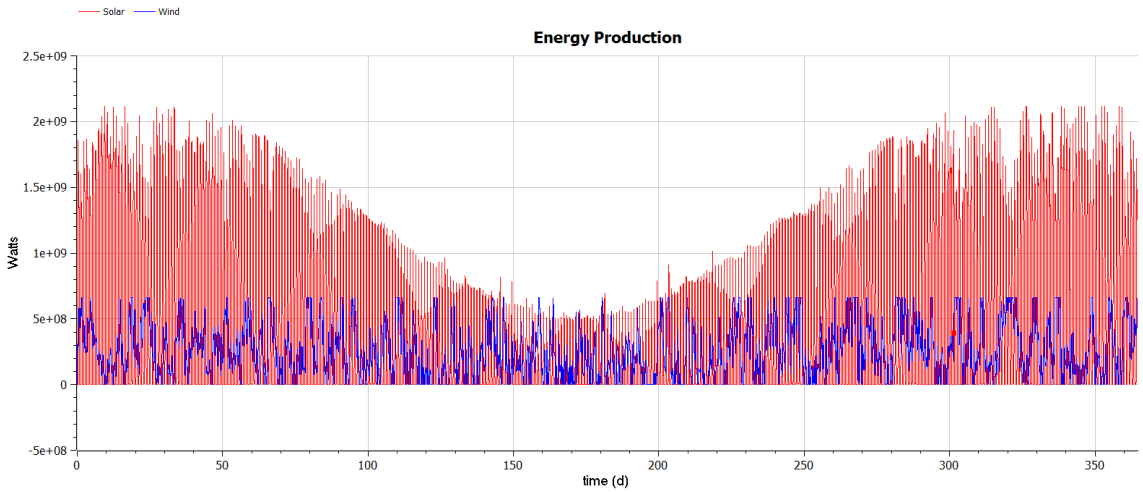


**Figure 5.15:** Solar and Wind power plant production during one year.

Further, the city and other industrial activity in the region is constantly drawing power as seen in figure 5.16. In the figure, a base load plus variable daily consumption is seen varying from 65 to 80 MW. This is built on a constant 50 MW from industries and consumption data for the scaled and mirrored (for hemisphere difference) Romanian dataset. It can be seen that during the night consumption is low, and during the day it increases, with peaks for morning and evening. Matching the example in figure 3.12 in the literature study.

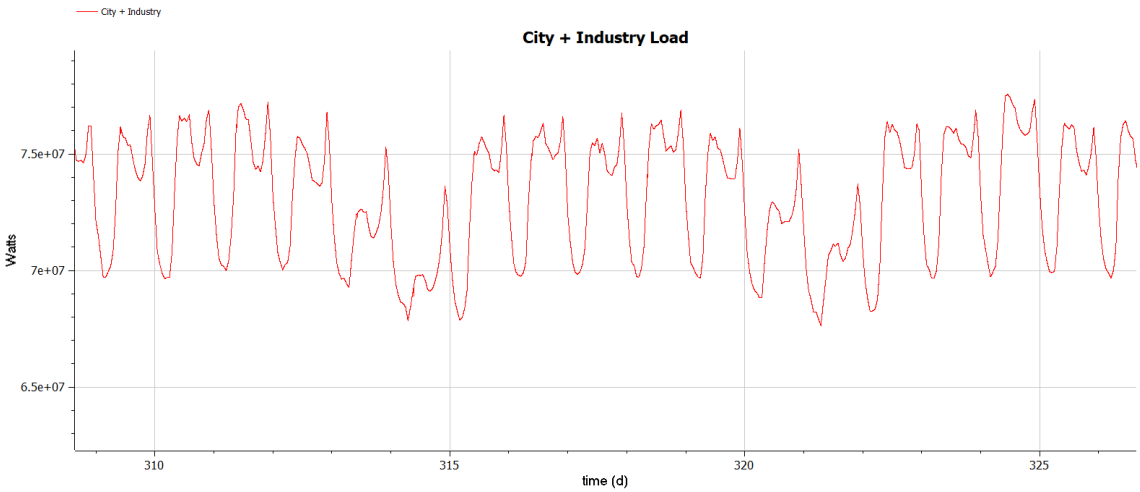


**Figure 5.16:** City and industry demand during 20 days

For the full year, the trend is seen in figure 5.17. The overall consumption trend is that people use more energy the colder season it gets, which validates the data set as energy consumption is higher the colder and darker it gets.

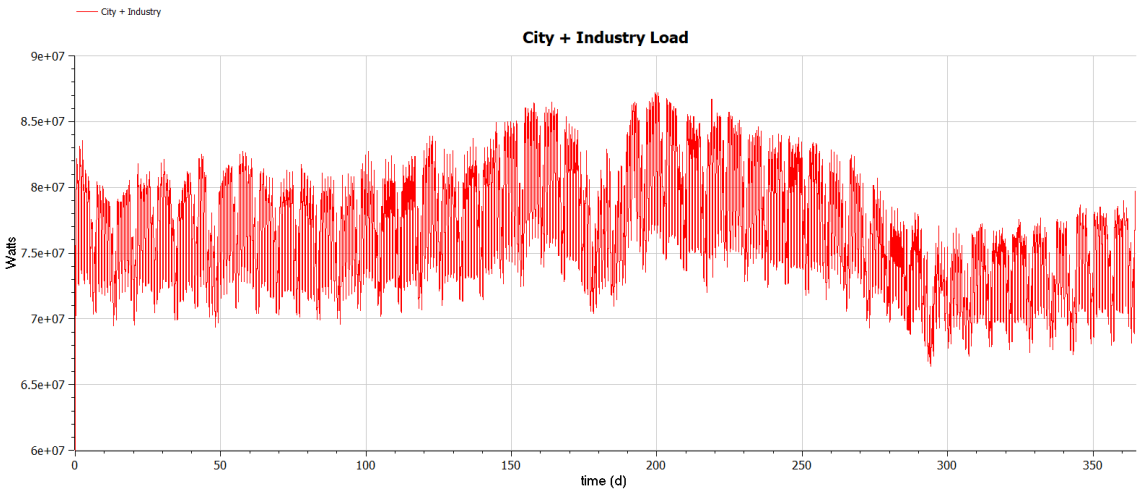


**Figure 5.17:** City and industry demand for the full year.

The water production in the DSP plant is seen in figure5.18 together with the water consumption. One can see that the stable production rate of 155 l/s is consumed with a variable consumption based on the operation of the electrolyzer, which consumes between 0 and 80 l/s by consuming 9 l per kg Hydrogen produced. Consumption also consists of a constant draw of 100 l/s for agriculture and 200 l per person per day from residents, as stated in table5.2.

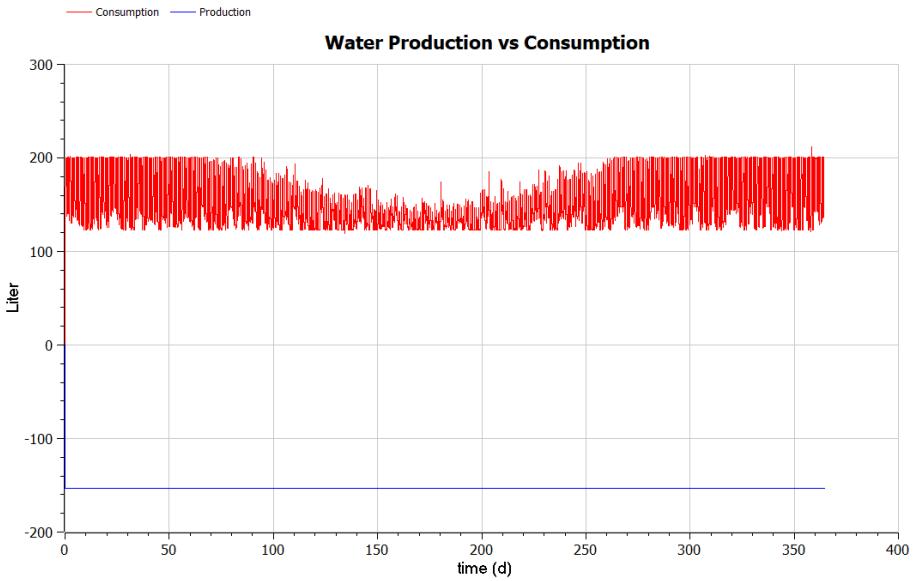


**Figure 5.18:** Desalinated water production and consumption

The main load in the system, which is the combined electrolyser and Haber Bosch process, is seen in figure 5.19, together with the total power production in the system. The red area seen in the figure is, therefore, curtailed or used to charge a battery or use domestic energy. In the figure, one can see that the capping mechanism of the electrolyzer works as intended, by never exceeding 1835 MW, and that the trend of the very variable wind can be seen by the "spikes" during the summer months exceeding the solar power generation.

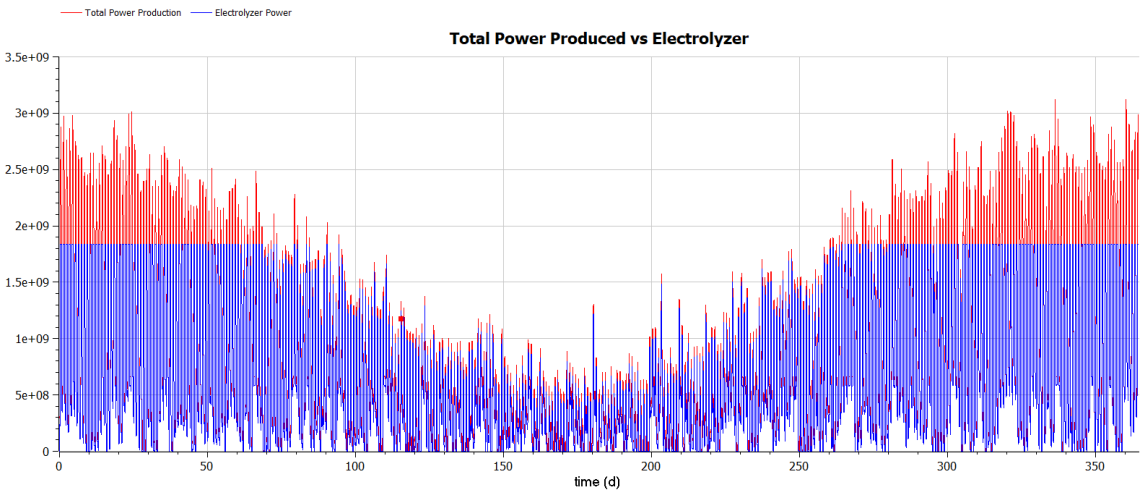


**Figure 5.19:** Total power potential vs electrolyzer+HB production

Most of the power exceeding the rated power of the electrolyzer is curtailed. The cumulative power for the entire year is shown in figure 5.20 together with the energy generation from the wind and solar production plants. In this graph, it can be seen that there is simply no curtailing during the South African winter, where the solar peaks are lower than the rated power of the electrolyzer.

Looking further into the figure, one can see that the power generation trend looks differently for wind and solar throughout the year. Looking at the steepness of the red curve the solar power produces much more during summer and the wind produces almost constantly over the year, with little seasonal variation for the Port Nolloth site. Looking at the end value of the cumulative graph Annual Energy Yield (AEY) values are seen. The AEY of solar energy generation is 4035 GWh, and for wind energy generation its is 2292 GWh and from curtailment it is 410 Gwh. The percentage of energy curtailed is given by dividing curtail with generated power and is 6.5 percent. Using the equation for capacity factor stated in literature study equation 3.1 the capacity factors for the solar and wind power generation are according to following calculations,

$$CF_{wind} = \frac{2292}{8760 * 640} = 0.408 \tag{5.1}$$

$$CF_{Solar} = \frac{4035 + 410}{8760 * 3022} = 0.168 \tag{5.2}$$

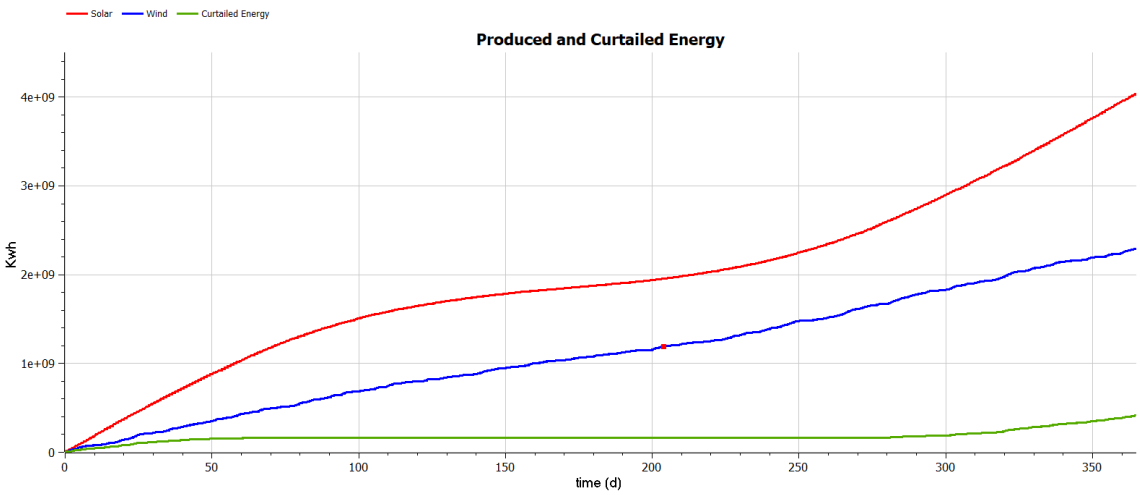


**Figure 5.20:** Cumulative produced power of Solar and Wind as well as total curtailed energy for the full year

The state of charge of the battery that ranges from 0.9 to 0.1 for the entire year is shown in figure 5.21. The performance of the battery vary greatly between seasons, where it is mainly regulated upward during the summer months and downward during the winter months.

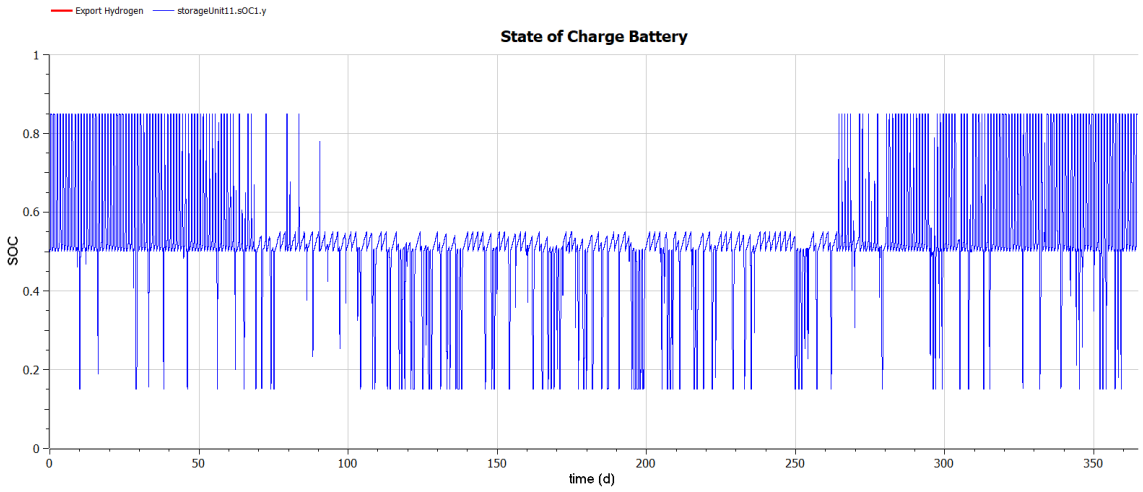


**Figure 5.21:** SoC for the BESS for the full year

This trend can be explained by looking at a zoomed version of the graph seen in Figure 5.22 where both voltage regulating up and down is seen for a period of 20 days. During winter, the photovoltaic system cannot produce enough power to supply the full installed capacity of the electrolyzer. Therefore, there is no excess power available to charge the battery. The system prioritizes ammonia production, which requires downward regulation. This is evident in the graph where the SoC of the battery remains relatively low and fluctuates with small peaks and deep troughs, which leads to limited charging and frequent discharging. When power production generates a net surplus, the electrolyzer controller prioritizes charging the battery by slightly reducing hydrogen production. This results in an increase in the SoC of the battery. As mentioned in the battery method 4.2.6, the battery is used for peak shaving, where the energy stored in the battery supports the operation of the electrolyzer during high demand periods, following the logic described in the electrolyzer method 4.2.9. When the SoC is even lower, and there is a long-term deficit of energy in the system, mainly during winter, the fuel cell is activated to produce electricity, compensating for the battery's inability to meet the power demand. This results in the observed deep troughs in the SoC graph during winter periods.

In contrast, during summer, the photovoltaic system generates enough power to reach the rated capacity of the electrolyzer, especially during the daytime, when solar power reaches full capacity. During these periods, excess power charges the battery, causing the SoC to rise. The battery begins to regulate upward, storing the surplus energy. At night, if wind power is not sufficient, the battery is discharged to supply the necessary power. This behavior is seen in the graph by higher SoC levels and daily charging cycles during the summer.

Using the method described in the data collection block 4.2.10 to determine battery cycles, one can see that the lifetime limit of 5000 cycles of the lithium battery is not exceeded while having a higher production, compared to not integrating peak shaving where the battery is used much less frequently.

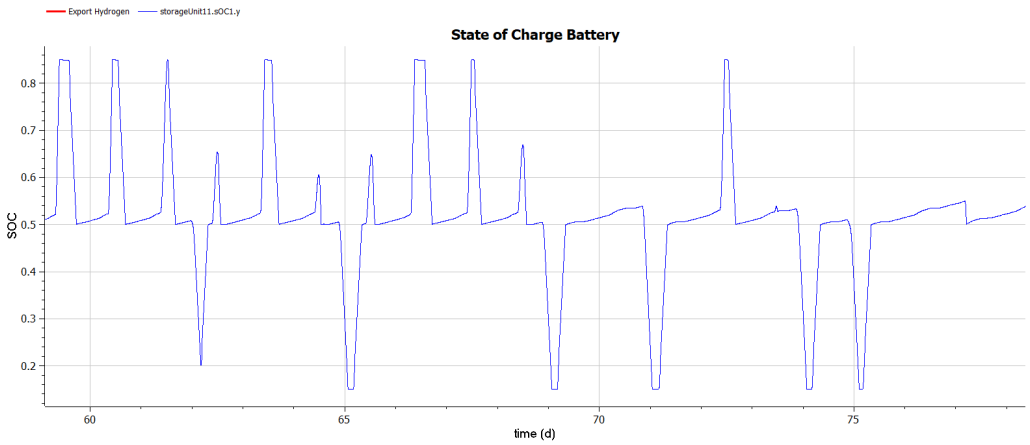


**Figure 5.22:** SoC for the BESS 20 days

To limit the CAPEX of the battery, its power is capped at 250 MW as stated in table 5.5. The power outage over the year is seen in figure 5.23 where the charging battery is negative power while the discharge is positive. From the graph, some clear trends are seen. First of all, the behavior of the battery is very different between summer and winter, as it is directly linked to the state of charge. In summer (start and end of graph), one can see that the curtailing logic works, where the battery is charged with a maximum of 200 MW. The battery is also drained with around 200 MW, when the SoC is high. During the entire time series, the positive load of around 80 MW is the city's demand during nights with no wind or solar generation. The higher negative peaks occur when the battery's SoC is low and the power generated should prioritize charging before producing hydrogen. During summer, the state of charge is lower and battery operation is less, when the electrolyzer rarely reaches its rated capacity.

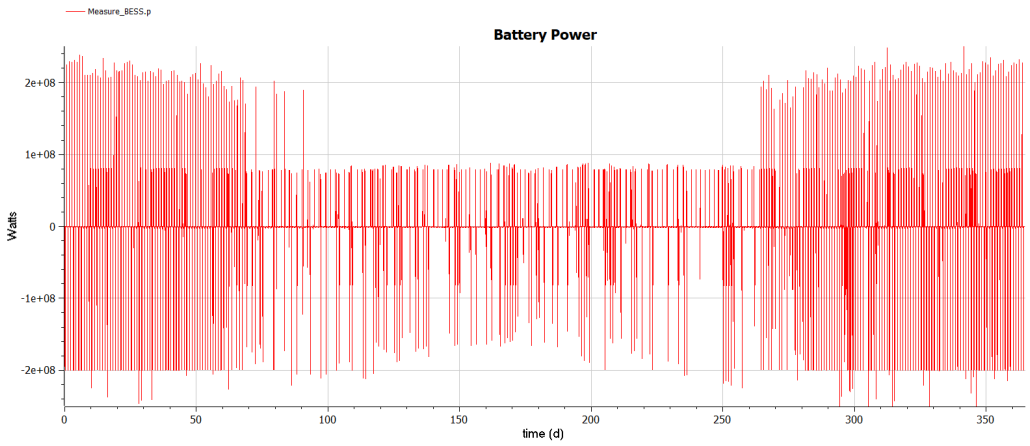


**Figure 5.23:** Power for the BESS not exceeding 250 MW for the full year

The fuel cell operation for the entire year can be seen in figure 5.24, where it can be seen that it starts frequently, but the power (maximum 90 MW compared to 1835 MW for ammonia production) and the operating time is low. When the SoC of the battery is lower than 15%, the fuel cell begins to activate the voltage regulation in the battery. The FC mechanism is made to consume as little hydrogen as possible matched to consumption at every moment.

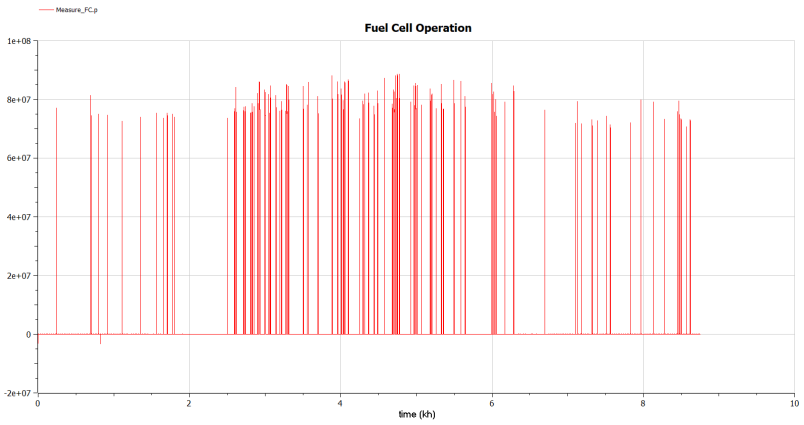


**Figure 5.24:** FC operation for the full year with maximum load of 90 MW

The total exported energy, which is the difference between ammonia production and consumption, is shown in Figure 5.25. In the figure, it is clear that the production is much higher in the summer. Overlapping this graph with the figure 5.20, it is clear that the solar generation flattens out during the summer, only managing to supply the city. Without wind power during winter, there would simply be no ammonia production, since solar energy does not provide sufficient power in winter. This underscores the importance of using wind energy, in addition to managing the day/night shift presented in 5.3. In the figure below, it is also evident that the consumption of ammonia is only a fraction of the production, even when a relatively small battery bank is used. Therefore, for this project setup, further optimizing the battery expenditure is not prioritized, the consumption is 0.53% of the production. With total export after 1 year of production of 720 Millions kg ammonia.

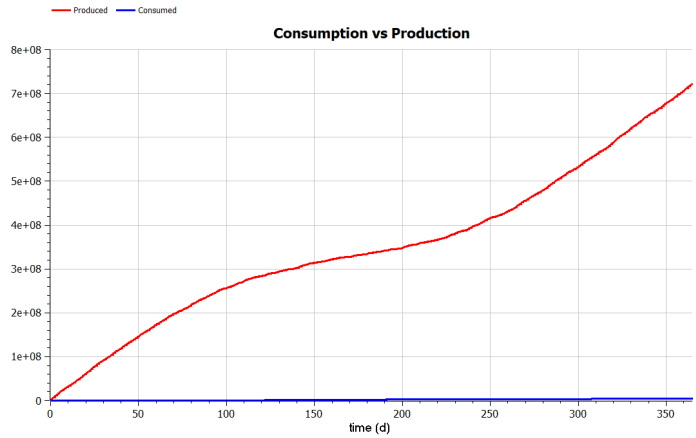


**Figure 5.25:** Cumulative kilograms of ammonia produced during one year.

Further interesting to present is the a wasted energy graph in 5.26. Here, the energy lost during the full year is illustrated. The loss of power in the system occurs in part by supplying the system with power through the conversion of ammonia, but also through the curtailment of existing power. In addition, it is evident that the energy lost by curtailing is much higher than the energy lost by running the fuel cell where the lost power through the use of FC only accounts for 15% of the lost power by curtailing.

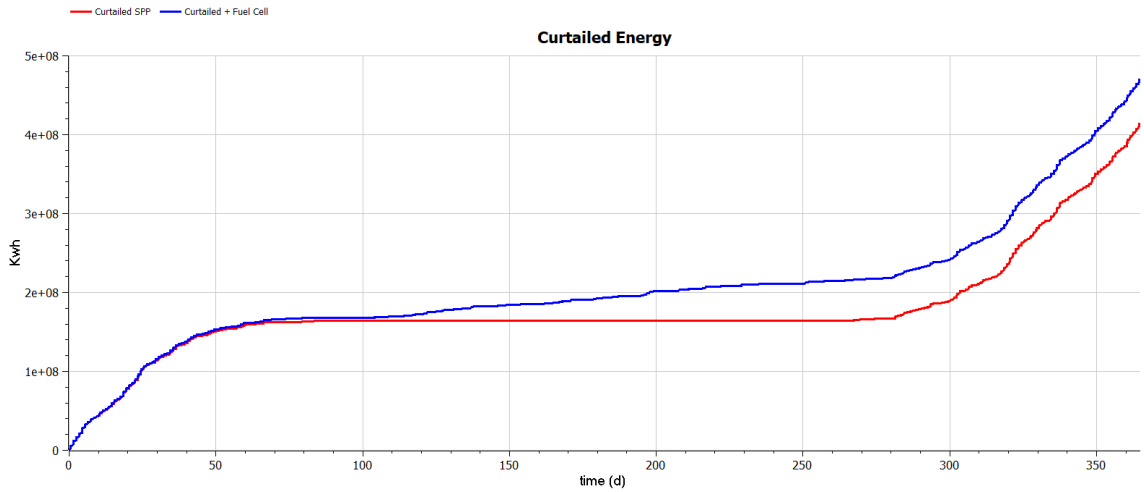


**Figure 5.26:** KWh of wasted energy from curtailing and the round trip energy use of fuel cell operation

The offloading operation of the ammonia storage is seen in the figure 5.27, which is the state of charge of the Ammonia storage for the full year. The size of the offloading is 10,000 tons, corresponding to a ship as stated in table 5.5. The time between offloading varies between 15 days in winter (low production) and 3 days in the summer (peak production). For the full year, 70 ships are therefore exporting ammonia from the project site. In the model, the offloading starts when the SoC reaches 90 % although in reality they need to be planned in advance. From this figure, the ammonia storage bank seems very over-dimensioned in the simulation model. This is because of preparation for land-based infrastructure and energy needs, where the idea is to have other offloading for local industries from which there will be a higher consumption variability.

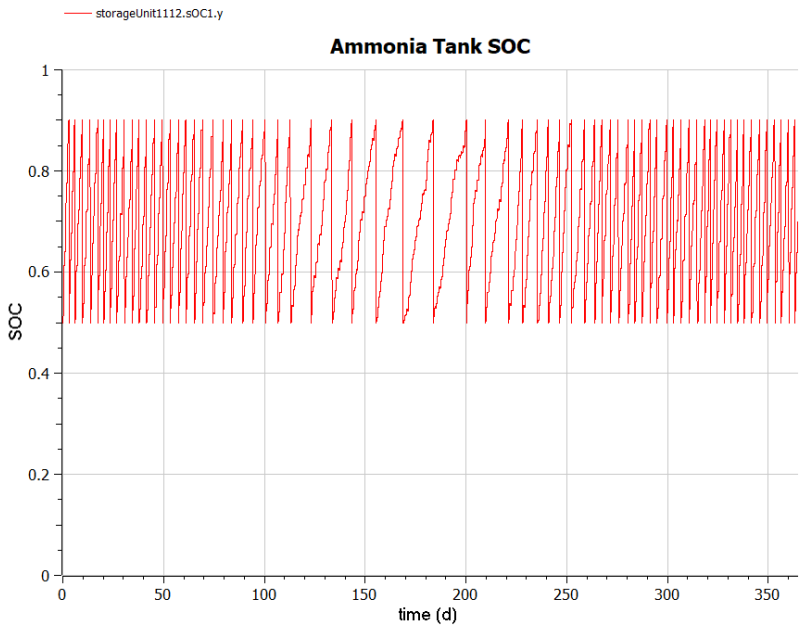


**Figure 5.27:** SoC for the hydrogen tank for the full year.

The SoC of the DSP tank is affected by the DSP production and offloading mechanism. The SoC results for the entire year are seen in Figure 5.28. In the figure, there is slight over-production throughout the year. This is needed because of comprehensive extra evaporation calculations varying from year to year. When the stores are full, the DSP can be turned off, or extra usage can be applied. Important to notice is that this assumes that no water can be reused in the system, so the overproduction will be even higher in reality, when including water treatment plant.

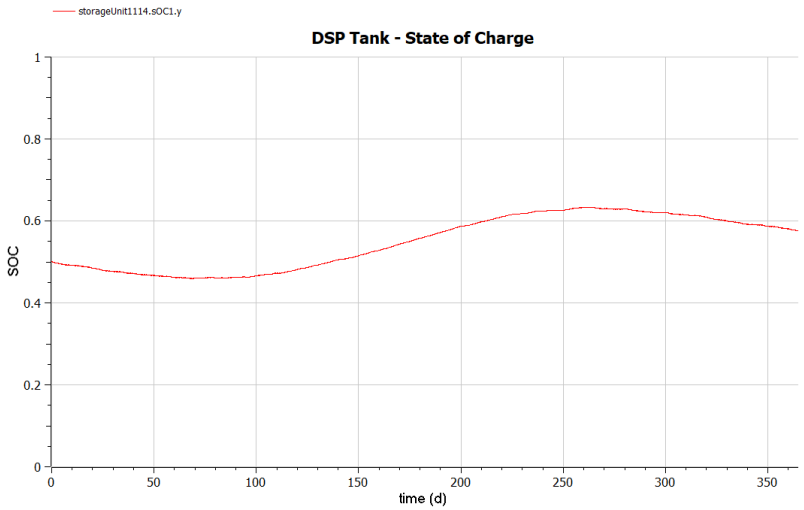


**Figure 5.28:** SoC of DSP tank for the full year

Lastly, a plot of the voltage in the system for the whole year is shown in figure 5.29. In the figure, small variations are seen, which are directly connected to the operation of the battery that is balancing the system, where a slight delay in response leads to a voltage drop or increase. The voltage is for the full year remaining stable at a level of 1 000 000 V +- 40 volt corresponding to a change of 0.004 percent.

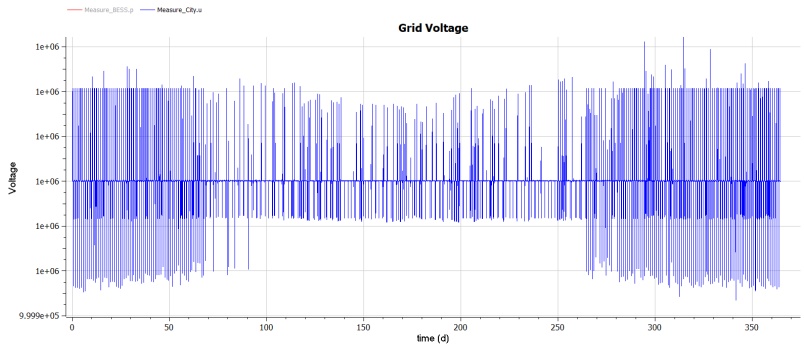


**Figure 5.29:** Voltage level of the DC grid during one year (V).

### 5.4.1 1 Year Result Summary

In table 5.10 all the outputs from the data collection block are stated. This presents the main simulation outputs after a full year of production. In the table, the total electricity production is the sum of wind power, solar power and curtailed electricity. Wasted energy is curtailed energy plus the losses from storing energy in ammonia to later be used in the system itself. The electricity consumption of ammonia production is all electricity consumed by the electrolyzer + HB, which generates the ammonia production. The consumption of ammonia occurs through FC operation, where the difference between these two is the exported ammonia. The electricity usage of the city, BESS and FC electricity production is also stated.

**Table 5.10:** Yearly Production Data summary

| Parameter | Value | Unit |
|---|---|---|
| Total electricity production (incl Curtailed) | $6.73697 \times 10^9$ | kWh |
| Wind electricity production | $2.29177 \times 10^9$ | kWh |
| Solar electricity production | $4.03509 \times 10^9$ | kWh |
| Curtailed electricity | $4.10118 \times 10^8$ | kWh |
| Wasted electricity | $4.76381 \times 10^8$ | kWh |
| Ammonia Production Electricity Consumption | $5.65589 \times 10^9$ | kWh |
| City electricity Usage | $6.69489 \times 10^8$ | kWh |
| BESS Bidirectional electricity usage | $1.75063 \times 10^8$ | kWh |
| Fuel Cell electricity Production | $3.01014 \times 10^7$ | kWh |
| Ammonia Production | $7.2609 \times 10^8$ | kg |
| Ammonia Consumption | $3.904 \times 10^6$ | kg |
| Exported Ammonia | $7.22185 \times 10^8$ | kg |

## 5.5 Final Economical Results for Project Lifetime

To have an idea of the final economics of the project, the LCOE of the production of Ammonia, hydrogen and electricity are presented in figure 5.11, togheter with the total production volume of each energy carrier is presented. These prices are based on the values in Table 5.6 and a project lifetime of 30 years with an interest rate of 8%. The LCOE prices have been calculated using the LCOE formula in equation 2.2 from Chapter 2. When calculating the LCOE of ammonia, simply all CAPEX and OPEX stated in table 5.6 are considered. The same applies for hydrogen, although in reality the Haber-Bosch process should not be considered. However, extra costs of storage and logistics for each respective energy carrier should be considered, but in this case the total economics are assumed to be similar for the two different generation plants. When calculating the LCOE for electricity, the CAPEX and OPEX of all technologies related to energy carrier production are disregarded, such as electrolyzer, haber-bosch, and ammonia storage.

**Table 5.11:** LCOE, LCONH3 LCOH for the full project life time with interest rate of 8 percent.

| Parameter | Value |
|---|---|
| Produced Ammonia (kg) | $7.21 \times 10^8$ |
| $LCONH_3$ ($/kg) | 0.865 |
| Produced Hydrogen (kg) | $1.02 \times 10^8$ |
| LCOH ($/kg) | 6.143 |
| Produced Electricity (kWh) | $6.75 \times 10^9$ |
| LCOE ($/kWh) | 0.059 |

### 5.5.1 Model Input Correction Results

The capacity factors calculated in equation 5.1 and 5.2 was 0.408 for wind power and 0.168 for solar power respectively. However, capacity factors of 0.56 for wind power and 0.24 for solar power was discovered in the case study in Section 2.7. In this following section, the result from scaling the electricity generation data taken from renewable ninja to match the annual output and capacity factors of the case study in section 2.7, is displayed. In addition, the efficiency of the electrolyzer is changed from 0.72 to 0.8 (which leads to 0.72 for electrolyzer + HB) and the efficiency of the fuel cell is changed from 0.72 to 0.6 (leading to 0.54 fuel cell + HB). Keeping the rest of the inputs from the previous results, the new outputs are presented in Table 5.12 in the same way as for 5.10. In Table 5.12 the new values are stated together with the old values and the percentual change.

Looking at the percentual change in the results, one can see that the change of capacity factors has a clear impact on the power generated, for both wind, solar and curtailed power. Both the power consumption and ammonia production increases due to increase electricity production. However, the percentual difference between them is due to the change in efficiency of the electrolyzer. The city consumption is kept constant, while the fuel cell operation is

lower, due to the higher availability of the wind during the night. The total output of the adjustments deliver 35% more ammonia. Meanwhile, the power produced increases, and the electrolyzer and other components remain at the same capacity.

The optimized techno-economical method therefore would have to be remade for the new inputs to find the optimal ratio, but due to time constraints it was not included in the scope of this thesis.

**Table 5.12:** Comparison of Yearly Production Data

| Parameter | Initial Value | New Value | Change (%) |
|---|---|---|---|
| Total electricity prod (incl Curtailed) | $6.73697 \times 10^9$ kWh | $9.56857 \times 10^9$ kWh | +42.0% |
| Wind electricity production | $2.29177 \times 10^9$ kWh | $3.21407 \times 10^9$ kWh | +40.2% |
| Solar electricity production | $4.03509 \times 10^9$ kWh | $4.60561 \times 10^9$ kWh | +14.1% |
| Curtailed electricity | $4.10118 \times 10^8$ kWh | $1.74907 \times 10^9$ kWh | +326.5% |
| Wasted electricity | $4.76381 \times 10^8$ kWh | $1.81677 \times 10^9$ kWh | +281.4% |
| Ammonia Prod. Electricity Cons. | $5.65589 \times 10^9$ kWh | $7.14184 \times 10^9$ kWh | +26.3% |
| City electricity Usage | $6.6947 \times 10^8$ kWh | $6.6947 \times 10^8$ kWh | 0% |
| BESS Bidirectional electricity usage | $1.75063 \times 10^8$ kWh | $2.17138 \times 10^8$ kWh | +24.0% |
| Fuel Cell electricity Production | $3.01014 \times 10^7$ kWh | $2.62323 \times 10^7$ kWh | -12.9% |
| Ammonia Production | $7.2609 \times 10^8$ kg | $9.78057 \times 10^8$ kg | +34.7% |
| Ammonia Consumption | $3.904 \times 10^0$ kg | $2.73355 \times 10^6$ kg | -44.7% |
| Exported Ammonia | $7.22185 \times 10^8$ kg | $9.75321 \times 10^8$ kg | +35.0% |

The increase in ammonia production has a direct effect on the levelized cost of ammonia (LCONH3), which together with LCOE and LCOH are calculated in the same way as before and shown in Table 6.1. The values are further compared to the previous ones by presenting the percentual change. As reasoned before, even though one can see a clear decrease in the levelized costs of energy, using the new model inputs, the techno-economical optimizing method would, as prevously mentioned need to be applied to have optimal production. Combining the results from the two presented simulations although delivers interesting findings and conclusions of the outcome of the project, stated in the discussion in chapter 6.

**Table 5.13:** Comparison of production and costs for the corrected values for LCOE, LCONH3 and LCOH.

| Parameter | Initial Value | Corrected Value | Change (%) |
|---|---|---|---|
| Produced Ammonia (kg) | $7.21 \times 10^8$ | $9.75321 \times 10^8$ | +35.4% |
| $LCONH_3$ ($/kg) | 0.865 | 0.639322769 | -26.1% |
| Produced Hydrogen (kg) | $1.02 \times 10^8$ | $1.444 \times 10^8$ | +41.6% |
| LCOH ($/kg) | 6.143 | 4.318178134 | -29.7% |
| Produced Electricity (kWh) | $6.75 \times 10^9$ | $9.5695 \times 10^9$ | +41.8% |
| LCOE ($/kWh) | 0.059 | 0.04127431 | -30.0% |

# Chapter 6

# Discussion

## 6.1 Result Discussion

The results of the study provided several interesting findings that align with the objectives of the thesis. The analysis was supported by various graphs and data visualizations that illustrate the insights gained from our investigations. By building a simulation model to validate the functionality of the system and then applying a techno-economic optimization method, the potential for floating wind was thoroughly investigated in off-grid P2X megaprojects. In this chapter, the results and findings are further discussed to lead to the final project conclusions.

### 6.1.1 Floating Wind Investment

The result of the economic analysis indicated that all the component ratios tested with the highest energy carrier production both incorporate solar and wind power, even though the LCOE value of wind power is substantially higher than that of solar. There are several reasons behind this. The wind conditions for the specific case study are quite unique, with properties such as a power shift in the evening and relatively small seasonal variations. This makes wind power a good complement to photovoltaic systems that have strong daily and seasonal variations, which suggests a balanced approach that harnesses the strengths of both renewable sources to achieve the most cost-effective and efficient production setup. The more wind power used, the stronger the effect of the power shift is, which apart from increasing ammonia production and limiting fuel cell usage decreases the cycles of the battery, which is of key interest for longer simulations where the BESS could have to be changed if 5000 cycles exceeded. The fact that the wind played a key role in the project could also be explained by the fact that the electrolyzer had relatively high CAPEX and OPEX. Although the electrolyzer consumption is elastic using PEM technology, the lost revenue from low-irradiance seasons

further consolidates the need to install wind power, since most of the electrolyzer capacity during summer otherwise is not used.

It was also discovered that the trend was not as strong for onshore wind conditions, further strengthening the choice of using floating turbines instead of onshore. The choice of offshore wind is also strengthened by its upscaling possibilities due to less area constraints at sea and the logistical possibilities of larger turbine size, making the conditions favorable over land-based wind. However, it could be criticized that the model does not include any share of onshore wind, but the use of another component with different wind data and other CAPEX and OPEX to include in the techno-economic optimization is out of the scope of this thesis.

### 6.1.2 Economical Method Evaluation

An interesting finding from the economical result is that although a failure was made by optimizing based on an interest rate of 0%, the optimal ratio still was the same when integrating the interest rate of 8 %. This can be explained by the fact that initial optimization based on CAPEX showed an economical ratio similar to the final results, including the interest rate. However, when testing for an interest rate of 0% the results become unrealistic. However, what this means is that it is possible that only local maximums around the tested combinations of installed capacities are analyzed, missing the global maximum. A better alternative would therefore be to include the interest rate from the beginning, but for this project there was not enough time to do it. Important to consider is, although, that even though the results might not lead to the optimal ratio, the main conclusions are still the same.

The reason why the CAPEX and Total economic ratios including the 8% interest rate for the final economics showed similar ratios was because the similar OPEX:CAPEX ratio shifts the installed capacity for different setups differently. A ratio with a high installed wind capacity (with its high OPEX ratio according to Figure 5.8) will now be less OPEX heavy due to discounting. This makes it possible to install more solar panels while keeping the budget, for example. Because electrolyzers have a high OPEX ratio, and solar panels have a low ratio and are coupled together for our simulation, the effects oppose each other, leading to very similar ratios to what we observed before, ending up with a result close to CAPEX.

The fact that the model is linearly scalable can also be criticized when it comes to economical optimization. Although using the methodology described, there is no alternative solution to doing so in the scope of this report when it comes to optimization. One way to generate more reliable calculations would be to redo the calculations based on the final dimensions. However, this takes the essence away from the striving toward simplicity in scaling the method itself. It is important to consider that for the scope of this master thesis, achieving precise economic accuracy is not prioritized in favor of building a tool which is scalable.

### 6.1.3 LCOE Analysis

Comparing the capacity factors from our data shown in Equations 5.1 and 5.2 with the background data in Section 2.7, our values of 0.168 for solar power and 0.408 for wind power are substantially lower than the values of 0.23 and 0.56 respectively. For solar, this means that the capacity factor is 27% lower than the reference value for the chosen site from the Global Solar Atlas, and for wind power, it is 29% lower than the reference value provided by Hexicon. This discrepancy likely occurred due to errors in the dataset provided by the Renewable Ninja. However, these capacity factors are not totally unrealistic, as the global average capacity factor for offshore wind is in the same range, and for solar it is usually between 0.10-0.25, as stated in the capacity factor section for both wind and solar power, seen in Sections 3.1.1 and 3.2.3.

Further analysis reveals that assuming that the fuel cell uses the same efficiencies as the electrolyzer can be questionable. Some sources show that the electrolyzer efficiency is generally higher than stated in the simulated setup. However, since fuel cell consumption is very low for the project, using more accurate numbers would not significantly impact the main outcome. The prediction of future efficiencies for technologies such as electrolyzers is uncertain, which affects the overall performance of the system.

Due to these inaccuracies in the model inputs, some of the simulations with the best results were rerun with the new capacity factors and efficiencies, to focus on the economic output of the project presented in Section 5.5.1. This was done to understand the range of forecasted LCOE values for such a setup. It is important to note that implementing these adjustments means that the techno-economical optimization is no longer valid, so the LCOE-values are expected to improve if all simulations are redone, and a ratio closer to optimum is found.

Although the inputs generating the main results are believed to be incorrect, the economic results are discussed based on both the new simulations (without economic optimization) and the old results. The levelized costs of hydrogen (LCOH), ammonia (LCONH3), and electricity (LCOE) from our results, shown in Table 6.1, are compared with forecast ranges and target prices from the literature study, shown in Table 3.2. This comparison is essential to understand the feasibility and potential impact of our production costs on the development of future infrastructure.

The LCOH in our analysis is $6.14/kg, which is within the predicted range of $5-$8/kg but higher than the government targets of $1-$3/kg. When adjusting the capacity factors, the LCOH is $4.318 per kilogram, which is closer to the governmental targets. The original prices can be interpreted as if the project was built in locations with wind and solar conditions similar to San Francisco or northern Portugal. The new prices, after adjustments, are within the range of what the prices are believed to be for the actual location, reflecting more accurate and favorable economic outcomes for the project.

The LCONH3 from our result is $0.87/ kg, which is within the predicted range of $0.475 to $0.95 per kilogram by 2030. After adjustments, the price is $0.639 per kilogram, indicating that ammonia production could be economically feasible in the near future.

The LCOE in our analysis is $0.059 per kWh, slightly above the forecasted estimates of $0.03 for solar energy and $0.054 for wind. With adjustments, the LCOE is $0.041 per kWh, which is more reasonable and falls between the two predicted values. Lower LCOE values are crucial for the economic viability of hydrogen and ammonia production, since electricity is a significant input cost.

**Table 6.1:** Literature LCOE Comparison with Initial and Corrected LCOE

| Parameter | Initial Value | Corrected Value | Literature Range |
|---|---|---|---|
| $LCONH_3$ ($/kg) | 0.865 | 0.6393 | 0.475 – 0.95 |
| LCOH ($/kg) | 6.143 | 4.3181 | 5-8 (1-3 target) |
| LCOE ($/kWh) | 0.059 | 0.0412 | 0.03-0.054 |

In summary, our analysis shows that the levelized costs for hydrogen, ammonia, and electricity production are within realistic and forecasted ranges, although some costs are on the higher end. The gap between our LCOH and government target prices highlights the challenges ahead. Bridging this gap is vital for the economic viability of hydrogen and the development of necessary infrastructure. The later analysis with higher capacity factors and efficiencies indicates closer alignment with the realization goals. Continued technological innovation, material cost reductions, and supportive policies are essential to achieving these goals.

The reasons why the location, which is expected to be one of the best in the world for solar and wind power production, does not provide the cheapest energy could vary. The CAPEX and OPEX prices are based on future price projections of other projects, which, of course, can vary. Examining the total economic pie chart in Figure 5.9 shows that lowering the CAPEX and OPEX prices for the main components would drastically affect the project outcome. The pie chart indicates that certain technologies, such as electrolyzers and floating wind power, are more expensive than others. This suggests that CAPEX and OPEX for specific components, such as electrolyzers and floating wind power, have a significant impact on the overall economic outcome of the project. Consequently, any cost reduction in these technologies could notably influence the project's financial viability. Economic optimization is also based on a trial-and-error method, where more advanced calculations could yield better ratios and lower costs. Additionally, the linear scaling of CAPEX/OPEX prices might not be valid for the tested dimensions, as it might lead to higher prices than reality, where the effect of economies of scale would apply.

### 6.1.4 Choice of Energy Carrier

Using our model for the Port Nolloth location in 2035, it was decided to focus solely on ammonia production. This choice was based on factors specific to this location and the setup of the project. However, it is worth noting that different locations and timeframes could lead to the production of different energy carriers. For our P2X setup, ammonia was chosen due to its ease of export and established market. However, in other locations, factors such as nearby

industries or pipeline options might make another energy carrier such as hydrogen a better choice. It is important to note that the choice of the energy carrier that should be produced is not set in stone. If the system is expanded or circumstances change, it is possible to easily switch to producing hydrogen or another energy carrier. This flexibility ensures that we can adapt to evolving needs and opportunities, maximizing the project's effectiveness in the long run.

### 6.1.5 Grid Connection

The decision to design the project without a grid connection is influenced by several factors, including the goal of achieving complete self-sufficiency, which makes it suitable for locations where no other options are available. This setup not only simplifies the simulation process but also provides a clearer view of the project's economic viability as a standalone entity, which might be needed in the future of P2X project due to the forecasted boom in future demand. Moreover, by operating as a large-scale production plant independent of the local grid, the project's impact on the regional grid is minimized. For example, if the project scaled up to the size discussed in the Boegoebaii report in South African case Study section 2.7, it would accurately simulate scenarios where production significantly exceeds the residual electrical consumption through the grid.

### 6.1.6 Seasonal Generation Advantage

When considering the location of the project, such as the case study location of Port Nolloth, its geographical position in the Southern Hemisphere is noteworthy. The results indicate that most of the electricity production occurs during the summer months of October-March. This timing is advantageous because it aligns with winter in the Northern Hemisphere, where a large portion of the global population resides and energy demand is present. During winters in the Northern Hemisphere, energy consumption increases significantly due to heating needs, resulting in higher energy prices. Meanwhile, renewable electricity production tends to decrease due to low irradiation. Therefore, having peak electricity production in the Southern Hemisphere during this period could potentially facilitate the export of energy at a higher price, which affects the profitability of the project.

## 6.2 Project Risks

Usually, these multi-billion dollar types of projects come with several great risks due to the size of the project. These risks can be in areas that project leaders have the power to avoid or mitigate, but they can also be on a larger scale, which cannot be avoided.

### 6.2.1 National Security

A risk of investing in a project in a country of high poverty and low GDP is that there are higher risks related to national security, where political instability and corruption are having a large impact on the outcome of the project. However, the size of the project itself does have a positive influence, as the bigger economical investment, the more resources can be put on security concerns.

### 6.2.2 Safety

A P2X project includes concerns about safety. The project is built in a climate of very harsh weather, with strong winds and gassing sun, which affects not only the technology but also the people involved. The handling of flammable, toxic, and explosive chemical energy carriers is also of great concern, which requires education and safety measures, as even minor incidents can have a catastrophic outcome.

### 6.2.3 Failure of Components

There are risks associated with failure of components. Since these types of systems have a large number of different types of components, failures and O& M are inevitable. Since systems are also so interconnected, some components are crucial for the system to run, and a failure of such components could be devastating. It could also be especially devastating if the location is remote and the competence and resources for O& M is far away.

### 6.2.4 Supply Chains

Due to the size of these types of project and the great amount of different components that are needed in a Power-to-X project, there are a lot of supply chains involved. In addition to this, there are many components in the system that are dependent on each other, making the project very vulnerable to unexpected difficulties in these supply chains. For example, if there would be a shortage of material for the battery production, the P2X system would not be able to run due to the battery having such an essential function in the system, which would cause a delay of the deployment of the project.

### 6.2.5 Component and Energy Prices

As mentioned in the result discussion, there are also risks coupled to the prices for the respective components in the system. In the literature study, the prices for the major components are based on literature with price predictions for 2035. So, if there would be a major price deviation for some of the components in reality, that would substantially affect the project

profitability and perhaps the dimensioning of the system. As previously mentioned, floating wind power for example is in an early commercial stage where it is yet to be scaled up, but at the moment it is rather expensive in comparison with other power generating alternatives. Since floating wind power constitutes a rather large portion of the total investment cost, its future price development will significantly affect the project. Many of the components are also currently in a phase of rapid technology development. In the case of the technology development, these types of project can be deeply affected depending on how the situation looks like 2035. Electrolyzer technology and solar power technology is currently under rapid development, and if both of these technologies were to increase in efficiency by just a couple of percentage units, that would correspond to a major increase of hydrogen and therefore the profitability of the whole project.

Obviously, the predicted selling price for the chemical energy carrier is of huge importance for a P2X project, as the use of the energy carrier, which reflects the prices of it, directly determines the outcome of this project. Important to consider is also that it is not the prices of a sole chemical energy carrier that decided the revenue of the project, but all P2X alternatives, this because the process itself is flexible and one energy carrier can be swapped for another if the outcome is more profitable.

## 6.3 Future Development in Port Nolloth

If the project presented in this report is realized, the steps forward are to attract industries and consumers. South Africa has, as stated in 2.7, great possibilities for many of the industrial uses discussed in Section 2.3, opening up good possibilities for agriculture and industrial applications such as steel production. In addition, the addition of green energy on this scale could attract other industries from the rest of the continent, which in many areas lacks a stable energy supply that does not rely on fossil fuels. Especially industries with flexible demand that could make use of buying the otherwise curtailed energy for prices close to zero. In addition to this, as mentioned in Section 2.7, the coastal area outside of Port Nolloth has great expansion possibilities for addition of renewable energy generation, with a potential of 26 GW of wind power and large areas suitable for the expansion of solar power generation. This could eventually lead to an expansion of the additional plans, which can attract more industries while keeping the optimal generation ratio.

When the industries are implemented, further expansion of generation and production is possible in the area and will be generated at prices lower than the competitor, as the main infrastructure is already in place. In addition, a possibility is to use the Port Nolloth site as a central hub on the South African continent, where cheap energy could be used to export components to surrounding P2X projects, such as along the South African and Namibian coasts, which have conditions very similar to the Port Nolloth site. When industries are attracted, the project can not only shift focus to more hydrogen production but also other chemical energy carriers such as methanol, which requires carbon from industries in combination with the clean energy to be created.

In a future stage of the project, when the remote location is connected to the rest of the

southern African grid, the generator park can also be used to sell energy for domestic use. At this stage, whether or not the weather production of the chemical carrier occurs depends on the long-term contracts and energy prices. In case of oveproduction, surplus energy could go to the grid. In addition, the produced hydrogen could be stored in large scale to support long-term seasonal imbalances in the grid. If the projects are of enough production capacity, this is although less realistic locally as the site will have an over-production all around the year to be able to sell produce and export the hydrogen.

## 6.4 Ethical Dilemmas

From an ethical point of view producing hydrogen P2X project locations in general, or South Africa in particular for export to Europe or other industrialized countries comes with both promising benefits and significant challenges. On the one hand, it offers potential solutions to issues such as job deficit, efficient land use, and technological development. Using underutilized land, hydrogen production maximizes land efficiency without compromising vital ecosystems, and as the climate crisis is a global concern, the decision by South Africa to let such a project pass is part of a decision limiting millions of tons of carbon emission. If the project is beneficial and expansion is allowed, it can not only deliver more job opportunities but also, when grid connection is implemented, stability in their power generation.

However, it also raises ethical and practical considerations that cannot be overlooked. Concerns about resource allocation arise, particularly in regions where basic necessities such as clean water, healthcare, education, and electricity supply are not accessible. Prioritizing the needs of local communities over export-oriented industries is necessary where balancing the combating of climate change with protecting local environments requires careful consideration.

These considerations, for the case of Europe and Africa, have to be treated with care because of the historical perspective. One could argue that such projects are part of modern colonialism, where dependency is reestablished. One key difference is, though, that the project does not have a permanent impact on the site, where only natural resources such as weather conditions are used. Another difference is that a P2X project benefits the entire world by cutting emissions. However, the coinciding with history when it comes to the main arguments of job creation and development aid cannot be unseen, and the discussion about the subject has to be treated with extra care as no one can oppose that Europe would do this investment primarily for their own benefit.

## 6.5 Future Development of MSc Thesis

### 6.5.1 Scaling of the System

The model, as well as the Port Nolloth project setup, offers great possibilities when it comes to up-scaling. Simulation-wise there are no big changes in the model which would be needed when up-scaling. However, the scaling of the project in practice also has an impact on the project when it comes to logistics as well as costs of the project. The Port Nolloth P2X project offers huge areas for wind and solar power generation. Space-restricted issues are therefore in theory not a problem for huge local upscaling.

Upscaling also has a positive impact on all CAPEX values. The bigger such a project is, the lower the CAPEX gets, as the logistics are in place and the supply chain is already there. Furthermore, when all local demand is met, the project site could be an interesting location for the construction of technology that could be distributed along the African coast, as prices are expected to be competitive for projects elsewhere, when port facilities and competence are established.

The project location is therefore not only suitable for local up-scaling but could also serve as a continental distribution center, where closest main options are cross-ocean in Europe or southeast Asia, by being able to cut the expenses for similar projects in the area.

### 6.5.2 Applying System for Other Case Studies

Using the model, it is possible to identify the result of the P2X project at other locations. This would drastically change the ratio of the installed component, with a potentially very different outcome. For example, for locations with better wind conditions compared to solar, more wind will be needed, and for sites without the power shift, less installed wind capacity would be needed. This is implemented in the P2X model by changing the generation input files and following the methodology. This tool is very important for the initial scouting of project locations, as a map of simple capacity factor overlays does not mean that the location coincides with the maximum hydrogen production because of the time aspect. In reality, using the same economical numbers for CAPEX and OPEX does not give an accurate representation, although the project setup is forecasted prices for situation 2035, the same assumptions would be made for this location if the model was built based on it.

### 6.5.3 Forecasting

When it comes to optimizing the modeling, the integration of forecasting would be handy for the project. By forecasting electricity production, one could limit wasted hydrogen consumption in the fuel cell, by charging the batteries before an energy deficit, and relatively

smoothly could be integrated in the battery controller. A faster response time for the electrolyzer would also be possible, making the voltage regulation for the battery less intensive.

### 6.5.4 Price Scenarios

As previously discussed, making model simulations based on different price scenarios for the different components would also be interesting. Currently, to do this the entire extensive economical method would have to be done all over again, which exceeds the time for this project. Putting more energy into this could eventually lead to interesting potential findings. As mentioned in section 6.2.5, the outcome of the project is very sensitive to the volatility of the prices. Simulating the economics for different price scenarios would therefore be interesting. This includes both comparing with other prices for energy and using other values for CAPEX/OPEX of the main components such as wind power and electrolyzer, which have a big impact on the outcome.

### 6.5.5 Hourly Data

With the current model, small fluctuations from minute to minute for generation do not occur. This is in part due to the delays in the parks, but also because hourly values are used. In reality, local variation from cloud coverage could for example occur, which would have a heavy impact on the ramp-up and downs of the electrolyzer as well as cycles of the battery. To use minute data for the region would therefore be favorable, even though it is difficult to find valid resources for such. In this scenario, the use of supercapacitors in combination with lithium batteries could become a relevant solution for handling the short-term power balance.

### 6.5.6 Alternative Controller Operation

Using minute data would also lead to increased battery usage as power generation would fluctuate much more. Even though the generation park placement is made to dampen the effect of this, for example, large clouds will cause a rapid decline in solar production, which energy the battery needs to input. This could also raise the cycles of the battery, which causes higher wear, meaning that the currectly used peakshaving logics in the model could have to be discarded, leading to lower production, but also consumption, as the SOC of the battery will be at higher charge most of the time.

Another way to lower the fuel cell consumption would be to directly run the fuel cell on hydrogen instead of ammonia in the model. Currently, the system converts the electrical energy to hydrogen and further ammonia, which is cycled the same way back to electricity supporting the battery when the SOC is low. A more efficient way would be to use a secondary hydrogen storage system for this purpose. The storage facility could be used for the other local uses of hydrogen.

### 6.5.7 Sensitivity Analysis

Performing a sensitivity analysis on the economic aspects and results of the model would further generate interesting results. This analysis aims to explore how variations in economic parameters affect the results. Specifically, sensitivity analysis could investigate how changes in factors such as costs, market prices, discount rates, or regulatory policies impact the economic performance of the model by varying the parameters and observing their effects on key economic indicators. However, it is worth noting that something similar is made throughout the methodology, as the model is subjected to tests of a wide range of ratios of installed capacities, as well as variation in interest rates. This evaluation of the model across various component ratios further highlights its robustness for various applications.

# Chapter 7

# Conclusion

Based on the investigated case study for year 2035, floating wind plays a key role for P2X projects even for one of the worlds best solar conditions. Although solar energy generates more peak power, the ability of wind energy to cover nights and seasons of low radiance motivates the use of it. This is both because of a higher capacity factor and because the wind produces when the solar system cannot, which makes the system less dependent on potentially expensive short-term storage systems. For the Port Nolloth site, although floating wind plays a key role, the LCOE of the energy is much higher than for solar, whereas for this project setup, the installed capacity is only a share of the total. However, for other locations, the result might look different.

In this P2X project, a scaleable tool for the analysis of the P2X system independent of the selected site selection has been built, which can be used to further investigate the role of the (floating) wind and the other main components for a P2X location.

The main cost drivers are for the P2X project identified as the development of floating wind power and electrolyzer technology, where cost reduction in these technologies could notably influence the financial viability of the P2X projects.

Considering simulation setups for different ratios of components, very different ratios have similar production output at the end of the year, even though the generation distribution looks different. There might therefore be alternatives, better than the one found in this report. The conclusion of this is that it is very hard to find trends in the optimal ratio for maximum production in the system. However, all integrated components, including floating wind, have a key role in the project based on the analysis made in the case study.

From the project, one can also see that although wind is many times more expensive in terms of costs, it is much more efficient regarding installed capacity. This is in part because of the higher capacity factor but also a more even power curve throughout the hours of the

day, which gives the electrolyzer allowance for constant production, while the solar produces excessive electricity for a couple of hours and then does not deliver anything.

Ammonia has been identified as the most suitable energy carrier for this specific project for a number of reasons. Ammonia is expected to be one of the main alternatives of the transition fuels and is already used in industries all over the world. The energy carrier is also suitable for storage and transportation. However, the disadvantages are the extra cost and loss in efficiency, as well as health concerns.

Another finding made through simulation is that the use of a fuel cell for a temporary energy need may be economically viable for emergency power generation. Investing in more batteries with higher efficiencies is an alternative to lower fuel cell consumption, but when the budget used for extra batteries instead is used on generation/production, a higher net export is achieved.

A finding made in the report is also that to use electricity directly in local industries, costs can be cut for multiple causes such as the expensive CAPEX and OPEX of hydrogen technology, as well as lost power because of low efficiencies. Moving industries to the location is therefore expected to be much cheaper than moving the energy.

The analysis suggests that the target prices for hydrogen, ammonia, and electricity production are challenging but realistic. Despite potential errors in our initial data, adjusted simulations indicate that our cost estimates fall within industry norms, validating our calculations and the reliability of our tool.

The location in Port Nolloth investigated in the case study is identified as a suitable location for the project for multiple reasons. The energy availability and overlap between wind and solar, space, port facilities, and temperature make the conditions favorable, as well as the possibility for expansion and applications of both electrical and chemical energy in local industries.

# References


[1] Kavlak, G., McNerney, J., and Trancik, J.E. Evaluating the causes of cost reduction in photovoltaic modules. *Energy Policy*, 123:700–710, (2018). https://doi.org/10.1016/j.enpol.2018.08.015.

[2] Power-to-x: paving the way for a greener future. *Ramboll*, (n. d). https://www.ramboll.com/net-zero-explorers/power-to-x-explained?utm_term=power%20to%20x%20definition&utm_campaign=RGR-NZE-Power-to-X&utm_source=adwords&utm_medium=ppc&hsa_acc=2148707682&hsa_cam=20527872846&hsa_grp=150125846541&hsa_ad=673305662311&hsa_src=g&hsa_tgt=kwd-2078547371926&hsa_kw=power%20to%20x%20definition&hsa_mt=p&hsa_net=adwords&hsa_ver=3&gad_source=1&gclid=Cj0KCQiA5rGuBhCnARIsAN11vgRSn_P2Uw_TKe1dWKkL772_eHkCsOZNxbpIp5N4-D02x-AcMpYmKrYaAlQLEALw_wcB.

[3] Hybrit demonstration. *Hybrit*, (n. d). https://www.hybritdevelopment.se/hybrit-demonstration/.

[4] Aagaard, P., Andersen, J. R., Wedege, K., Nauclér, T., and Prabhala, P. From green ammonia to lower-carbon foods. *McKinsey*, (2022). https://www.mckinsey.com/industries/agriculture/our-insights/from-green-ammonia-to-lower-carbon-foods.

[5] Teter, J. and Voswinkel, F. Transport. *IEA*, (2023). https://www.iea.org/energy-system/transport.

[6] Ipceis on hydrogen. *European Commission*, (2022). https://single-market-economy.ec.europa.eu/industry/strategy/hydrogen/ipceis-hydrogen_en.

[7] Korea hydrogen economy roadmap 2040. *IEA*, (2020). https://www.iea.org/policies/6566-korea-hydrogen-economy-roadmap-2040.

[8] Biden-harris administration announces $7 billion for america's first clean hydrogen hubs, driving clean manufacturing and delivering new economic opportunities nationwide. *U.S Department Of Energy*, (2013). https://www.energy.gov/articles/bi

den-harris-administration-announces-7-billion-americas-first-clean-hydrogen-hubs-driving/.

[9] How to calculate the levelized cost of energy (lcoe)? *GreenMatch*, (n. d). https://www.greenmatch.ch/en/knowledge-center/how-to-calculate-the-levelized-cost-of-energy-lcoe/.

[10] Bilicic, G. and Scroggins, S. 2023 levelized cost of energy+. *Lazard*, (2023). https://www.lazard.com/research-insights/2023-levelized-cost-of-energyplus/.

[11] Global wind atlas. *Global Wind Atlas*, (2024). https://globalwindatlas.info/en.

[12] Key sectors. *Zuidafrika*, (n. d). https://zuidafrika.nl/trade-investment/key-sectors/.

[13] Our mission. *NCGH2*, (2023). https://www.ncgh2.co.za/.

[14] Global solar atlas. *Global Solar Atlas*, (2024). https://globalsolaratlas.info/map.

[15] Introduction. *Open Modelica*, (n. d). https://openmodelica.org/.

[16] About. *Renewable Ninja*, (n. d). https://www.renewables.ninja/about.

[17] Solar explained. *U.S Energy Information Administration*, (2023). https://www.eia.gov/energyexplained/solar/photovoltaics-and-electricity.php.

[18] K.V. Vidyanandan. An overview of factors affecting the performance of solar pv systems. *Energy Scan (A house journal of Corporate Planning, NTPC Ltd.)*, 27:2–8, 02 (2017). https://www.researchgate.net/publication/319165448_An_Overview_of_Factors_Affecting_the_Performance_of_Solar_PV_Systems.

[19] 2030 solar cost targets. *US Energy - Solar Energy Technologies Office*, (2022). https://www.energy.gov/eere/solar/articles/2030-solar-cost-targets.

[20] Utility-scale pv. *NREL*, (2023). https://atb.nrel.gov/electricity/2023/utility-scale_pv.

[21] Wiser, U., Ryan, H., Bolinger, M. and Seel, J. Benchmarking utility-scale pv operational expenses and project lifetimes: Results from a survey of u.s. solar industry professionals. *Berkley Lab*, (2020). https://emp.lbl.gov/publications/benchmarking-utility-scale-pv.

[22] What is capacity factor and how do solar and wind energy compare. *WhatNextNow*, (2011). https://www.whatnextnow.com/home/solar/what-is-capacity-factor-and-how-does-solar-energy-compare.

[23] Stc and noct – solar panel test conditions explained. *SolarDesignGuide*, (n. d). https://solardesignguide.com/stc-and-noct-solar-panel-test-conditions-explained/.

[24] K. Lu. Comparison and evaluation of different types of solar cells. *Applied and Computational Engineering*, 23:263–270, 11 (2023). https://www.researchgate.net/publication/375449186_Comparison_and_Evaluation_of_Different_Types_of_Solar_Cells.

[25] van de Ven, D-J., Capellán-Pérez, I., Arto, I., Cazcarro, I., Castro, C., Patel, P., and González-Eguino, M. The potential land requirements and related land use change emissions of solar energy. *Scientific Reports*, 11, 02 (2022). https://www.nature.com/articles/s41598-021-82042-5.

[26] Maia, A. S., Culhari, E., Fonseca, V., Milan, H., and Gebremedhin, K. G. Photovoltaic panels as shading resources for livestock. *Journal of Cleaner Production*, 258:120551, 02 (2020). https://www.researchgate.net/publication/339246522_Photovoltaic_panels_as_shading_resources_for_livestock.

[27] Bošnjaković, M., Santa, R., Crnac, Z., and Bošnjaković, T. Environmental impact of pv power systems. *Sustainability*, 15(15), (2023). https://www.mdpi.com/2071-1050/15/15/11888.

[28] Guaita-Pradas, I., Marqués, I., Gallego, A., and García del Río, B. Analyzing territory for the sustainable development of solar photovoltaic power using gis databases. *Environmental Monitoring and Assessment*, 191, 12 (2019). https://www.researchgate.net/figure/Main-criteria-used-in-the-site-selection-model-for-PV-power-plants_fig5_337401410.

[29] Solar pv issues: Top solar energy system losses. *SolarSME*, (2023). https://solarsme.com/top-solar-energy-system-losses/.

[30] Wind explained - electricity generation from wind. *EIA*, (2023). https://www.eia.gov/energyexplained/wind/electricity-generation-from-wind.php.

[31] Wind energy capacity. *OurWorldInData*, (2023). https://ourworldindata.org/grapher/cumulative-installed-wind-energy-capacity-gigawatts?country=~OWID_WRL.

[32] Wind turbine. *Wikipedia*, (n. d). https://en.wikipedia.org/wiki/Wind_turbine.

[33] History of europe's wind industry. *WindEurope*, (2024). https://windeurope.org/about-wind/history/#.

[34] Rapacka, P. Offshore wind turbines will be larger and more economical than predicted. *BalticWind*. https://balticwind.eu/offshore-wind-turbines-will-be-larger-and-more-economical-than-predicted/.

[35] Onshore vs offshore wind energy: what's the difference? *NationalGrid*, (2022). https://www.nationalgrid.com/stories/energy-explained/onshore-vs-offshore-wind-energy.

[36] Horwath, S., Hassrick, J., Grismala, R., Diller, E., Krebs, J., and Manhard, R. Comparison of environmental effects from different offshore wind turbine foundations. *BOEM*, (2021). https://www.boem.gov/sites/default/files/documents/environment/Comparison-Environmental-Effects-Different-OWT-Foundations-2021.pdf.

[37] Deep water: The next step for offshore wind energy. *European Wind Energy Association*, (2013). https://www.ewea.org/fileadmin/files/library/publications/reports/Deep_Water.pdf.

[38] Koefoed Jensen, M. Lcoe. *National Renewable Energy Laboratory*, (2022). https://www.nrel.gov/wind/assets/pdfs/engineering-wkshp2022-1-1-jensen.pdf.

[39] What is the Cost of Offshore Wind Energy? *Windustry*, (n. d). https://www.windustry.com/what-is-the-cost-of-offshore-wind-energy.htm.

[40] Operations and maintenance. *Guide to a Floating Offshore Wind Farm*, (n. d). https://guidetofloatingoffshorewind.com/guide/o-operations-and-maintenance/).

[41] Average capacity factor for offshore wind power worldwide from 2010 to 2022. *Statista*, (2022). https://www.statista.com/statistics/1368679/global-offshore-wind-capacity-factor/.

[42] Hywind scotland remains the uk's best performing offshore wind farm. *Equinor*, (2022). https://www.equinor.com/news/archive/20210323-hywind-scotland-uk-best-performing-offshore-wind-farm.

[43] Y. Katsigiannis and G. Stavrakakis. Estimation of wind energy production in various sites in australia for different wind turbine classes: a comparative technical and economic. *Renew Energy*, 67:1–7, 01 (2013). https://www.researchgate.net/figure/Typical-wind-turbine-power-curve_fig3_312786418.

[44] Yuan, W., Feng, J-C., Zhang, S., Sun, L., Cai, Y., Yang, Z., and Sheng, S. Floating wind power in deep-sea area: Life cycle assessment of environmental impacts. *Advances in Applied Energy*, 9:100–122, (2023). https://www.sciencedirect.com/science/article/pii/S266679242300001X.

[45] Patonia, A., Lenivova, V., Poudineh, F. R., and Nolden, C. Hydrogen pipelines vs. hvdc lines: Should we transfer green molecules or electrons? *Oxford Institute for Energy Studies*, (2023). https://www.connaissancedesenergies.org/sites/connaissancedesenergies.org/files/pdf-pt-vue/ET27-Hydrogen-pipelines-vs.-HVDC-lines_HG_AP_2.pdf.

[46] Alam, M., Rahaman, M. and Foysal, D. Technical comparison of modern hvac and hvdc transmission system along with cost analysis. *Journal of Control and Instrumentation Engineering*, 8:10, 02 (2022). https://www.researchgate.net/figure/Cost-break-down-HVDC-LCC-Overhead-transmission-line-for-3-000-MW-of-500-kV-for-600-km_fig3_358460206.

[47] Liun, E. Stochastic methodology to estimate costs of hvdc transmission system. 02 (2016). https://www.researchgate.net/figure/HVDC-Submarine-cable-cost_tbl1_293959228.

[48] Murphy, L. and Allen, S. Everything you need to know about gas piping. *Forbes*, (2023). https://www.forbes.com/home-improvement/plumbing/what-is-gas-piping/.

[49] Contracts Signed for Construction of Ammonia-Fueled Ammonia Gas Carrier. *Nippon Yusen Kabushiki Kaisha)*, (2024). https://www.nyk.com/english/news/2024/20240125_02.html.

[50] Infrastructure costs. *Supply Chain Management Outsource*, (n. d). https://www.scmo.net/infrastructure-costs.

[51] Martin, P. Maersk orders world's biggest ammonia carriers from hyundai to ship hydrogen derivative across oceans. *Hydrogeninsight*, (2023). https://www.hydrogeninsight.com/transport/maersk-orders-worlds-biggest-ammonia-carriers-from-hyundai-to-ship-hydrogen-derivative-across-oceans/2-1-1563932?zephr_sso_ott=hn8F6h.

[52] Chen, T., Jin, Y., Liu, M., Chen, B., and Xie, Y. Applications of lithium-ion batteries in grid-scale energy storage systems. *Transactions of Tianjin University*, (2020). https://doi.org/10.1007/s12209-020-00236-w.

[53] Rapier, R. Estimating the carbon footprint of utility-scale battery storage. *Forbes*, (2022). https://www.forbes.com/sites/rrapier/2020/02/16/estimating-the-carbon-footprint-of-utility-scale-battery-storage/.

[54] Lithium-ion battery pack prices hit record low of $139/kwh. *BloombergNEF*, (2023). https://about.bnef.com/blog/lithium-ion-battery-pack-prices-hit-record-low-of-139-kwh/.

[55] Grid scale storage. *IEA*, (2023). https://www.iea.org/energy-system/electricity/grid-scale-storage.

[56] Northvolt develops state-of-the-art sodium-ion battery validated at 160 wh/kg. *Northvolt*, (2023). https://northvolt.com/articles/northvolt-sodium-ion/.

[57] Cole, W. and Karmakar, A. Cost projections for utility-scale battery storage: 2023 update. *National Renewable Energy Laboratory*, (2023). https://www.nrel.gov/docs/fy23osti/85332.pdf.

[58] Xu, B., Oudalov, A., Ulbig, A., Andersson, G., and Kirschen, D.s. Modeling of lithium-ion battery degradation for cell life assessment. *IEEE Transactions on Smart Grid*, 99:1–1, 06 (2016). https://www.researchgate.net/publication/303890624_Modeling_of_Lithium-Ion_Battery_Degradation_for_Cell_Life_Assessment.

[59] Making batteries work. *WSP*, (n. d.). https://www.google.com/url?sa=i&url=https%3A%2F%2Fwww.wsp.com%2F-%2Fmedia%2Finsights%2Fuk%2Fdocument

s%2Fmaking-batteries-work290920.pdf&psig=AOvVaw2lOO91kmlurYzoQZt6LC1d&ust=1714810528161000&source=images&cd=vfe&opi=89978449&ved=0CAcQrpoMahcKEwiAn6GUhfGFAxUAAAAAHQAAAAAQBA).

[60] Roy, P. K., Karayaka, H., He, J. and Yu, Y-H. Economic comparison between a battery and supercapacitor for hourly dispatching wave energy converter power. *NREL*, (2022). https://www.nrel.gov/docs/fy21osti/77398.pdf.

[61] Söderbom, J. Unlocking new possibilities through innovative energy storage the role of ultracapacitors in the energy transition. *EIT*, (2020). https://eit.europa.eu/sites/default/files/white_paper_on_ultracapacitor_technology.pdf.

[62] Breeze, P. Chapter 8 - hydrogen energy storage. pages 69–77, (2018). https://www.sciencedirect.com/science/article/pii/B9780128129029000080.

[63] Hydrogen production related links. *US Office of ENERGY EFFICIENCY & RENEWABLE ENERGY*, (2022). https://www.energy.gov/eere/fuelcells/hydrogen-production-related-links#targets/.

[64] Electrolyzers. *IEA*, (n. d.). https://www.iea.org/energy-system/low-emission-fuels/electrolysers.

[65] Jiahui, Y. The world's first direct seawater electrolysis for hydrogen production driven by offshore wind power successfully tested in fujian. *College of Civil and Transportation Engineering, Shenzhen University*, (2022). https://ce.szu.edu.cn/info/1355/5893.htm.

[66] Cost reduction and performance increase of pem electrolysers. *Fuel Cells and Hydrogen Joint Undertaking*, (2018). https://www.fch.europa.eu.

[67] Sun, Y., Hu, X., Gao, J., Han, Y., Sun, A., Zheng, N., Shuai, W., Xiao, G., Guo, M., Ni, M., and Xu, H. Solid oxide electrolysis cell under real fluctuating power supply with a focus on thermal stress analysis. *Energy*, 261:125096, (2022). https://www.sciencedirect.com/science/article/pii/S0360544222019910.

[68] Hodges, A., Hoang, A. L., Tsekouras, G., Wagner, K., Lee, C-Y., Sweigers, G. F., and Wallace, G. G. A high-performance capillary-fed electrolysis cell promises more cost-competitive renewable hydrogen. *Nature Communications*, (2022). https://doi.org/10.1038/s41467-022-28953-x.

[69] Comparison of fuel cell technologies. *Hydrogen and fuel cell office Energy GOV*, (n. d.). https://www.energy.gov/eere/fuelcells/comparison-fuel-cell-technologies.

[70] Reversible Solid Oxide Electrolyser (rSOC) for resilient energy systems. *European Commission*, (2024). https://cordis.europa.eu/programme/id/H2020_FCH-02-3-2017.

[71] Collins, L. Green hydrogen price in europe unlikely to fall below €5/kg by 2030, putting off potential offtakers: analyst. *Hydrogeninsight*, (2023). https://www.hydrogeninsi

ght.com/production/green-hydrogen-price-in-europe-unlikely-to-fall-below-5-kg-by-2030-putting-off-potential-offtakers-analyst/2-1-1537520.

[72] The future of Hydrogen. *International Energy Agency*, (2019). https://iea.blob.core.windows.net/assets/9e3a3493-b9a6-4b7d-b499-7ca48e357561/The_Future_of_Hydrogen.pdf.

[73] Christensen, A. Assessment of hydrogen production costs from electrolysis: United states and europe. *International Council on Clean Transportation*, (2020). https://theicct.org/wp-content/uploads/2021/06/final_icct2020_assessment_of-_hydrogen_production_costs-v2.pdf.

[74] Patonia, A. and Poudineh, R. Ammonia as a storage solution for future decarbonized energy systems. *Oxford Energy*, (2020). https://www.oxfordenergy.org/wpcms/wp-content/uploads/2020/11/Ammonia-as-a-storage-solution-for-future-decarbonized-systems-EL-42.pdf.

[75] Aziz, M., Wijayanta, A. T., and Nandiyanto, A.B.D. Ammonia as effective hydrogen storage: A review on production, storage and utilization. *Energies*, 13(12), (2020). https://www.mdpi.com/1996-1073/13/12/3062.

[76] The role of hydrogen and ammonia in meeting the net zero challenge. *The Royal Society*, (2021). https://royalsociety.org/-/media/policy/projects/climate-change-science-solutions/climate-science-solutions-hydrogen-ammonia.pdf.

[77] Müller, M., Pfeifer, M., Holtz, D., and Müller, K. Comparison of green ammonia and green hydrogen pathways in terms of energy efficiency. *Fuel*, 357:129843, (2024). https://www.sciencedirect.com/science/article/pii/S0016236123024572.

[78] Zhang, H., Wang, L., Van herle, J., Maréchal, F., and Desideri, U. Techno-economic comparison of green ammonia production processes. *Applied Energy*, 249, (2020). https://www.sciencedirect.com/science/article/pii/S0306261919318227.

[79] Cheddie, D. Ammonia as a hydrogen source for fuel cells: A review. (2012). https://doi.org/10.5772/47759.

[80] Brown, T. Development of direct ammonia fuel cells. *ammoniaenergy*, (2017). https://www.ammoniaenergy.org/articles/development-of-direct-ammonia-fuel-cells/.

[81] Lövdahl, J. and Magnusson, M. Evaluation of ammonia as a potential marine fuel. *Chalmers*, (2019). https://odr.chalmers.se/server/api/core/bitstreams/a9eedd5c-0c25-4d53-b6c0-7003522a4363/content.

[82] IRENA and AEA. Innovation outlook: Renewable ammonia. *International Renewable Energy Agency*, (2023). https://www.irena.org/publications/2022/May/Innovation-Outlook-Renewable-Ammonia.

[83] Fúnez Guerra, C., Reyes-Bozo, L., Vyhmeister, E., M. Jaén Caparrós,, Salazar, J. L., and Clemente-Jul, C. Technical-economic analysis for a green ammonia production plant in chile and its subsequent transport to japan. *Renewable Energy*, 157:404–414, (2020). https://www.sciencedirect.com/science/article/pii/S0960148120307394.

[84] Gallardo F. and Frisk A. Green ammonia production: harnessing green hydrogen. *Hydrogen Tech World*, (2023). https://hydrogentechworld.com/green-ammonia-production-harnessing-green-hydrogen.

[85] Herber, G. Plant prices: The costs of constructing a desalination plant and facility. *Medium*, (2024). https://medium.com/@desalter/plant-prices-the-costs-of-constructing-a-desalination-facility-2c31f7fcb690.

[86] The role of desalination in an increasingly water-scarce world. *World Bank Group*, (2019). https://documents1.worldbank.org/curated/en/476041552622967264/pdf/135312-WP-PUBLIC-14-3-2019-12-3-35-W.pdf.

[87] Vad är vätgas? *Vätgas Sverige*, (n. d). https://www.vatgas.se/.

[88] Nayak-Luke R. M., Forbes C, Cesaro Z, Bañares-Alcántara R, and Rouwenhorst K. H. R. *Techno-Economic Aspects of Production, Storage and Distribution of Ammonia*, pages 191–207. Elsevier, (2022). https://ris.utwente.nl/ws/portalfiles/portal/276441421/3_s2.0_B9780128205600000084_main.pdf.

[89] Storage tank costs: storing oil, energy, water and chemicals? *Thunder Said Energy*, (n. d). https://thundersaidenergy.com/downloads/storage-tank-costs-storing-oil-energy-water-and-chemicals/.

[90] Klopčič, N., Grimmer, I., Winkler, F., Sartory, M., and Trattner, A. A review on metal hydride materials for hydrogen storage. *Journal of Energy Storage*, 72:108456, (2023). https://www.sciencedirect.com/science/article/pii/S2352152X23018534.

[91] C. Drawer, J. Lange, and M. Kaltschmitt. Metal hydrides for hydrogen storage – identification and evaluation of stationary and transportation applications. *Journal of Energy Storage*, 77:109988, (2024). https://www.sciencedirect.com/science/article/pii/S2352152X2303387X.

[92] Vestas v236-15.0. *Wind-turbine-models*, (2024). https://en.wind-turbine-models.com/turbines/2317-vestas-v236-15.0.